Tradeoff Evaluation of Scheduling Algorithms for Terminal-Area Air Traffic Control

by

Hanbong Lee
Bachelor of Science in Mechanical and Aerospace Engineering
Seoul National University, South Korea, 2002

Submitted to the Department of Aeronautics and Astronautics
in partial fulfillment of the requirements for the degree of

Master of Science in Aeronautics and Astronautics

at the

MASSACHUSETTS INSTITUTE OF TECHNOLOGY

June 2008

© Massachusetts Institute of Technology 2008. All rights reserved.

Author .....
Department of Aeronautics and Astronautics
May 23, 2008

Certified by .....
Hamsa Balakrishnan
Assistant Professor of Aeronautics and Astronautics and Engineering Systems
Thesis Supervisor

Accepted by .....
David L. Darmofal
Associate Department Head
Chair, Committee on Graduate Students

MASSACHUSETTS INSTITUTE OF TECHNOLOGY
AUG 0 1 2008
LIBRARIES
ARCHIVES

Tradeoff Evaluation of Scheduling Algorithms for Terminal-Area Air Traffic Control

by

Hanbong Lee

Bachelor of Science in Mechanical and Aerospace Engineering

Seoul National University, South Korea, 2002

Submitted to the Department of Aeronautics and Astronautics
on May 23, 2008, in partial fulfillment of the
requirements for the degree of
Master of Science in Aeronautics and Astronautics

Abstract

The terminal-area surrounding an airport is an important component of the air transportation system, and efficient and robust terminal-area schedules are essential for successfully meeting the projected increase in air traffic demand. Aircraft arrival schedules are subject to a variety of operational constraints, such as minimum separation requirements for safety, required arrival time-windows, limited deviation from a nominal or FCFS sequence, and precedence constraints on the arrival order. With these constraints, there is a range of desirable objectives associated with multiple stakeholders that could be optimized in these schedules. The schedules should also be robust against the uncertainty around the terminal-area.

A dynamic programming algorithm for determining the minimum cost arrival schedule, given the aircraft-dependent delay costs, is presented in this thesis. The proposed approach makes it possible to determine various tradeoffs between multiple objectives in terminal-area operations. The comparison of schedules that maximize throughput to those that minimize average delay shows that the benefit from maximizing throughput could be at the expense of an increase in average delay, and that minimizing average delay is the more advantageous of the two objectives in most cases. A comprehensive analysis of the tradeoffs between throughput and fuel costs, and throughput and operating costs is conducted, accounting for both the cost of delay (as reported by the airlines) and the cost of speeding-up when possible (from models of aircraft performance). It is also demonstrated that the proposed aircraft scheduling algorithm can be applied to the optimization problem for the coupled operations of arrivals and departures on a single runway.

Using the same framework, a dynamic programming algorithm for robust scheduling in terminal-area is also developed. This algorithm is designed to minimize the possibility that an air traffic controller has to intervene the initially determined sched-

ule under the uncertainty of the landing time accuracy due to the aircraft equipage. The result from the proposed approach is a tradeoff curve between runway throughput and robustness.

Thesis Supervisor: Hamsa Balakrishnan
Title: Assistant Professor of Aeronautics and Astronautics and Engineering Systems

Acknowledgments

This research was funded by NASA under the NGATS-ATM Airspace and NGATS-ATM Airportal Programs.

First of all, I would like to thank my advisor, Professor Hamsa Balakrishnan for her guidance and support through this work. She has always listened to my opinions carefully and led my research in the right direction with her great insights. I am so fortunate to have Hamsa as an advisor.

I thank the labmates at International Center for Air Transportation (ICAT) for making a passionate research atmosphere in the lab. In particular, Jonathan Histon deserves special credit for kind advices and helps that he gave me when I started my research at ICAT.

I appreciate all of my friends at MIT, including Korean Aero/Astro graduate students and SSHS friends, who have made my life in Boston delightful. Especially, I would like to thank SeungBum Hong who encouraged me to study at MIT. I also appreciate Jaemyung Ahn for his outstanding advices about my research and academic career.

I also thank Gun-yeong Lee, a director of aircraft design development team in Korean Air Aerospace division, and Dong-jun Lee, a group manager in the team. They understood my academic aspiration and allowed me to go abroad for my study, in spite of suffering from a manpower shortage for the B787 development program.

Thanks to my lovely wife, Rosa Cho. You have always stayed with me, supported me in various ways including delicious food, and cheered me up whenever my confidence was shaken. I love you.

Lastly, I would like to thank my dear family, grandmother, mother, and sister, as well as my parents-in-law. I really appreciate you for your constant trust, understanding, and love.

Contents

List of Figures

List of Tables

Chapter 1

Introduction

Air traffic congestion is considered one of the principal constraints to the future growth of the global air transportation industry [5]. The increasing demand and the capacity limitations of the current system have resulted in a significant increase in system delays. The Department of Transportation estimates that commercial aviation delays cost U.S. airlines over $3 billion per year in direct operating costs alone [6]. With air transportation having become the backbone of global commerce and transporting 36% by value of all international freight, the indirect costs to passengers and businesses are much higher [7].

Airports and the airspace surrounding airports (terminal-areas) have traditionally been the most capacity constrained elements of the air transportation system. Airport capacity expansion through additional physical infrastructure (such as, for example, runway expansion projects) is not easy and requires long-term planning and significant investment. This has motivated efforts to improve the use of airspace resources through Air Traffic Management (ATM) to accommodate the growing traffic demand.

1.1 The Current Air Traffic Control System

The current air traffic control (ATC) system is typically composed of three types of facilities: airport air traffic control towers, terminal airspace control facilities, and en

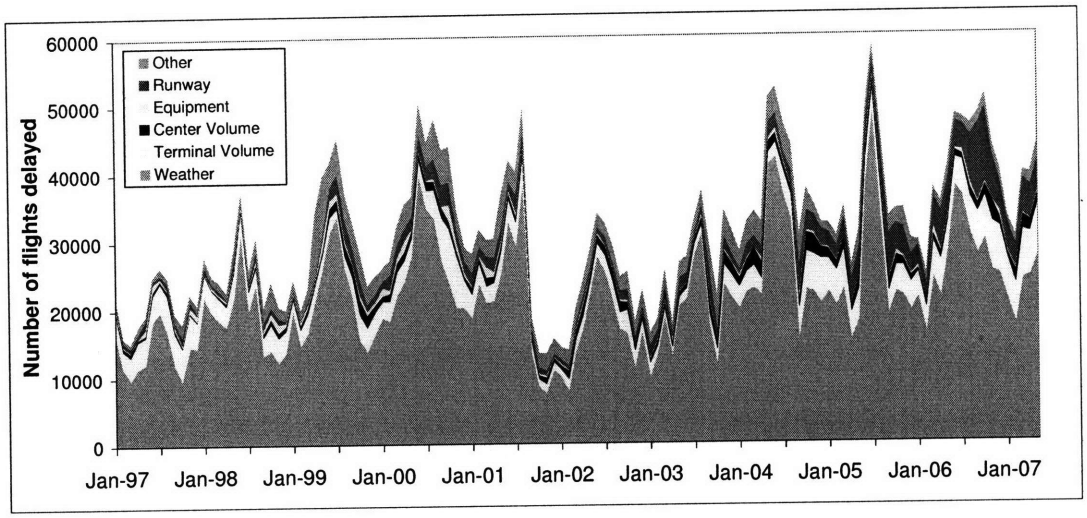

Figure 1-1: The area chart shows the total number of flights delayed by causes, between 1997 and 2007 [2].

route control centers. Airport air traffic control towers monitor aircraft on the ground and give takeoff and landing clearances. Terminal airspace control facilities handle aircraft ascending and descending to and from airports. In the United States, these facilities are called approach control facilities or Terminal Radar Approach Control (TRACON) facilities. En route control centers, known as Air Route Traffic Control Centers (ARTCC), or more simply, Centers in the US, handle aircraft flying between airports at the higher altitudes [5,8].

1.1.1 Terminal-area air traffic control

The terminal-area, generally a region of radius 30-40 miles around an airport, forms the critical interface between the airspace and the airport (surface). The terminal-area is also a significant bottleneck in the ATC network, resulting in delays. Figure 1-1 shows the total number of flights delayed per month in the United States between January 1997 and May 2007. The delayed flights are categorized by six causes of delay: weather, terminal volume, center volume, equipment, runway, and other. The largest cause of delay is weather, but it is noted that the delays due to terminal volume and runways also account for a large portion of the delayed flights.

Possible solutions for improving congestion in the terminal-area fall into four cat-

egories [9]:

- Reorganizing the existing schedule (reduced ticket prices in off-peak periods)
- Rationing the use of existing capacity (increasing landing fees during peak time or limiting the number of landing slots)
- Physically increasing the landing capacity (expanding existent airports or building new airports)
- Using existing airport capacity more efficiently (improving air traffic flow and control in terminal-area)

Among these proposed solutions, the last one, namely, the efficient use of existing airport capacity by improving air traffic flow in terminal-area, is the focus of this thesis since it potentially requires less long-term planning and investment than the other options. In other words, increasing the efficiency of arrival and departure operations in the terminal-area has the potential to be toward successfully meeting the increased demand for air traffic services.

1.1.2 Decision support tools (DSTs) for terminal-area operations

To help air traffic managers and tower controllers manage arrival and departure operations in the terminal-area efficiently, several automated decision support tools (DSTs) have been developed and used at airports. These include COMPAS (Computer Oriented Metering, Planning and Advisory System) in Frankfurt [10], MAESTRO (Means to Aid Expedition and Sequencing of Traffic with Research of Optimization) in Paris [11], and CTAS (Center-TRACON Automation System) in Dallas Fort Worth [12]. The decision support tools suggest optimum landing sequences and schedule, resulting in minimizing airport delays and alleviating controller workload.

1.1.2.1 COMPAS

COMPAS is a computer-controlled planning system which helps air traffic controllers plan and control the inbound flow of air traffic into the terminal control area (TMA)

of an airport more efficiently. The operational objectives of COMPAS are to achieve the best possible usage of the available but limited runway landing capacity, to avoid unnecessary delays, and to apply economical approach profiles whenever possible. The operational COMPAS system was designed and tested for Frankfurt/Main ATC center environment [10].

1.1.2.2 MAESTRO

MAESTRO is a metering and spacing tool for arrival management at airports. This tool provides a proposal for arrival sequencing and indication for actions leading to the proposed sequence for assisting air traffic controllers in planning the optimum landing sequence. The system consists of four basic functions, that is, estimated time computation, sequence elaboration, user assistance provision for actions to be undertaken, and a man-machine interface. MAESTRO has been operated at Paris Orly airport since 1989 and is currently used at several airports in Europe such as Paris and Lyon in France and Copenhagen in Denmark [11].

1.1.2.3 Center-TRACON Automation System (CTAS)

NASA Ames Research Center has developed a new set of decision support tools, known as the Center-TRACON Automation System (CTAS), for efficient air traffic management within each ARTCC and TRACON in a cooperative program with the Federal Aviation Administration (FAA). This system generates air traffic advisories designed to increase fuel efficiency, reduce delays, and provide automation assistance to air traffic controllers in achieving acceptable aircraft sequencing and separation as well as improved airport capacity, without decreasing safety or increasing controller workload.

The CTAS consists of three types of integrated tools that provide computer-generated advisories for both en route and terminal-area controllers to manage and control arrival traffic efficiently [13]. The first tool, Traffic Management Advisor (TMA), provides Traffic Management Coordinators (TMCs) and en route controllers with trajectory prediction, runway assignments, landing sequences and times, traffic

flow visualization, and controller advisories [14,15]. The second tool, En route Descent Advisor (EDA), generates clearances for en route controllers handling arrival flows to metering gates by providing fuel efficient metering-conformance advisories that are integrated with conflict detection and resolution capabilities [16,17]. The third tool, Final Approach Spacing Tool (FAST), provides terminal-area controllers with landing sequences, landing runway assignments, and speed and heading advisories, to help produce an accurately spaced flow of aircraft onto the final approach course [18,19].

1.2 Future Air Transportation Systems

The demand for air traffic is expected to increase to between 2 and 3 times current values by the year 2025 [20]. Failure to address the impact of air travel congestion could cost U.S. consumers up to $20 billion a year by 2025 [21]. However, it is expected that the evolutionary improvements of the existing air traffic control system alone cannot accommodate the increase of air traffic demand in the future. In order to achieve a significant increase in capacity and throughput while improving safety and efficiency, the traditional systems and methods of air traffic control require new approaches that constitute paradigm shifts, such as the automation of separation monitoring and control, and delegation of the separation assurance function to systems on the ground and in the cockpit [22]. This realization has motivated research efforts to develop new air transportation systems for the future in both the United States (Next Generation Air Transportation System, NextGen) and Europe (Single European Sky ATM Research, SESAR) [21,23].

1.2.1 Next Generation Air Transportation System (NextGen)

In the United States, a mandate for the design and deployment of an air transportation system to meet the nation's needs in 2025 was established in the "Vision-100" legislation (Public Law #108-176) signed by President Bush in December 2003. The legislation led to the formation of the Joint Planning and Development Office (JPDO)

to carry out this mission. The main goal of NextGen is to establish a safe, efficient, reliable, and secure air transportation system that can accommodate the increased demand in 2025 [20].

NASA is also working to develop, validate, and transfer advanced concepts, technologies and procedures for supporting NextGen through partnership with the FAA and other government agencies represented in the JPDO, and in cooperation with the U.S. aeronautics industry and academia. NASA's Airspace Systems Program is responsible for developing concepts, capabilities, and technologies for high-capacity, efficient, and safe airspace and airportal systems. The program integrates two projects: NGATS ATM-Airspace Project and NGATS ATM-Airportal Project.

1.2.1.1 Airspace project

The primary focus of the Airspace project is predominantly to develop integrated solutions that will safely expand capacity in the en route airspace. The development of core capabilities includes performance-based services, trajectory-based operations, super-density operations, weather assimilated into decision making, and equivalent visual operations. The general areas of primary interest are automated separation assurance, traffic flow management, dynamic airspace configuration, and system design tools [24].

1.2.1.2 Airportal project

The Airportal project focuses on key capabilities that will increase throughput of an airport runway complex and achieve the highest possible efficiencies in the use of airportal resources such as runways, taxiways, terminal airspace, gates, and aircraft servicing equipment. The primary capabilities addressed are super-density operations, equivalent visual operations, and aircraft trajectory-based operations. Primary research areas in this project are safe and efficient surface operations, coordinated approach/departure operations management, and airportal transition and integration management [25].

1.2.2 Single European Sky ATM Research (SESAR)

The SESAR program is the European Air Traffic Management modernization program. The objectives of SESAR are to eliminate the current fragmented approach to ATM, transform the European ATM system, synchronize the plans and actions of the different partners, and federate resources. SESAR will be run in three major phases: Definition, Development, and Deployment. EUROCONTROL, which is the European organization for the safety of air navigation, will adapt its activities to realize the ATM transformation that will be recommended by SESAR. In order to take full account of the requirements of the various stakeholders, a European ATM Master Plan is being developed by a consortium that is representative of the entire ATM community, comprising of many companies and associated organizations in Europe [26].

The key goals of the future European ATM system for 2020 and beyond are to, relative to today's performance, enable a 3-fold increase in capacity which will reduce airborne and ground delays, improve safety performance by a factor of 10, reduce environmental effects by 10%, and provide ATM services at a cost to the airspace users which is at least 50% less than current costs [27].

1.3 Scope, Contributions and Organization of This Thesis

1.3.1 Terminal-area scheduling

One of the key goals for the smooth functioning of the future air transportation system is to improve the efficiency of super-density operations at the busiest airports. While efficiency in terminal-area operations is cardinal, airport runway schedules are limited by the different operational constraints that are imposed by the system, such as separation requirements for safety, air traffic controller flexibility, airline equity concerns, and the performance envelopes of aircraft.

Under these constraints, air traffic controllers need to determine the appropriate

aircraft sequences and schedules for safe and efficient operations. While scheduling runways, they have to decide what objectives will be optimized. In addition, they also need to consider uncertainties that may occur in aircraft operations.

1.3.1.1 Multiple objectives

The air traffic control system is a complex system involving many public and private stakeholders. These include commercial airlines, general aviation (GA) operators, passengers, air traffic controllers and airports. While scheduling runways, different stakeholders have different needs, and these needs may conflict each other. For example, from the perspective of air traffic control, throughput and average delay are important metrics, while from the airline perspective, operating costs, especially fuel costs, are critical. To determine optimal solutions that balance as many of the objectives of different stakeholders as possible, it is often necessary to make tradeoffs between these objectives when scheduling aircraft operations.

1.3.1.2 Uncertainty

In addition to the need to evaluate and manage tradeoffs between multiple objectives, air traffic controllers are faced with another challenge, namely, the uncertainty in the air traffic control system. In order to determine a suitable schedule for runway operations, controllers estimate meter fix and runway arrival times based on the times at which aircraft cross the Center boundary [28]. The uncertainties associated with this estimate may lead to wrong predictions of the estimated times of arrival. The sources of uncertainty include weather effects such as winds and thunderstorms, the limitations imposed by the precision of on-board equipment, as well as the uncertainty in pushback times and runway times of arrival for departing aircraft [29,30,31].

Since wrong estimates of the arrival times perturb schedules and pose a challenge to efficient operations, it is desirable to develop robust schedules that account for the uncertainty. Furthermore, the uncertainty in the system could make aircraft violate safety constraints, which may result in frequent intervention from air traffic controllers. Therefore, robustness in the presence of uncertainty is another important

objective while optimizing runway schedules. In other words, determining optimal schedules that minimize the likelihood that an air traffic controller needs to intervene is also important for improving safety and reducing the air traffic controllers' workload.

1.3.2 Contributions and organization

1.3.2.1 Contributions

This thesis focuses on aircraft sequence and schedule optimization for air traffic control in terminal-areas. Appropriate algorithms for various objectives described above are developed, and using these techniques, several tradeoffs between the different objectives are evaluated.

The key contributions of this research are as follows:

1) A dynamic programming-based scheduling algorithm for optimizing the sum of general aircraft-dependent delay costs is developed, by extending a framework previously used for determining the tradeoff between schedule robustness and throughput [32,33]. Given arbitrary delay cost functions for each aircraft in the schedule, the proposed approach can determine the schedule that minimizes the total delay cost in computation time that scales linearly in the number of aircraft and as the square of the largest difference between the latest and earliest arrival time over all aircraft.

2) This research also attempts to analyze tradeoffs between multiple objectives of different stakeholders. For example, the tradeoffs between throughput or average delay (for air traffic control) and fuel cost or direct operating cost (for airlines) are investigated with real scenarios based on Dallas Fort Worth international airport (DFW). In addition, Monte Carlo simulations are used to evaluate the tradeoffs between throughput and average delay.

3) The proposed algorithm considers both Constrained Position Shifting (CPS) and Time Advance (TA) strategies simultaneously while optimizing the schedule, and determines the optimal level of speed-up for each aircraft in order to minimize the total fuel cost.

4) The possibility of applying the proposed algorithms to the coupled operations of arrivals and departures on a single runway is studied with data from Incheon international airport (ICN) in South Korea.

5) Another runway scheduling algorithm that optimizes robustness against the uncertainty is developed. We propose and optimize a new notion of robustness, different from the one previously developed for maximizing reliability of a schedule [32].

1.3.2.2 Organization

This thesis is structured as follows. Chapter 2 introduces sequencing methods such as First-Come, First-Served (FCFS), Time Advance (TA), and Constrained Position Shifting (CPS), and surveys previous research related to aircraft sequencing and scheduling.

In Chapter 3, the problems to be addressed in this thesis are defined, and the relevant constraints and objectives are described in detail.

Chapter 4 presents an algorithmic framework to be used for both the minimum landing cost solution and the maximum robustness solution. The dynamic programming algorithm for minimizing landing cost is also proposed in this chapter.

Chapter 5 shows that the optimization algorithm developed in the previous chapter can be used for the evaluation of the tradeoff studies between various objectives such as throughput, average delay, fuel cost, and operating cost. In this chapter, the algorithm is applied to real-world scenarios at Dallas Fort Worth international airport (DFW) for analyzing the fuel cost and operating cost, and at Incheon international airport (ICN) for expanding this algorithm to arrival and departure coupled operations.

In Chapter 6, a dynamic programming algorithm for robust runway scheduling is proposed, and the related tradeoffs are analyzed.

Chapter 2

Background

The terminal-area is a dynamic and uncertain environment, with constant updates to aircraft states being obtained from surveillance systems and airline reports [34]. The dynamic nature of the terminal-area necessitates the development of scheduling algorithms that are computationally efficient, and therefore amenable to replanning when new events occur or new data updates are obtained [33].

This chapter will introduce basic runway sequencing methods used for the air traffic control system in terminal-area and describe the prior research in the area of aircraft arrival and departure scheduling.

2.1 Sequencing Methods

The "sequence" refers to the order in which aircraft are scheduled to arrive at or depart from the airport. For air traffic controllers to determine the most efficient landing order and assign optimally spaced landing times to all arrivals, several important sequencing and scheduling methods have been developed and applied to the air traffic control system. These strategies are briefly described below.

2.1.1 First-Come, First-Served (FCFS)

The most common and straightforward approach to assign the landing order of aircraft is to maintain the First-Come, First-Served (FCFS) order. In a FCFS schedule, aircraft land in order of their estimated arrival times at the runway, and air traffic controllers are merely required to add the proper delay times required for keeping the minimum separation requirements (which depend on the weight classes of consecutive aircraft).

There are two advantages to FCFS scheduling. Firstly, the FCFS schedule is relatively easy to implement and therefore promotes safety because this method does not increase controllers' workload. The other advantage is that the FCFS order maintains a sense of fairness, since aircraft simply land in the order in which they arrive at the runway. Also, the FCFS schedule minimizes the standard deviation of the delays when all aircraft are to be spaced equidistant from each other [35].

However, because the FCFS algorithm creates groups of tightly sequenced aircraft with large gaps between individual groups, the first aircraft in a group requires no delay whereas succeeding aircraft, on the average, require increasingly larger delays [35,36].

2.1.2 Time Advance (TA)

An effective method of reducing the average delay time without changing the existing FCFS order is the Time Advance (TA) method. In this approach, the first aircraft in a group is speeded up to arrive sooner than its nominal ETA, as a result of which all aircraft in the group following it can reduce their delays by the same amount of time. Since speedup requires a greater amount of fuel, the first aircraft in the sequence is speeded up only when at least the aircraft immediately following has incurred a delay, which may be decreased if the leading aircraft arrives earlier than its original estimated time of arrival. This method also reduces the intergroup gaps which occur naturally in FCFS schedules during heavy traffic [35,36].

However, there are additional costs associated with TA, since acceleration from

the nominal speed results in greater fuel consumption by the aircraft. As a result, there is a point beyond which the cost of speeding-up outweighs the benefit (in terms of delay reduction) of time advance.

2.1.3 Constrained Position Shifting (CPS)

By changing the order of the arriving aircraft, throughput of air traffic flows can be improved because the spacing requirements between adjacent two aircraft are dependent upon their weight classes, and these differences in the spacings may provide the opportunity to optimize the landing sequence. However, it is often unrealistic to allow large deviations from the nominal sequence for two reasons: (i) the system may afford controllers limited flexibility in reordering aircraft, and (ii) large deviations from a nominal or "priority" schedule may be unacceptable to airlines from a fairness standpoint.

This observation led to the Constrained Position Shifting (CPS) framework for scheduling aircraft, first proposed by Dear [37], which stipulates that an aircraft may be moved up to a specified maximum number of positions from its FCFS order. For example, if the maximum position shift allowed is 2, an aircraft that is in the 8^{th} position in the FCFS order can be located in the 6^{th}, 7^{th}, 8^{th}, 9^{th}, or 10^{th} position in the final sequence [33].

The CPS method assumes that the initial landing order is determined by the FCFS sequence and is most beneficial when all aircraft are tightly packed, that is, the inter-arrival separations are at a minimum. By rearranging the landing order, and yet not shifting any aircraft from its original position in the sequence by more than a few places, the total time between the landings of the first aircraft and the last one can often be reduced [35,36]. An additional advantage of CPS is that the restricted deviation from the FCFS order helps maintain a sense of fairness in the perception of the airlines that operate the aircraft, and also increases the predictability of landing times and positions for the pilots [1].

Although the CPS method is conceptually straightforward, its implementation in a real-time situation is more complex because of grouping and of gaps in the arrival

sequence, which arise from the randomness of the arrival times of aircraft in the terminal area [35,36].

2.2 Literature Survey

2.2.1 Review of existing scheduling algorithms

Several approaches have been previously proposed for solving the optimal aircraft sequencing and scheduling problem for runways and terminal-areas. The goal of runway scheduling is to simultaneously achieve safety, efficiency and equity, which are often competing objectives [31,38,39], and doing so in a reasonable amount of time. While there is broad consensus on what constitutes safety (wake-vortex avoidance, downstream metering constraints), efficiency (high throughput, low average delay), and equity (limited deviation from the nominal order), adequately modeling and optimally solving the runway scheduling problem in a computationally tractable manner has remained a challenge. One reason for this computational hurdle is that most runway scheduling models are, from a theoretical perspective, inherently hard to solve [40]. As a result, most solution approaches rely on heuristic or approximate approaches to produce "good" solutions in reasonable computation times [38,41,42].

Dear [37] first proposed the CPS method, in which deviations from FCFS are limited, and solved the aircraft sequencing problem by enumerating all possible sequences to find an optimal sequence. This approach was not practical for large numbers of aircraft. Dear and Sherif [43] presented a heuristic algorithm for single runway scheduling, in which they considered separation requirements and the maximum position shift (MPS) parameter, enforcing the constraint that an aircraft cannot be shifted by more than this parameter from the FCFS order.

Neuman and Erzberger evaluated a variety of scheduling algorithms including modified FCFS, heuristic TA, fuel saving TA, optimal CPS with one position shift, and heuristic CPS and statistically analyzed these algorithms with various scenarios [35, 36]. While investigating them, they considered arrival time-windows and did not

allow overtaking along jet routes.

Some researchers have modeled the aircraft sequencing problem as a job shop scheduling problem. From this point of view, runways and aircraft represent machines and jobs, respectively. However, due to separation requirements between aircraft, the processing time of a job on a machine depends on the following job on the same machine. Therefore, the aircraft sequencing problem is a special case of the job shop scheduling problem with the sequence-dependent processing times and time-windows, as Beasley et al. [40] pointed out.

Psaraftis [44] incorporated CPS within a dynamic programming recursion for solving the aircraft arrival sequencing problem at a single runway as a special application of the job shop scheduling problem. Although he could solve the problem in polynomial time, he did not take into account the constraint that the landing time of each aircraft must be restricted to fall within a specific range, as known as its arrival time-window. Venkatakrishnan et al. [45] modified Psaraftis' formulation in a heuristic manner to consider earliest and latest times when they investigated the separation times observed between landings at Logan airport in Boston. Trivizas [46] proposed a dynamic programming approach to compute the optimal CPS landing sequence, but precedence relations between aircraft were not considered. However, precedence constraints are important because (i) overtaking on the same jet route is not allowed in many cases in current air traffic control systems, and (ii) airlines may have preferences in precedence relations due to their banking strategies [1].

There have also been several attempts to apply techniques such as integer programming to the problem. Bianco et al. [47,48] adopted a job shop scheduling view for the aircraft sequencing problem and solved the single runway landing problem using a mixed integer linear program. They provided a tree search procedure based on Lagrangian lower bounds and developed a heuristic approach for the problem. Abela et al. [49] presented a mixed-integer 0-1 formulation of the single-runway aircraft landing problem together with a heuristic based on a genetic algorithm. Beasley et al. [40] extended this mixed-integer linear program to the case of both single and multiple runways. With the integer programming method, they could reflect con-

straints such as time-windows, precedence relations, and limits on the maximum number of position shifts, but the solution times were often too long to utilize the method as a real-time decision support tool (DST). Ernst et al. [50] developed a fast simplex-based lower-bounding method for the aircraft scheduling problem and used it for solving single and multiple runway problems with a heuristic, as well as with an exact branch-and-bound method.

Bayen et al. [51] formulated the aircraft sequencing problem as a single machine scheduling problem and presented approximation algorithms to alternatively minimize the sum of delays and the landing time of the last aircraft in the sequence (the makespan). The approximation algorithm was slower than a heuristic algorithm, but provided guarantees on suboptimality and performed more robustly for a range of sequences than a greedy heuristic algorithm [52]. In this approach, they assumed that the spacing between landings is the same between any two aircraft, regardless of their weight classes. However, in practice, this assumption could lead to inefficient and conservative results because it would be necessary to choose the largest among all possible spacings as the required minimum separation for all aircraft pairs, for safety.

Recently, Balakrishnan and Chandran posed the runway scheduling problem as a modified shortest path problem on a network and solved it with a dynamic programming algorithm. They showed that the approach could handle all the operational constraints that may arise in practice and its computation time was sufficiently small to enable real-time implementation [1,32,33]. In this thesis, we extend this approach to the problem of runway scheduling with a variety of objectives, and evaluate the tradeoffs involved.

2.2.2 Tradeoff studies between multiple objectives

In prior research, runway scheduling algorithms have been designed to optimize several objectives representing the interests of multiple stakeholders. Neumann and Erzberger [35] developed heuristics that optimized average delay and fuel costs per aircraft when evaluating various techniques for sequencing and spacing arrivals. Balakrishnan and Chandran [1] investigated the problem of maximizing runway through-

put under CPS. Milan [53] considered a model of assigning priorities for landings at a congested airport. Carr et al. [54] also introduced the concept of airline priority scheduling for air traffic control automation and performed fast-time simulations for statistical evaluation. However, the sequencing algorithm illustrated that there are some deviations between preferred sequences and the resulting sequences due to the presence of separation requirements. A heuristic approach for minimizing the passenger-weighted sum of arrival times (with no time advance, arrival time-windows or precedence constraints) was also proposed [45].

However, to the best of our knowledge, there have been no comprehensive studies in recent years on the tradeoffs between multiple objectives associated with terminal-area schedules. The objective of this thesis will be the investigation of tradeoffs between schedules optimized for various objectives.

2.2.3 Robust runway scheduling

Most algorithms reviewed above were developed for deterministic environments. However, the presence of uncertainty due to factors such as weather and the limited accuracy of aircraft equipment perturbs schedules, with the aircraft no longer landing at the intended landing times [32]. This implies that distributions representing the probabilities that aircraft can use the runway at a particular time need to be introduced, addition to just time-windows for the times at which an aircraft can utilize the runway. In other words, runway scheduling is a fundamentally stochastic problem which requires robust solutions, and requires coordination between decision support tools and human controllers [31].

Using stochastic terminal-area scheduling simulations for FCFS sequencing with multiple arrival runways, Meyn and Erzberger showed that improved arrival time accuracies could increase airport efficiency and reduce potential separation violations [30]. In the simulations, a separation buffer was added to all the runway separation minima for reducing the the likelihood that separation requirements will be violated when flights miss their scheduled runway arrival time. This form of buffering would be useful if all aircraft separations were likely to be perturbed by some fixed

fraction.

However, Chandran and Balakrishnan showed that buffering all aircraft could be suboptimal in practice, since all aircraft may not be equally equipped. They also noted that a tradeoff between robustness (the probability of controller's intervention) and efficiency (runway throughput) was involved while scheduling runways under uncertainty [32]. Since the dynamic programming-based technique proposed by them is computationally efficient and accommodates various operational constraints imposed by the terminal-area, we extend their approach to another possible notion of schedule robustness.

Chapter 3

Runway Scheduling: Problem Definition

Runway schedules are subject to several operational constraints, which need to be satisfied by any approaches that can be implemented in practice. These constraints include the limited flexibility afforded to air traffic controllers, available arrival time windows, minimum separation requirements, and precedence conditions between aircraft pairs. While ensuring that these constraints are met, the problem of optimizing runway schedules can be defined in various ways depending on the objective function to be optimized.

This thesis deals primarily with the scheduling of arrivals at a single runway, but the techniques described can also be extended for departure runway scheduling. We briefly demonstrate this in Section 5.3, when we consider the problem of simultaneously scheduling arrival and departure operations at Incheon International Airport in South Korea.

3.1 Constraints

We begin with a description of the sources of the different operational constraints that need to be satisfied by runway schedules.

Category	Definition	Examples
Heavy	Aircraft capable of takeoff weights of more than 255,000 pounds whether or not they are operating at this weight during a particular phase of flight	A380, B747, A300
Large	Aircraft of more than 41,000 pounds, maximum certificated takeoff weight, up to 255,000 pounds	B737, DC9
Small	Aircraft of 41,000 pounds or less maximum certificated takeoff weight	Beach 99

Table 3.1: Weight classes of aircraft

	Trailing Aircraft		
Leading Aircraft	Heavy	Large + B757	Small
Heavy	4	5	5/6
B757	4	4	5
Large	2.5 (or 3)	2.5 (or 3)	3/4
Small	2.5 (or 3)	2.5 (or 3)	2.5 (or 3)

Table 3.2: Minimum separation (in miles) between landings

3.1.1 Separation requirements

The Federal Aviation Administration (FAA) regulates the minimum spacing between landing aircraft to avoid the danger of wake turbulence. The FAA classifies aircraft into three weight classes (heavy, large, and small) based on the maximum take-off weight [55]. These weight classes and representative examples of each class are shown in Table 3.1.1.

The FAA defines minimum separation distance requirements depending on the weight classes of both the leading aircraft and the trailing aircraft during instrument flight rules (IFR) approaches (Table 3.2).

These separation requirements in miles can be transformed to the minimum time separation required between landings, assuming a 5 nmi final approach path and a nominal approach speed [5]. The matrix of minimum separation times (in seconds) for different weight classes of leading and trailing aircraft is shown in Table 3.3.

Leading Aircraft	Trailing Aircraft		
	Heavy	Large	Small
Heavy	96	157	196
Large	60	69	131
Small	60	69	82

Table 3.3: Minimum separation (in seconds) between landings

3.1.2 Limited deviation from FCFS

The terminal area is very dynamic environment, and resequencing aircraft increases the workload of air traffic controllers. Due to limited flexibility, it might not be possible for controllers to implement an efficient sequence that deviates significantly from the nominal or First-Come, First-Served (FCFS) order. This is the basic motivation for Constrained Position Shifting (CPS) methods. CPS, first proposed by Dear [37], stipulates that an aircraft may be moved up to a specified maximum number of positions from its FCFS order. The maximum number of position shifts allowed is denoted by k ($k \leq 3$ for most runway systems), and the resulting environment is referred to as a k-CPS scenario. We also refer to the sequences that satisfy the condition that the maximum number of position shifts incurred by any aircraft with respect to the FCFS order as k-CPS sequences.

According to Neuman and Erzberger [35], the FCFS sequence shows the minimum value of the standard deviation of delays among the possible sequences having the same average delay. In other words, the sequence that deviates overly from the FCFS sequence could lead to some benefit as a whole, but several aircraft postponed from their original positions in the nominal sequence experience disadvantage in their arrival times. This unfairness is another reason why the maximum deviation from the FCFS sequence should be limited. The restricted deviation from the FCFS order helps maintain equity among aircraft operators, and also increases the predictability of landing times [1].

3.1.3 Arrival time windows

Once an arriving aircraft is at the boundary of the Center (about 45-60 min from the destination airport), tools such as the Trajectory Synthesizer (a decision-support system developed by NASA that predicts a complete time-based trajectory along the expected path [56]) may be used to determine the estimated time of arrival (ETA) at which the aircraft will land on an assigned runway, assuming it follows a nominal route and speed profile [35].

If the aircraft is speeded up, the actual time of arrival will be earlier than the estimated time of arrival. The earliest time of arrival is usually limited to one minute before the ETA because of the resultant fuel expenditure. In Section 5.2.3, we investigate the possibility of allowing greater amounts of speed-up (Time advance), and the resultant fuel cost tradeoffs. The latest arrival time is determined either by fuel limitations or by the maximum delay that an aircraft can incur. The earliest and latest arrival times of aircraft i are denoted by $E(i)$ and $L(i)$, respectively. In general, it is also possible that the allowable time-windows are given by discontinuous time intervals [51]. The methods presented in this thesis can be easily extended to such scenarios.

3.1.4 Precedence constraints

There could also be precedence constraints imposed on the landing sequence. These are constraints of the form "aircraft i must land before aircraft j," and arise due to overtaking constraints, airline preferences from banking operations or high priority flights. Precedence relations are represented by a matrix $\{p_{ij}\}$ such that element $p_{ij} = 1$ if aircraft i must land before aircraft j, and $p_{ij} = 0$ otherwise.

3.2 Objective Functions

There are several possible objective functions that may have to be optimized while determining arrival runway schedules. An important objective is maximizing run-

way throughput (or alternatively, minimizing the completion time of a sequence of aircraft), which was considered in [1] with a dynamic programming based solution approach. Minimizing the average delay or minimizing a weighted sum of delays, where the weights represent the relative priorities of flights (based on factors such as crew schedules, passenger and fleet connectivity, turnaround times, gate availability, on-time performance, fuel status and runway assignments), are also desirable objectives [54]. There are inherent tradeoffs involved between these objectives, and the schedules that maximize throughput are not necessarily the same as those that minimize the average or the weighted sum of delays. For instance, when the cost per unit delay differs considerably between aircraft, the schedule with the minimum total landing cost may differ significantly from the schedule with the maximum throughput.

3.2.1 Delay costs, fuel costs, and operating costs

To encompass all the objective functions described above, a general landing cost function is introduced. Given a landing cost function, $c_i(t_i)$, which corresponds to the cost of landing aircraft i at time t_i, the objective function is to minimize the sum of the landing costs of all aircraft in the schedule. Examples of the landing cost include the fuel cost (in dollars), the total fuel burn, and the direct operating costs of the schedule. For instance, if the objective is to minimize the weighted sum of delays, where w_i is the weighting factor of aircraft i, then $c_i(t_i) = w_i t_i$. When all the weights are equal, minimizing the weighted sum is analogous to minimizing the total delay, or equivalently, the average delay of the schedule.

3.2.2 Schedule robustness

Another possible objective function may be one designed for robust runway scheduling. The robustness of a schedule for runway operations in the uncertain environment of the terminal-area can be defined in several ways. From a standpoint of airlines, the robustness of a schedule or the reliability of a schedule may be measured in terms of how many passengers from a bank of arriving flights can be successfully connected

to departing flights at major hub airports in the event of weather disruptions. From the perspective of safety and controller workload, the robustness of a schedule may be gauged by the probability that no pair of aircraft violates the separation requirements. Because of various elements of uncertainty around the airport, there is almost always a difference between the estimated time of arrival (or departure) predicted by a controller and the actual time that the aircraft uses the runway. If this difference causes the violation of the separation constraints between two consecutive aircraft, i.e. if the leading aircraft lands much later than the estimated time of arrival and/or the following aircraft arrives at the runway earlier than it was expected, the air traffic controller would have to intervene to enforce spacing between the two aircraft. This intervention in turn may affect the separations between the other aircraft in a given sequence, requiring readjustment of the whole runway schedule.

Taking these conditions into account, Chandran and Balakrishnan developed a dynamic programming based runway scheduling algorithm to maximize the reliability of the initially fixed landing schedule [32]. They defined *reliability* as the probability that every pair of adjacent aircraft in a given sequence will not violate the separation requirements. The tradeoffs between reliability and throughput were also computed.

However, the objective function proposed in this optimization algorithm could potentially result in scenarios in which one pair of aircraft in a given sequence incurred greater risk of violating separation requirements in order to increase the reliability of the sequence as a whole. For example, when there are four equally distributed aircraft in a landing sequence, if the second aircraft's landing time is shifted to land later than the initial schedule and the third aircraft is moved to the earlier time, the probability of not violating the separation constraints between these aircraft will decrease, but the probabilities of violating the spacing requirements between the first and second aircraft and between the third and fourth aircraft will increase. As a result, while the reliability of the sequence as a whole may increase, the spacing requirement between the second and third aircraft is more likely to be violated. Therefore, it is important to also try to minimize the probability of violating separation requirements between individual pairs of aircraft, instead of just the reliability of the sequence.

Finding the weakest point among all inter-aircraft spacings in a landing sequence and rescheduling the landing times to minimize the probability of violating the spacing constraint at this point may be good approach to improving the robustness. In this thesis, a robust runway schedule is defined as one that minimizes the maximum value among the probabilities that the separation requirements between two successive aircraft in a given sequence will be violated. This maximum probability will be referred to as the *weakness* of the schedule in this thesis.

Let $t_i \nleftrightarrow t_j$ represent the event that the minimum spacing between two aircraft i and j (denoted δ_{ij}) will be violated, given that a leading aircraft i is scheduled to land at t_i and the trailing aircraft j is scheduled to arrive at t_j. If the scheduled arrival times are denoted $s(\cdot)$ and the actual landing times are denoted $a(\cdot)$, then

$t_i \nleftrightarrow t_j \Rightarrow \{a(j) < a(i) + \delta_{ij} \mid s(i) = t_i \wedge s(j) = t_j\}$.

Given a sequence of aircraft $\{1, 2, \cdots, n\}$ for which the corresponding scheduled times of arrival are $\{t_1, t_2, \cdots, t_n\}$, the weakness of the schedule, denoted by $W(t_1, t_2, \cdots, t_n)$, is the maximum value among the probabilities that the minimum spacing requirement between two adjacent aircraft is violated.

$W(t_1, t_2, \cdots, t_n) = \max\{\Pr\{t_1 \nleftrightarrow t_2\}, \Pr\{t_2 \nleftrightarrow t_3\}, \cdots, \Pr\{t_{n-1} \nleftrightarrow t_n\}\}$

With this definition, a dynamic programming algorithm to minimize the weakness of a sequence of aircraft will be developed in this thesis.

3.3 Problem Statement

This thesis primarily considers two problems: total landing cost optimization and robustness optimization. Given a sequence of n aircraft, without loss of generality, aircraft can be labeled (1, 2, ... , n) according to their position in the FCFS sequence. These problems are stated below:

3.3.1 Minimizing total landing cost

Integrating the constraints and the objectives related to delay costs, the problem of scheduling arrivals on a runway can be posed as follows:

Given n aircraft, earliest and latest arrival times $E(i)$ and $L(i)$ for the i^{th} aircraft, separation matrix S, precedence matrix $\{p_{ij}\}$, costs $c_i(t_i)$ for aircraft i landing at time t_i, and the maximum number of position shifts k, we would like to compute the optimal k-CPS sequence and corresponding landing times (t_i) to minimize the total landing cost, that is, the sum of the individual landing costs.

3.3.2 Maximizing robustness

Similarly, the problem of robust runway scheduling can be described as follows:
Given n aircraft, earliest and latest arrival times $E(i)$ and $L(i)$ for the i^{th} aircraft, separation matrix S, precedence matrix $\{p_{ij}\}$, the probability $\Pr\{t_i \nrightarrow t_j\}$ that the separation requirements between two successive aircraft i and j (with i scheduled to land at time t_i and j scheduled at time t_j) will be violated, and the maximum number of position shifts k, we would like to compute the optimal k-CPS sequence and corresponding landing times (t_i) to minimize the weakness $W(t_1, t_2, \cdots, t_n)$, that is, the maximum value among probabilities of violating the separation requirements between two successive aircraft in the sequence.

Chapter 4

CPS Framework for Runway Scheduling

In this chapter, we describe an algorithmic framework to solve runway scheduling problems under Constrained Position Shifting (CPS). We begin with a description of prior work, where it had been shown that every feasible k-CPS sequence can be represented as a path in a directed graph whose size is polynomially bounded in n and k [1]. This enables us to solve the problem of minimizing landing costs using dynamic programming, as is demonstrated in this chapter.

4.1 The CPS network [1]

The CPS network consists of n stages, in addition to a source and a sink. Each stage corresponds to an aircraft position in the final sequence. A node in stage p of the network corresponds to a subsequence of aircraft of length $\min\{2k+1, p\}$, where k is the maximum position shift. For example, $n = 5$ and $k = 1$, the nodes in stages $3, \cdots, 5$ represent all possible subsequences of length $2k+1 = 3$ ending at that stage, while the stage 1 contains a node for every possible sequence of length 1 ending (and starting) at position 1 and the stage 2 contains a node for every possible sequence of length 2 ending at position 2. The network is generated using all possible aircraft assignments to each position in the sequence (Table 4.1).

n=5, k=1	Stage 1	Stage 2	Stage 3	Stage 4	Stage 5
Possible	1	1	2	3	4
last	2	2	3	4	5
aircraft		3	4	5	

Table 4.1: Possible aircraft assignments for n=5, k=1.

For convenience, we refer to the last aircraft in a node's sequence as the *final aircraft* of that node. For each node in stage p, we draw directed arcs to all the nodes in stage $p + 1$ that can follow it. Figure 4-1 shows the network for $n = 5$ and $k = 1$. For example, the node (2–1–3) in stage 3 is a successor of node (2–1) in the previous stage (stage 2) and can precede the nodes (1–3–4) or (1–3–5) in the next stage (stage 4). The path (2)→(2–1)→(2–1–3)→(1–3–4)→(3–4–5) represents the sequence (2–1–3–4–5).

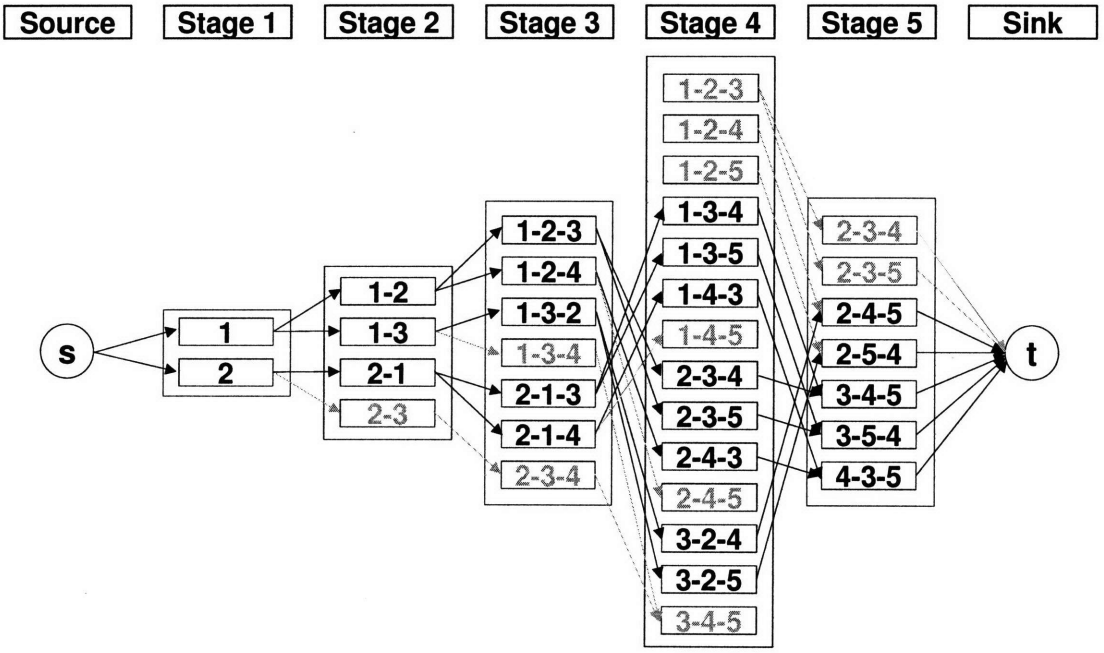

Figure 4-1: Network for $n = 5$, $k = 1$.

Some nodes that violate precedence constraints or are not part of a path from source to sink are removed from the network. These nodes are shown in gray in Figure 4-1. By this process, we can produce a "pruned" network, which is significantly smaller than the original network. Precedence constraints further reduce the size of

the network.

In prior work [1], the following properties of this network were proved:

(i) Every possible k-CPS subsequence of length $2k + 1$ or less is contained in some node of the network.

(ii) Every feasible sequence (one that satisfies maximum position shift constraints and precedence constraints) can be represented by a path in the network from a node in stage 1 to a node in stage n.

(iii) Every path in the network from a node in stage 1 to a node in stage n represents a feasible k-CPS sequence.

4.2 Dynamic Programming Algorithm for Minimizing Total Landing Cost

4.2.1 Bounding the makespan

Given a set of arriving aircraft, the *makespan* is defined as the arrival time of the last aircraft, or in other words, the completion time of the landing sequence. For a fixed set of aircraft (the static case), minimizing the makespan is equivalent to maximizing the throughput of the schedule, and is desirable from the perspective of system performance. As mentioned earlier, since the schedule with the minimum total landing cost could be different from the schedule with the maximum throughput, a determination of the tradeoffs between throughput and landing costs is needed. A possible approach to determining these tradeoffs, and one adopted in this thesis, is to determine the minimum landing cost schedule that can be achieved for every feasible value of the throughput. As a first step, given a FCFS schedule, we first determine a range of feasible values of the throughput. A trivial lower bound on the makespan is the minimum value among the earliest arrival times of all aircraft that could land last in the sequence. Similarly, the maximum value among the latest arrival times of all aircraft that could land last in the sequence would provide an upper bound on the makespan.

4.2.2 Minimizing the total landing cost

For each feasible value of the makespan, we consider all possible k-CPS sequences, and determine the optimal schedule that has the minimum total landing cost. This is performed using a dynamic programming recursion for minimizing the total landing cost. We first define the following variables:

$\ell(x)$: The last aircraft of node x

$\ell'(x)$: The second from last aircraft of node x

$P(x)$: Set of nodes that are predecessors of x

$\mathcal{I}(j)$: Set of times during which aircraft j could land

$c_j(t)$: Cost of landing aircraft j at time t

t_j: Scheduled time of arrival (STA) of aircraft j

Let $W_x(t_j)$ be the minimum value of the sum of landing costs that is accumulated until $l(x)$ lands at time t_j. The objective is to minimize the total landing cost, that is, the sum of landing costs of all aircraft.

$$\text{Total landing cost} = \sum_{i=1}^{n} c_i(t_i)$$

For an arc (x, y) in the CPS network, the sum of landing costs from the first aircraft of the sequence to the last aircraft i of node x, $W_x(t_i)$, is used to calculate the sum of landing costs from the first aircraft to the last aircraft j of node y, $W_y(t_j)$ using the following dynamic programming recursion:

$$W_y(t_{\ell(y)}) = \min_{x \in P(y)} \left\{ W_x(t_{\ell(x)}) \right\} + c_{\ell(y)}(t_{\ell(y)}),\ \forall\ t_{\ell(y)} \in \mathcal{I}(\ell(y)) : t_{\ell(y)} - t_{\ell(x)} \geq \delta_{\ell(x),\ell(y)}$$

The proof of correctness of this recursion follows standard techniques for proving the validity of dynamic programming recursions, and is presented below for completeness.

Proof: We first observe that, by construction, $\ell(x) = \ell'(y)$ for $x \in P(y)$. Therefore, $W_y(t_{\ell'(y)}) = W_y(t_{\ell(x)})$.

Since $W_y(t_{\ell(y)})$ is the minimum value of total landing cost over all paths leading to node y,

$$W_y(t_{\ell(y)}) \leq W_x(t_{\ell(x)}) + c_{\ell(y)}(t_{\ell(y)}),$$
$$\forall\, x \in P(y), t_{\ell(x)} \in \mathcal{I}(\ell(x)), t_{\ell(y)} \in \mathcal{I}(\ell(y)), \text{ where } t_{\ell(y)} - t_{\ell(x)} \geq \delta_{\ell(x),\ell(y)}.$$

This means that, in particular,

$$W_y(t_{\ell(y)}) \leq \min_{x \in P(y)} \left\{W_x(t_{\ell(x)})\right\} + c_{\ell(y)}(t_{\ell(y)}),$$
$$\forall\, x \in P(y), t_{\ell(x)} \in \mathcal{I}(\ell(x)), t_{\ell(y)} \in \mathcal{I}(\ell(y)), \text{ where } t_{\ell(y)} - t_{\ell(x)} \geq \delta_{\ell(x),\ell(y)}.$$

To complete the proof, we only need to show that the above relationship can never hold as a strict inequality. For contradiction, suppose that

$$W_y(t_{\ell(y)}) < W_x(t_{\ell(x)}) + c_{\ell(y)}(t_{\ell(y)}),\ \forall\, x \in P(y), t_{\ell(x)} \in \mathcal{I}(\ell(x)), t_{\ell(y)} \in \mathcal{I}(\ell(y)).$$

This is equivalent to

$$W_y(t_{\ell(y)}) - c_{\ell(y)}(t_{\ell(y)}) < W_x(t_{\ell(x)}),\ \forall\, x \in P(y), t_{\ell(x)} \in \mathcal{I}(\ell(x)),\ \text{and } t_{\ell(y)} \in \mathcal{I}(\ell(y))$$
$$\Longrightarrow W_y(t_{\ell(y)}) - c_{\ell(y)}(t_{\ell(y)}) < \min_{\substack{z \in P(y) \\ t_{\ell(z)} \in \mathcal{I}(\ell(z))}} \left\{W_z(t_{\ell(z)})\right\}\ \forall\, t_{\ell(y)} \in \mathcal{I}(\ell(y)).$$

However, $W_y(t_{\ell(y)}) - c_{\ell(y)}(t_{\ell(y)})$ is the total landing cost of the subsequence of $W_z(t_{\ell(z)})$ that ends at node z and time $t_{\ell(z)}$. This contradicts the minimality of $W_x(t_{\ell(x)})$ for $x = z$. ∎

For a node y in the first stage, since there are no previous landing costs, the landing cost is given by $W_y(t_i) = c_i(t_i)$, where i is the last aircraft of the node. For example, i can be 1, 2, or 3, when the maximum number of position shifts allowed, $k = 2$.

Since the state space for $W(\cdot)$ is infinite, the recursion is not computationally practical. In order to implement the algorithm, we discretize time into periods of length ϵ. Since radar update rates are once every 10-12 seconds [13], it would be reasonable to set ϵ to a value between 1 and 10 seconds. The pseudocode for the algorithm is presented in Figure 4-2.

The dynamic programming recursion presented above determines the landing cost

```
procedure MinLandingCost:
    begin
        Set W(·) for all nodes in the network to ∞;
        for each node y in stage 1 do
            for each t_{ℓ(y)} ∈ I(ℓ(y)) do
                W_y(t_{ℓ(y)}) ← c_{ℓ(y)}(t_{ℓ(y)});
        for each stage p = 2, ··· , n − 1 do
            for each node x in stage p do
                for each t_{ℓ(x)} ∈ I(ℓ(x)) do
                    for each arc (x, y) do
                        for each t_{ℓ(y)} ∈ I(ℓ(y)) : t_{ℓ(y)} − t_{ℓ(x)} ≥ δ_{ℓ(x),ℓ(y)} do
                            W_y(t_{ℓ(y)}) = min {W_y(t_{ℓ(y)}), W_x(t_{ℓ(x)}) + c_{ℓ(y)}(t_{ℓ(y)})};
    end
```

Figure 4-2: Algorithm for computing the minimum landing cost.

W for all nodes in stage n for all feasible time periods. The minimum cost schedule for a given makespan t is the minimum over all x in stage n of $W_x(t_{\ell(x)})$, such that $t_{\ell(x)} = t$. Comparing $W_x(t_{\ell(x)})$ for all nodes x in stage n, we can also determine the sequence and arrival times of aircraft that minimizes the total landing cost of the schedule.

4.2.3 Complexity

It was shown in [1] that the number of nodes in the CPS network is $O(n(2k+1)^{(2k+1)})$ and the number of arcs is $O(n(2k+1)^{(2k+2)})$. In the present case, we have to assign the arrival times of aircraft (and therefore the weight) associated with each arc (x, y) in the given time-window. We need to consider all possible landing times for the last aircraft in node x and the last aircraft of the current node y. When we assume that the length of the largest interval of feasible arrival times among all aircraft is L and the accuracy is ϵ, there are at most (L/ϵ) time-periods in a given arrival time-window. The computational work done per arc in the CPS network is therefore $O((L/\epsilon)^2)$.

Lemma 1 : The complexity of the proposed dynamic programming algorithm is $O(n(2k+1)^{(2k+2)}(L/\epsilon)^2)$, where n is the number of aircraft, k is the maximum allowed number of position shifts, L is the largest difference between the latest and earliest arrival times over all aircraft, and ϵ is the desired resolution.

The proposed method is computationally tractable and amenable to real time implementation because the complexity scales linearly with the number of aircraft and as the square of the largest difference between the latest and earliest arrival times over all aircraft. While the computational complexity is exponential in k, we note that k is small (typically less than or equal to three).

Chapter 5

Minimizing Delay Costs

In this chapter, we use the algorithm proposed in Chapter 4 to optimize the total delay costs incurred by aircraft, and also evaluate the tradeoffs between delay costs and schedule throughput.

5.1 Evaluating Tradeoffs between Objectives

Typically, there are three methods to simulate the aircraft landing situation and evaluate its effectiveness and impact on the sequencing and scheduling: fast-time simulation, real-time simulation, field test and evaluation [54]. In this thesis, fast-time simulation is performed through the generation of randomized instances for the statistical evaluation of CPS sequencing and scheduling algorithms having different objectives.

5.1.1 Minimizing average delay

In Chapter 4, we presented an algorithm for minimizing the sum of landing costs (or equivalently, the sum of delay costs), given the cost of landing each aircraft at a particular time. The problem of minimizing the sum of arrival times of all aircraft can be solved by setting the cost of landing an aircraft at a particular time to be equal to that time (that is, $c_i(t_i) = t_i$). Since the average delay of a given group of

aircraft is equal to the sum of the individual delays (differences between the actual and estimated arrival times) divided by the number of aircraft, we can write:

$$\text{Average delay} = \frac{1}{n}(\sum_{i=1}^{n} t_i - \sum_{i=1}^{n} ETA_i).$$

The sum of estimated arrival times is a constant, therefore the problem of minimizing the sum of arrival times is equivalent to that of minimizing the average delay.

We consider a random instance of scheduling a sequence of 30 aircraft on a single runway. The mix of aircraft types is assumed as 40% Heavy, 40% Large, and 20% Small. A discussion of the dependencies of the results on the arrival rates and the fleet mix is beyond the scope of this thesis, and can be found in [1]. We choose parameters that maintain pressure on the arrival runway (about an aircraft a minute), and a reasonably heterogeneous mix of aircraft. Precedence constraints are imposed by not allowing overtaking between aircraft arriving on the same flight jet route, which is assigned to be one of four possible routes. The earliest arrival time is equal to the ETA ($E(i) = ETA_i$) and the maximum allowed delay is 60 min. Table 5.1 shows the *makespan* (the arrival time of the last aircraft in the group) and the *average delay* for the FCFS and CPS sequences. The throughput of the schedule is given by the number of aircraft in the sequence divided by the makespan of the schedule. When the objective is to minimize average delay (columns 2 and 3 in Table 5.1), we note that as the maximum number of position shifts k increases, the average delay decreases. We also compare the schedule that minimizes the average delay with the one that minimizes the makespan (using the CPS framework [1]). For each value of k, for the minimum value of the makespan, we determine the minimum achievable value of the average delay (shown in Table 5.1). We note that the decrease in makespan (increase in throughput) is achieved at the cost of an increase in the average delay. While it is true that minimizing the makespan frequently results in an improvement in the average delay [1], this is not necessarily the case. Similarly, minimizing the average delay may result in an increase in makespan (or equivalently, a decrease in

Procedure	Min. average delay		Min. makespan	
	Makespan	Average delay	Makespan	Average delay
FCFS	3296	134.27	3296	134.27
1-CPS	3247	101.03	3247	101.03
2-CPS	3247	94.13	3242	103.90
3-CPS	3247	92.30	3232	121.00

Table 5.1: Comparison of the makespan and average delay of various scheduling procedures for two objectives: 1) minimizing average delay and 2) minimizing the makespan

throughput).

The minimum average delay and minimum makespan schedules for $k = 2$ are shown in Figure 5-1 in a form popularized in [36], known as the "comb diagram". In Figure 5-1, the horizontal lines on the top represent time-lines for each jet route. The dots on each horizontal time-line show when an aircraft is crossing the Center boundary on a given jet route. The time-scales for ETAs and STAs (FCFS and 2-CPS in this instance) have been shifted by a constant amount to make the figure more compact, with the assumption that all aircraft take the same amount of time to travel from the Center boundary to the runway. This can be easily extended to the case where the different travel times are known from the Trajectory Synthesizer [1,56]. The time-scale given above the comb diagram is for the time-lines of ETAs and STAs. A straight line from a given jet route is connected to the ETA. This time represents the time the aircraft would arrive at the runway, if there was no interference from any other aircraft or from unknown navigation errors and environmental conditions. The sequence of all ETAs determines the FCFS order to be preserved for fair scheduling. The horizontal component of the line between ETA and FCFS in the diagram represents the sequenced delay to meet spacing requirements. If the line connecting the ETA of an aircraft to the FCFS schedule is vertical, no delay is required for that particular aircraft; the greater the deviation of the line from the vertical, the more the assigned delay. The crossing of lines connecting the FCFS and 2-CPS schedules denotes the resequencing or exchange of aircraft positions. The vertical line beneath each aircraft on the 2-CPS schedule indicates the weight class of the aircraft: a long

line denotes Heavy, a medium line denotes Large, and a short line denotes Small [35]. The makespan of the sequence and the average delay per aircraft in seconds are shown at the bottom of the diagram for each objective function. The two comb diagrams in Figure 5-1 illustrate that the position swaps and arrival times in the optimal schedule depend on the objective function, and can yield different values of makespan and average delays.

5.1.2 Analysis of tradeoffs between delay and throughput

We further investigate the tradeoff between average delay and throughput that was demonstrated in the previous section using Monte Carlo simulations. We generate 1,000 instances of 30-aircraft sequences, with the aircraft types and jet routes assigned randomly using appropriate probability distributions. Precedence constraints are imposed among aircraft using the same jet route, and time-windows are assigned with the ETA as the earliest arrival time and a maximum delay of 60 min. For each of these generated instances, we optimize the schedule for two different objectives: minimizing the average delay and minimizing the makespan (or maximizing the throughput).

The comparison between the two solutions is shown in Figure 5-2 (left). The horizontal axis corresponds to the maximum throughput solution and shows its normalized improvement in throughput, $\frac{(CPS\ throughput)-(FCFS\ throughput)}{(FCFS\ throughput)}$. The vertical axis corresponds to the minimum average delay solution and shows its normalized decrease in average delay, which is calculated as $\frac{(FCFS\ avg.\ delay)-(CPS\ avg.\ delay)}{(FCFS\ avg.\ delay)}$.

We note that about 45% of the instances in Figure 5-2 (left) lie on the vertical axis. This means that in 45% of the instances, there is little or no benefit (over the FCFS schedule) in minimizing the throughput of the sequence, although there are instances in which a 14% improvement in throughput can be achieved through resequencing the arrival sequence. In contrast, as the histogram in Figure 5-2 (right) shows, larger improvements in average delay (as high as 50%) can be achieved through resequencing, while the throughput improvements are typically smaller.

Figure 5-3 (left) shows the makespan values of both the minimum makespan schedule and the minimum average delay schedule. We note that the makespan of the

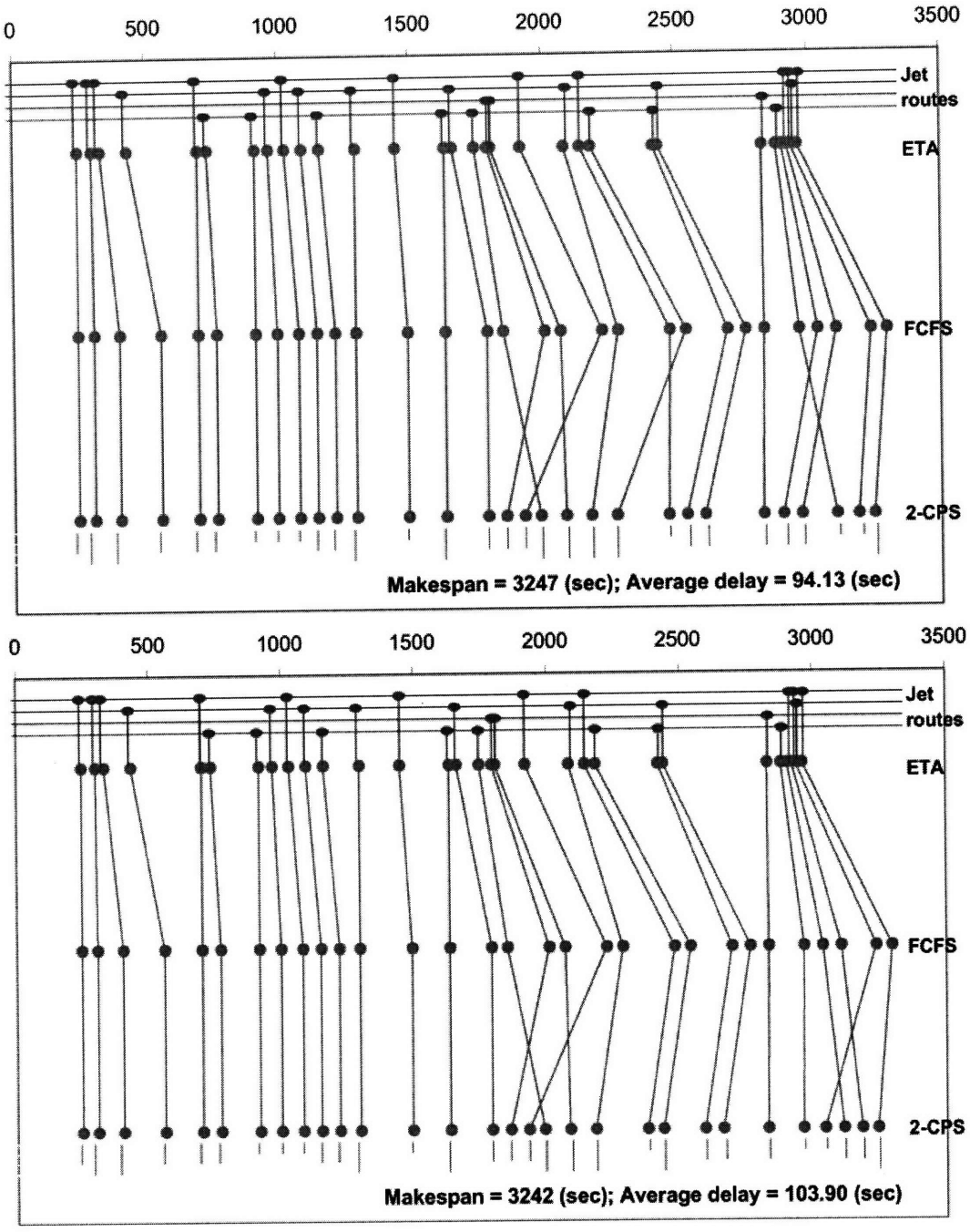

Figure 5-1: Simulated arrival traffic for (top) minimum average delay and (bottom) minimum makespan, with 2-CPS. The horizontal axes denote the time line. The ETAs correspond to the estimated time of arrival at the airport if the aircraft flies at its nominal speed and route.

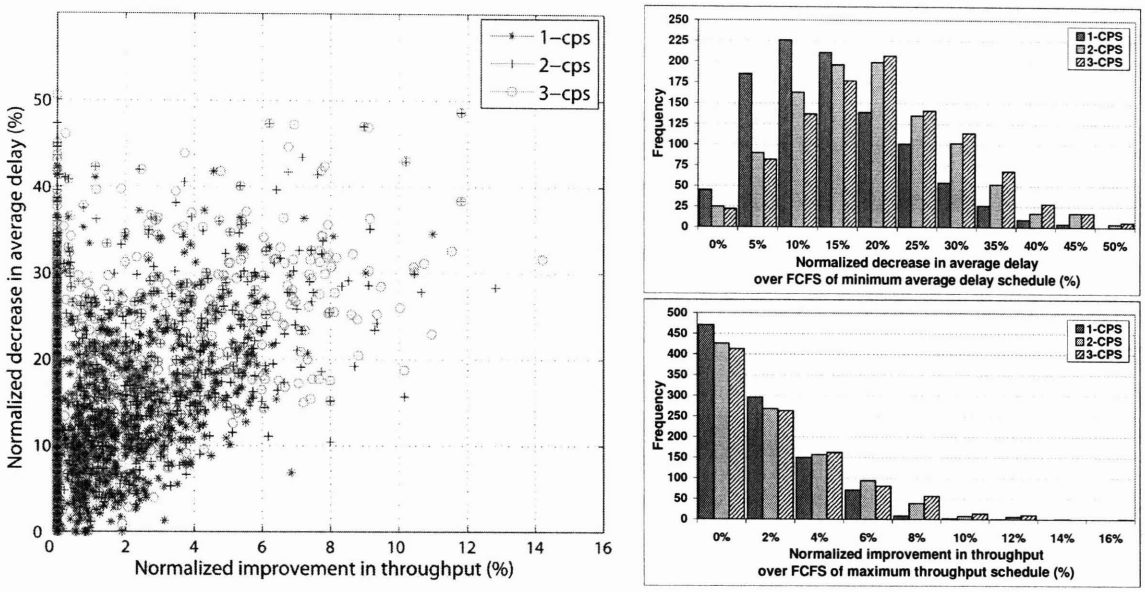

Figure 5-2: (Left) Normalized runway throughput vs. normalized average delay. (Right) Histograms corresponding to the normalized runway throughput vs. normalized average delay solutions.

schedule that minimizes the average delay does not differ very much from the minimum makespan values. Figure 5-3 (right) shows the average delay values of both the minimum makespan and the minimum average delay schedules. While in a large number of instances the average delay values are not much larger than the minimum, there are instances in which the average delay corresponding to the minimum makespan solution is significantly greater than the minimum value that can be achieved. In other words, while maximizing the throughput of the sequence, the benefit frequently comes at the expense of an increase in the average delay incurred by the aircraft.

We also compare the minimum average delay and maximum throughput schedules to the nominal FCFS schedules. The rationale behind this is as follows: since the minimum average delay solution can have a sub-optimal throughput, it is possible that the throughput of the minimum average delay solution is actually *lower* than the FCFS throughput. Similarly, the average delay of the minimum makespan solution may be higher than the FCFS average delay. Therefore, for the Monte Carlo simulations, we also compare the ratio of the makespan of the minimum average delay schedule to the FCFS makespan (x-axis in Figure 5-4) and the ratio of the average

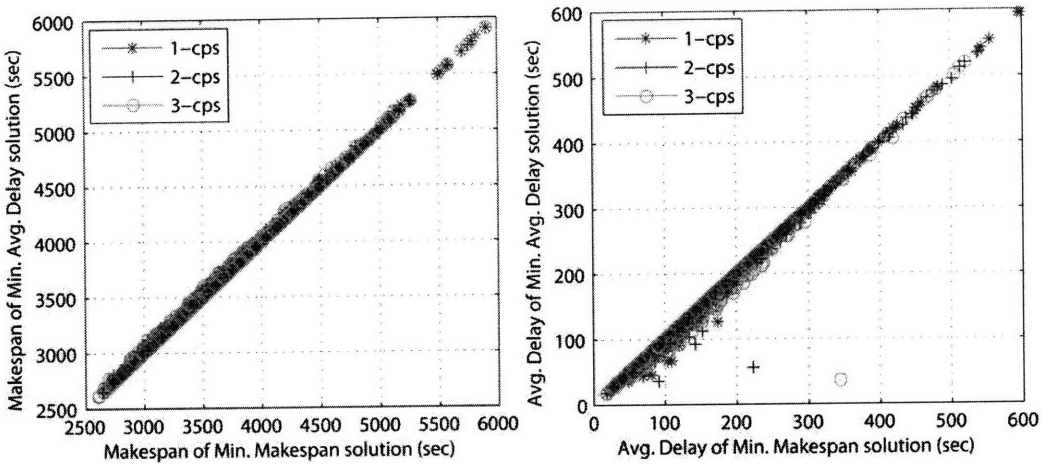

Figure 5-3: Comparison between the objectives of minimizing average delay and minimizing makespan in terms of (left) Makespan and (right) Average delay.

delay of the minimum makespan schedule to the FCFS average delay (y-axis in Figure 5-4).

In most samples, these ratios are less than one, that is, the resequencing using CPS improves both the makespan and the average delay, when compared to the FCFS solution. However, some instances have a ratio greater than one, implying a worse throughput or average delay than the FCFS schedule. The results are summarized in Table 5.2. For example, in about 4% of instances, the schedule that minimizes the average delay (with $k = 3$) has a worse throughput than the FCFS schedule. The maximum throughput schedule (with $k = 3$) has a worse average delay than the FCFS schedule in about 5% of instances.

In addition, we note that there are a handful of points that are significant outliers in both Figure 5-3 and Figure 5-4. As we have noted earlier, the minimum makespan solution on average appears to improve the average delay, but can sometimes (depending on the FCFS sequence and arrival times) have an adverse effect on the delay. The Monte Carlo simulations show that instances in which the adverse effect is large do occur, but are infrequent.

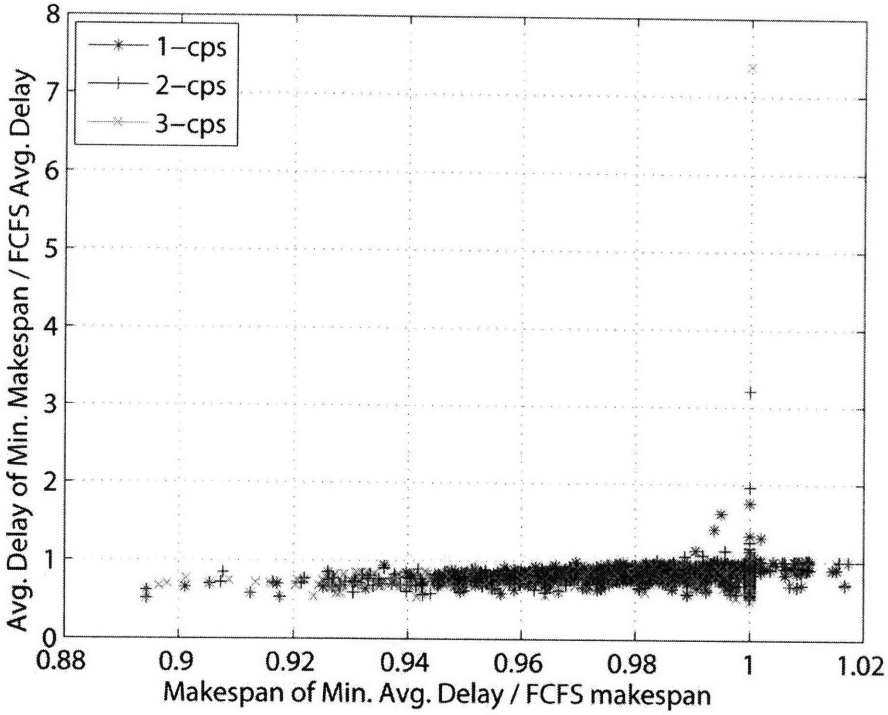

Figure 5-4: Comparison between optimal and FCFS schedules.

	Minimum average delay schedule has larger makespan than FCFS	Minimum makespan schedule has larger average delay than FCFS
1-CPS	3.6 %	4.0%
2-CPS	4.0 %	4.5%
3-CPS	3.7 %	5.3%

Table 5.2: Summary of comparison between optimal and FCFS schedules.

5.1.3 Weighted sum of delays

While the previous section dealt with the tradeoffs between the average delays and the throughput, it is possible that all the flights may not have equal importance. Some of the possible objectives that could be considered are the passenger-weighted delays or the airline priority weighted delays. We consider an instance similar to the scenarios seen previously for the average delay, but with weighting factors. The instance is summarized in Table 5.3, which shows the estimated arrival times of 30 aircraft, weighting factors of 1 or 9, and resultant schedules based on FCFS and resequencing to minimize the weighted sum of delays, with a maximum of k position shifts. For each schedule, the total landing cost (sum of delay multiplied by corresponding weighting factors) is computed. As expected, minimizing the weighted sum of delays under CPS tries to land aircraft with large weighting factors as early as possible. In this example, resequencing can help save 40-60% of the weighted sum of delays when compared to the FCFS schedule.

In addition, Figure 5-5 depicts the relation between the possible throughput and the minimum weighted sum of delays that can be obtained at the throughput for the instance through the k-CPS resequencing. In general, as the throughput increases, the weighted sum of delays decreases. However, it is noted that while by minimizing the makespan it is possible to increase the throughput from 37.8 aircraft/hour to 38.2 aircraft/hour, but this increase in throughput is achieved at the expense of a 17% increase in the weighted sum of delays.

5.2 Tradeoff Studies for DFW

We apply the proposed algorithm to the problem of minimizing the fuel costs of the arrival schedule at Dallas/Fort Worth International Airport (DFW). The airport is located in the Fort Worth Center (ZFW) airspace and its distance from the Center boundary and other major airports makes it possible to easily determine traffic flow patterns to and from DFW. It is also one of the busiest airports in the United States.

Fuel costs account for almost 50% of the total operating costs per block hour for

Aircraft ID	Weighting factor	ETA (sec)	Scheduled Time of Arrival (sec)			
			FCFS	1-CPS	2-CPS	3-CPS
Ac1	9	87	27	27	27	27
Ac2	9	101	184	184	184	184
Ac3	9	308	248	248	248	248
Ac4	9	472	412	412	412	412
Ac5	9	587	527	527	527	527
Ac6	9	596	587	656	656	656
Ac7	9	603	744	596	596	596
Ac8	1	702	875	852	852	852
Ac9	9	821	944	1003	1003	1003
Ac10	1	930	1075	934	934	934
Ac11	9	1080	1144	1072	1072	1072
Ac12	9	1106	1204	1132	1132	1132
Ac13	1	1395	1400	1335	1335	1335
Ac14	9	1398	1469	1404	1404	1404
Ac15	9	1426	1529	1464	1533	1533
Ac16	1	1448	1725	1660	1821	1821
Ac17	9	1475	1794	1729	1473	1473
Ac18	9	1551	1863	1798	1690	1690
Ac19	1	1579	1994	1929	1903	1903
Ac20	1	1630	2076	2011	1985	1985
Ac21	9	1831	2136	2140	2114	2279
Ac22	9	1845	2293	2080	2054	2054
Ac23	9	1934	2362	2297	2340	2436
Ac24	9	2057	2422	2426	2496	2496
Ac25	9	2084	2579	2366	2271	2123
Ac26	9	2095	2639	2522	2400	2183
Ac27	9	2517	2796	2775	2749	2749
Ac28	9	2544	2856	2618	2592	2592
Ac29	9	2620	3013	2844	2818	2818
Ac30	9	2650	3073	2904	2878	2878
Weighted sum of delays =			46974	31961	27075	26139

Table 5.3: Minimizing the weighted sum of delays.

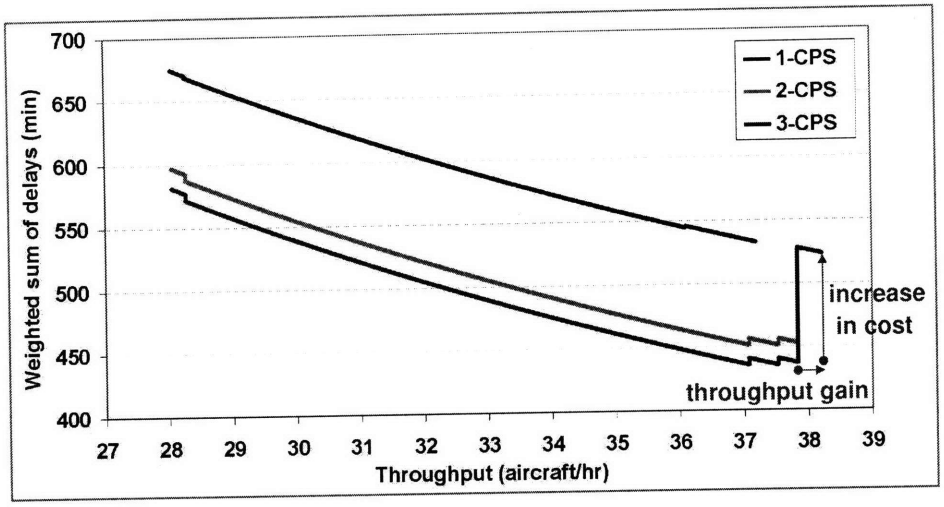

Figure 5-5: An illustration of the tradeoffs between the weighted sum of delays and the throughput.

most airlines [57]. Operating costs, including the cost of fuel consumed per unit delay, are dependent on the specific aircraft types and the airlines. In this study, we use the latest operating costs based on Form 41 data, in which each airline provides the operating cost breakdown (crew costs, fuel costs, insurance, tax, and maintenance costs per block hour of operation) for each aircraft type that it operates [57]. The fuel costs per unit delay can be derived from this database. A schematic showing the fuel costs, and a graph showing the fuel costs of landing an aircraft at a particular time are shown in Figure 5-6 for the top 10 aircraft types that operate at DFW.

5.2.1 Dallas Fort Worth international airport (DFW) information

Most arrivals into DFW pass through one of four arrival gates, BYP (NE gate), CQY (SE gate), JEN (SW gate), and UKW (NW gate), before they enter DFW TRACON airspace (Figure 5-7). Precedence constraints on the landing sequence are imposed based on aircraft that arrive on the same jet route. Runways 18R and 17C are usually used for arrivals. In this study, it is assumed that runway assignments are decided on the basis of gate usage: Since terminals A, C, and E are located on the east side, we assume that all aircraft using terminal A, C, and E land on runway 17C, and that

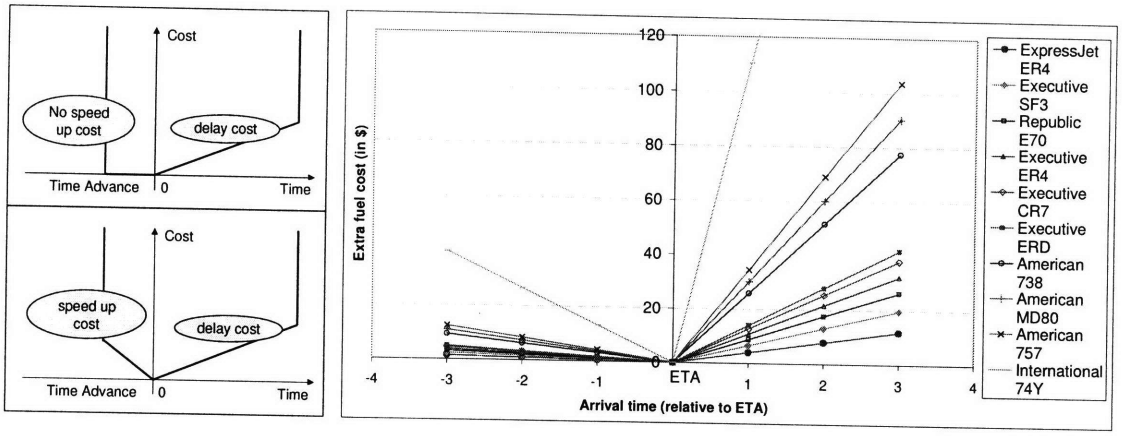

Figure 5-6: (Left) Schematic of fuel costs, depending on whether speed-up costs are accounted for. (Right) Fuel component of landing costs for the top 10 aircraft types that operate at DFW.

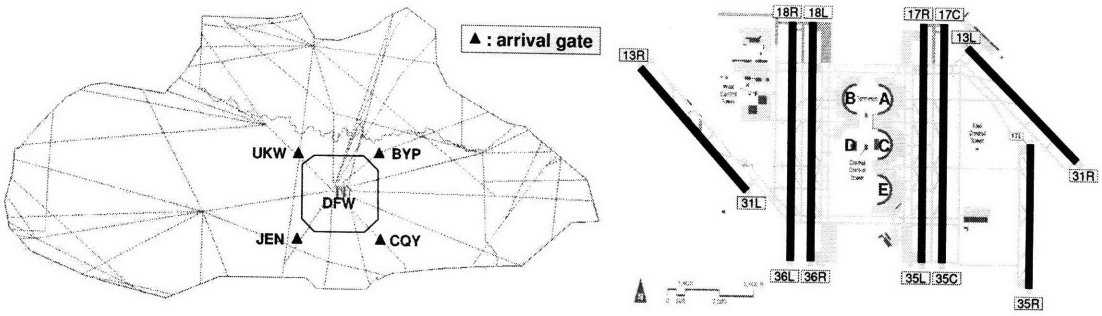

Figure 5-7: (Left) The ZFW airspace, showing jet routes and arrival gates. (Right) The DFW airport layout, showing runways and terminals [3,4].

aircraft using terminals B and D land on 18R. Most of the arrivals at DFW are heavy or large aircraft, with a few small aircraft. It is also assumed that all small aircraft land on 18R, since the south west area in the terminal is used for general aviation parking. This thesis focuses on scheduling arrivals onto Runway 18R.

5.2.2 Time Advance

Neuman and Erzberger noted that if an aircraft was allowed to speed up and land before its ETA, it could potentially result in significant savings in delay for the aircraft that follow it [35]. This procedure of allowing the earliest arrival time $E(i)$ to be less than the ETA is known as *Time Advance*. However, this decrease in delay (and the associated savings in fuel consumption) is achieved at the expense of the extra fuel

that is consumed in speeding up from the nominal velocity profile.

Using the fuel consumption rates, costs and elapsed times for both the nominal speed profile and the accelerated profile corresponding to various initial speeds and altitudes [35] and calibrating the fuel costs for the nominal profile with the block hour fuel costs of the American Airlines MD80 aircraft (which account for a significant fraction of operations at DFW), the cost per minute of time advance for each airline and aircraft type can be estimated.

The earliest time of arrival is determined by the number of minutes of time advance that is allowed, while the latest time of arrival is chosen such that no aircraft incurs more than 60 min of delay. We consider resequencing with the maximum number of position shifts k varying between 1 and 3, and determine the arrival schedule that minimizes the total fuel cost, accounting for both the fuel cost of delay and that of time advance for each aircraft.

5.2.3 Results: Fuel cost vs. Allowed time advance

The ETAs are assumed to be equal to the original scheduled times of arrival, as announced by the airlines [58]. Aircraft are unable to land at the ETAs in practice primarily because of the minimum separation requirements imposed, in addition to the inability to overtake along a jet route. The FCFS landing sequence therefore produces delay, and as a consequence, additional fuel consumption. The data described in the previous sections determines the cost of unit delay and that of unit time advance for each aircraft in the schedule. The extra fuel costs compared to ETAs for scheduling under CPS are calculated, and the benefits of the CPS schedule relative to FCFS are evaluated.

We consider intervals of one hour, between 8:00AM and 2:00PM. Table 5.4 shows extra fuel costs for the different time-windows, k, and the allowed time advance. As expected, as k increases, the fuel cost savings increase. Similarly, as the allowed speed up increases, the extra fuel cost decreases. However, it is important to note that the marginal benefit decreases, and the curve seems to level off around a value of 3 minutes time advance (Figure 5-8). This means that an increase in the cost of fuel

Extra fuel cost ($)	**8AM-9AM (n=35)**				**9AM-10AM (n=32)**			
	FCFS	1-CPS	2-CPS	3-CPS	FCFS	1-CPS	2-CPS	3-CPS
No TA	1113	924	838	748	1321	958	887	834
TA 1min	758	590	538	449	987	637	593	568
TA 2min	474	356	324	275	779	493	458	429
TA 3min	306	236	207	185	649	419	388	352
TA 4min	290	215	192	183	590	392	366	309
TA 5min	320	215	192	183	592	392	363	309
Extra fuel cost ($)	**10AM-11AM (n=26)**				**11AM-12PM (n=38)**			
	FCFS	1-CPS	2-CPS	3-CPS	FCFS	1-CPS	2-CPS	3-CPS
No TA	564	486	419	406	2474	2085	1602	1343
TA 1min	391	301	257	250	1870	1464	981	860
TA 2min	274	195	168	168	1333	973	625	542
TA 3min	221	152	135	135	913	620	416	351
TA 4min	220	147	130	130	698	449	320	268
TA 5min	237	147	130	130	561	354	287	240
Extra fuel cost ($)	**12PM-1PM (n=41)**				**1PM-2PM (n=41)**			
	FCFS	1-CPS	2-CPS	3-CPS	FCFS	1-CPS	2-CPS	3-CPS
No TA	2585	2112	1715	1527	7208	6099	5232	4851
TA 1min	2050	1621	1268	1080	6978	5870	5020	4639
TA 2min	1547	1187	940	733	6978	5870	5020	4633
TA 3min	1140	866	687	546	6978	5870	5020	4633
TA 4min	859	611	485	443	6978	5870	5020	4633
TA 5min	694	433	390	369	6978	5870	5020	4633

Table 5.4: Extra fuel cost incurred compared to ETAs for the time-windows between 8AM and 2PM.

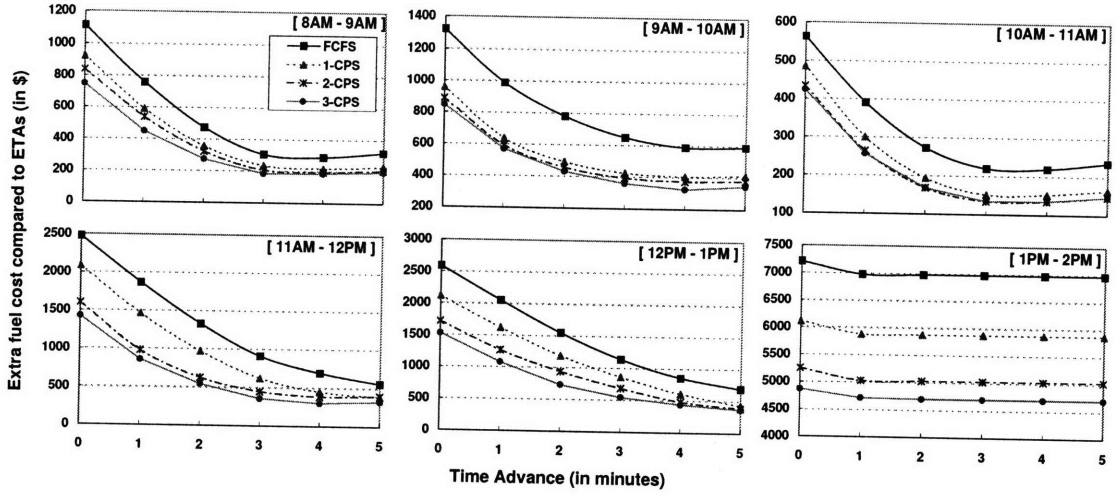

Figure 5-8: Extra fuel cost compared to the ETAs vs. the allowed time advance for the minimum fuel cost schedules, for different time-windows.

required for acceleration begins to offset the fuel-cost benefits of time advance for the rest of the aircraft. It is interesting to note that while the 12PM-1PM and the 1PM-2PM time-windows have the same number of aircraft ($n = 41$), the form of the plot is quite different, with there being little benefit to time advance of more than a minute in the latter case. A closer look at the schedules for the time-windows shows that while the 12PM-1PM window has 23 precedence constraints, the 1PM-2PM window has 33 precedence constraints. The heavily constrained sequence prevents aircraft from deriving benefit from time-advance.

The average delay values for the 8AM-9AM time-window are shown in Figure 5-9. This figure shows that the average delay values do decrease as the amount of time advance increases (this was the primary motivation for time advance). However, for a fixed amount of time advance, the decrease in fuel cost may be achieved at the expense of an increase in average delay.

It is also possible to evaluate the tradeoffs between the minimum fuel cost and maximum throughput objectives, as shown in Figure 5-10. The mean decrease in throughput (increase in makespan) experienced due to minimizing the fuel cost is 1.7% of the FCFS throughput (with a standard deviation of 2% and a maximum value of 8%); while when maximizing throughput, the mean increase in fuel cost (over the optimum value) is 1.4% with a standard deviation of 3% and a maximum

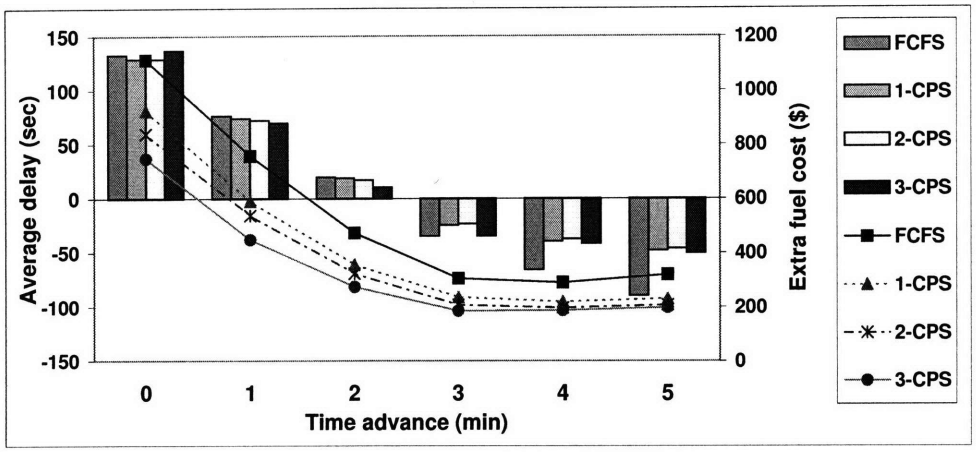

Figure 5-9: Extra fuel cost and average delay vs. allowed time advance for the time interval 8-9AM. The columns show the average delay and the lines show the extra fuel cost incurred.

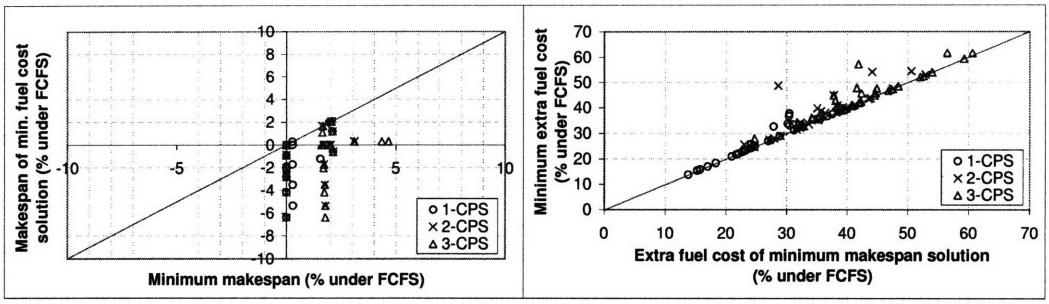

Figure 5-10: Tradeoffs between maximizing throughput and minimizing the fuel costs. The objectives are evaluated relative to the FCFS schedule – for example, the $x-$axis on the left figure is computed as 100*(FCFS makespan - min. makespan)/(FCFS makespan).

value of 20%. This suggests that the throughput is on average a (slightly) better objective function since optimizing it only results in a mean increased fuel cost that 1.4% of the FCFS cost; however, considering the worst-case scenarios, it is important to note that the maximum increase in fuel cost for the instances seen is 20% compared to a maximum 8% decrease in the throughput.

5.2.4 Minimizing flight operating costs

The above experiments are repeated using the total block hour (BH) operating costs reported by the airlines in the Form 41 data, instead of only the fuel costs. The

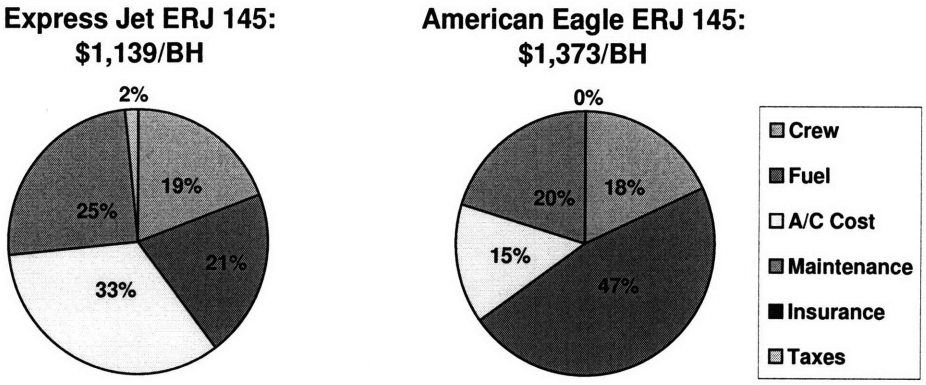

Figure 5-11: Split of the total cost of operating an ERJ145, for two different aircraft operators, ExpressJet and American Eagle. While the total Block Hour (BH) operating costs are comparable, the fuel costs are very different.

resultant objective functions can be significantly different, as is illustrated in Figure 5-11. While the total block hour operating costs of the ERJ145 are comparable for aircraft being operated by either ExpressJet (a regional jet operator based in Houston) or American Eagle, the fuel costs are very different – about 2.7 times as expensive for the latter as for the former. We note that part of this difference can be attributed to the different prices that airlines pay for fuel.

As previously seen for fuel costs in Section 5.2.3, it is possible to compute the benefit of different amounts of time advance, when the total operating costs are being minimized (Figure 5-12). In contrast to minimizing fuel costs, it appears that there is no point at which the delay benefits in terms of operational costs are offset by the fuel cost of speedup. From the point of view of minimizing total operating costs, it is therefore desirable to allow as much time advance as is practically feasible by aircraft (about 5 minutes).

The tradeoffs between the total operating cost and throughput objectives are also analyzed, as done previously for average delay vs. throughput and fuel cost vs. throughput. The results are shown in Figure 5-13. This figure shows the tradeoff between the maximum throughput and minimum operating cost solutions. The mean decrease in throughput (sub-optimality in the throughput objective) due to minimizing the total operating cost is 0.87% of the FCFS throughput, with a standard

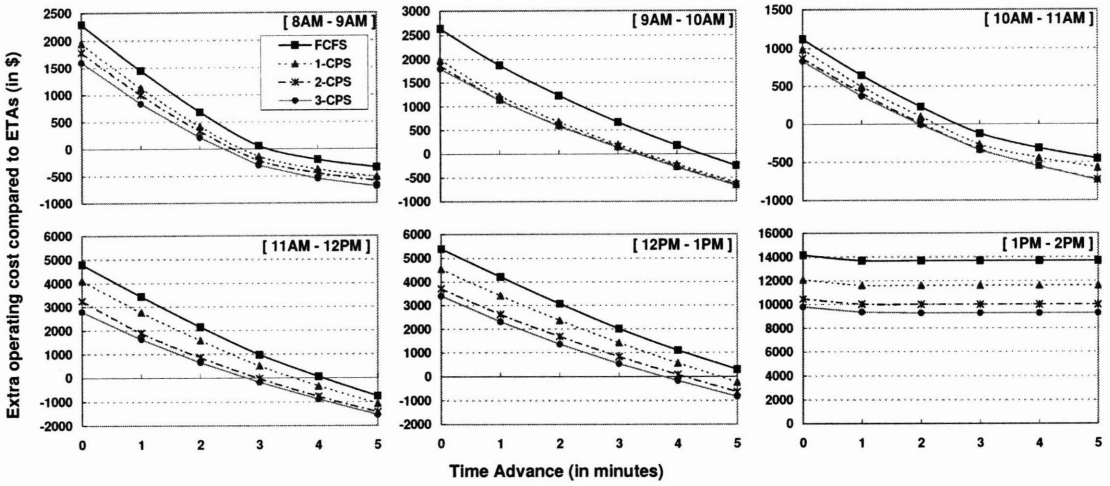

Figure 5-12: Increase in operating costs (over the ETA schedules) vs. length of allowed time advance for different 1-hour intervals in the day.

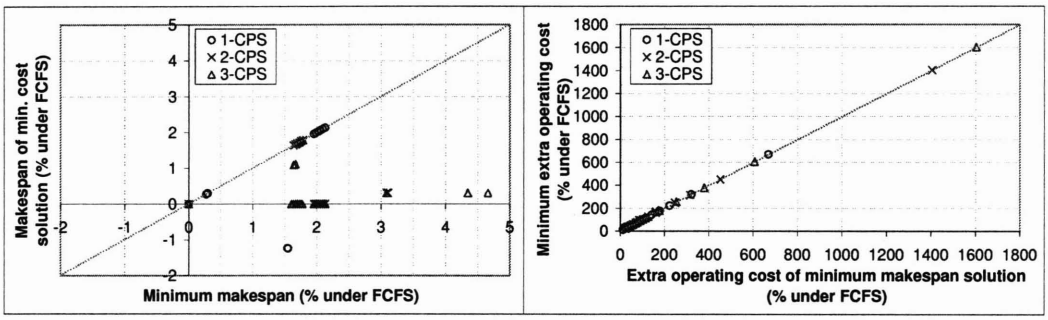

Figure 5-13: Tradeoff between maximizing throughput and minimizing the operating costs.

deviation of 1.3%, while the mean increase in the operating cost (sub-optimality in the operating cost objective) due to maximizing throughput is 0.76% of the FCFS operating cost with a standard deviation of 1.85%. This would suggest that maximizing the throughput on average leads to a (slightly) lower sub-optimality in operating cost than the reverse; however, the maximum increase in operating cost for the instances seen is 9% compared to a maximum 4.3% decrease in the throughput.

5.3 Minimizing Average Delays in the Coupled Operation of Arrivals and Departures: ICN Case Study

The proposed algorithm has so far been applied to arrival operations only, but can be extended to the coupled operation of arrivals and departures. Some airports around the world have only one runway which might have to accommodate both arrivals and departures. In addition, some airports in which two parallel runways are close to each other are sometimes treated as single runway airports because independent arrivals or departures on the closely spaced parallel runways are not allowed due to safety concerns. For example, Newark airport (EWR) has a primary pair of dependent runways oriented in a NE/SW configuration (4/22 R/L) [59]. Seattle airport (SEA) also has two parallel runways which are closely spaced.

In an airport with a single runway, arrivals and departures are coupled. Air traffic controllers at such an airport typically assign aircraft to runways, considering departures and arrivals together. Therefore, while the proposed algorithm has so far focused on the problem of scheduling aircraft landings, the algorithm should also deal with the problem of scheduling runway usage, in which we need to determine when arriving or departing aircraft use a shared runway for their landings or takeoffs.

To make the problem easier, it is assumed that the departure queue for a runway can be treated as similar to one of the jet routes for arrivals. In general, departing aircraft move from gates to the runway through taxiways after getting pushback clearance and wait for their takeoffs in a departure queue. In an airport operating a single runway, a local controller can assign the departing aircraft to use the runway during the time gap between arriving aircraft. On the other hand, an arrival control position in the TRACON determines a proper arrival sequence among aircraft approaching on jet routes from all directions. Assigning departing aircraft between arrivals at the runway is similar to assigning arriving aircraft coming from a specific jet route into an arrival sequence for final approach. From the standpoint of runway usage including

both departures and arrivals, determining the optimal runway usage sequence therefore is as same as deciding the optimal landing sequence for the aircraft approaching from various jet routes that include a virtual route representing the departure queue.

In addition, once a departing aircraft is in the departure queue, the sequence to use the runway is usually fixed: in other words, overtaking is not allowed in the departure queue. This is also similar to the precedence constraint for arrivals, that is, overtaking is not allowed between the aircraft approaching on the same jet route.

With the assumption described above, we will apply the proposed algorithm to the coupled operation optimization problem of departures and arrivals.

5.3.1 Incheon International Airport (ICN)

In this section, we demonstrate using a real-world scenario that the proposed scheduling algorithm can determine the optimal schedule which minimizes average delay for coupled arrival and departure operations. For this case study, the Incheon international airport (ICN) in South Korea was selected. ICN is a desirable location for a case study due to the reasons listed below:

1) Single runway operations

The Incheon airport currently has two parallel runways as shown in Fig 5-14, and a new third runway will be open in July, 2008. The 33 R/L runways are mainly used for departures and arrivals along the dominant wind direction. The distance between the centerlines of these parallel runways is about 1,300ft. Because the runway centerlines are close, the runways are treated as a single runway [5].

2) Heavy traffic during peak times

Air traffic demand in the Northeast Asia region is growing significantly. Since Incheon International Airport is the main hub airport to get access to Seoul (the capital of South Korea) by air travel, the air traffic demand of ICN has been increasing dramatically. As a result, the demand for operations sometimes exceeds the operational capacity of the airport, especially during peak time. The fact that the resultant delays are severe in this airport suggests that airport performance may be improved through the efficient operation of runways.

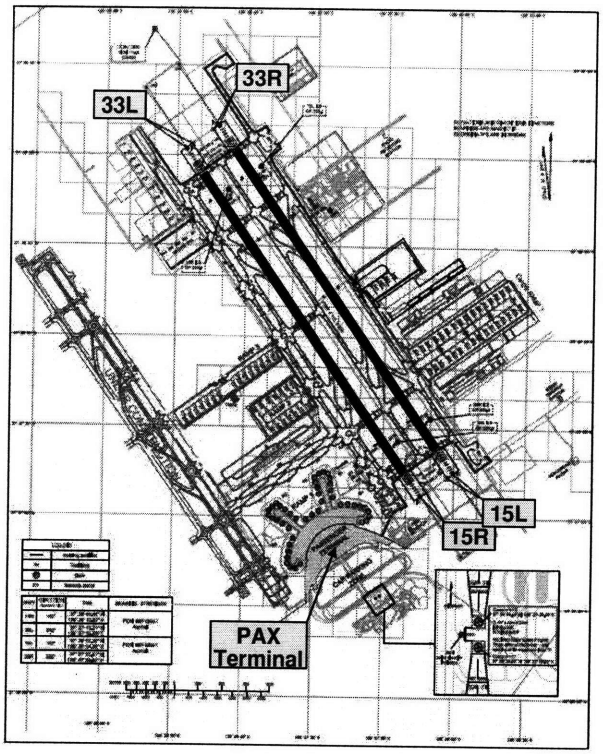

Figure 5-14: Incheon international airport layout

3) Availability of flight schedule information

In some airports, small aircraft, typically General Aviation (GA) or Very Light Jets (VLJ), form a significant fraction of the total traffic. However, it is not easy to obtain the actual departure or arrival times of these aircraft. On the other hand, the Incheon international airport mainly serves commercial flights with large and heavy types of aircraft, for which flight information is reported to the public. According to airport statistics, small aircraft account for only a small fraction. Therefore, it is reasonable to assume that the flight information provided by airlines to customers, including aircraft types, flight schedules, and actual arrival and departure times, reflects all the arrival and departure operations at ICN.

5.3.2 Separation requirements at ICN

Incheon international airport follows the separation rules defined by ICAO. The ICAO separation requirements between arrivals are shown in Table 5.5. These separation

Leading Aircraft	Trailing Aircraft		
	Heavy	Large	Small
Heavy	4	5	6
Large	3	3	4
Small	3	3	3

Table 5.5: Minimum separation (in miles) between arrivals at ICN airport

Leading Aircraft	Trailing Aircraft		
	Heavy	Large	Small
Heavy	105	128	195
Large	83	83	165
Small	83	83	105

Table 5.6: Minimum separation (in seconds) between consecutive arrivals at ICN airport

requirements in miles can be transformed to the minimum time separation required between landings, assuming a 4 nmi final approach path and an appropriate approach speed [5]. The matrix of the minimum time separation between arrivals is given in Table 5.6.

The separation requirement for successive departures basically follows 2 minute spacing, but the separation can be reduced, depending on the weight class of the first departing aircraft. The matrix of the minimum time separation between departures is shown in Table 5.7.

When arrival is followed by departure, the separation time is determined by the runway occupancy time of landed aircraft. The typical occupancy time on a runway is 55 seconds regardless of the aircraft type. However, in this study, a buffer time of

Leading Aircraft	Trailing Aircraft		
	Heavy	Large	Small
Heavy	90	120	120
Large	90	90	90
Small	60	60	60

Table 5.7: Minimum separation (in seconds) between consecutive departures at ICN airport

Leading Aircraft	Trailing Aircraft		
	Heavy	Large	Small
Heavy	70	70	70
Large	70	70	70
Small	70	70	70

Table 5.8: Minimum separation (in seconds) between arrival and departure at ICN airport

Leading Aircraft	Trailing Aircraft		
	Heavy	Large	Small
Heavy	60	60	60
Large	60	60	60
Small	60	60	60

Table 5.9: Minimum separation (in seconds) between departure and arrival at ICN airport

15 seconds is added for conservative analysis, as shown in Table 5.8.

In case of a departure followed by an arrival, the separation time is decided by the runway occupancy time of the departing aircraft. It is known that a departing aircraft usually occupies the runway for 40-45 seconds regardless of the aircraft type. Similarly to the case of an arrival followed by a departure, a buffer time of 15 seconds is added to the separation time in this case study (Table 5.9).

5.3.3 Input data for ICN case study

For this case study, actual operations data from ICN were used. These data include estimated times of arrival (ETAs), estimated times of departure (ETDs), jet routes for arriving aircraft, and aircraft types.

Most arrival flights into the ICN airport use one of three jet routes, B576, G597, and Y64. Precedence constraints on the landing sequence are imposed based on aircraft that arrive on the same jet route. The precedence constraints are also applied to departing aircraft in a departure queue because these aircraft take off the runway in FCFS order. The operating time of the schedule is chosen to be one hour during peak time. The detailed schedule data are provided in Appendix B with jet routes

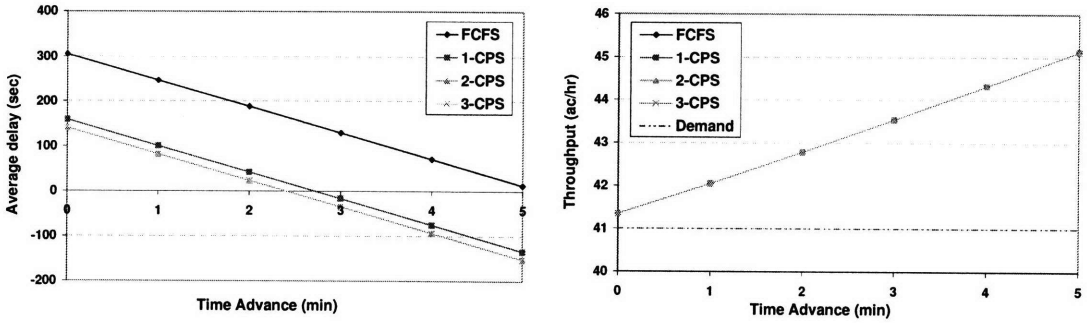

Figure 5-15: Optimization results to minimize the average delay: (left) average delay and (right) throughput.

and aircraft types.

The earliest time of runway usage is determined by the number of minutes of time advance that is allowed, while the latest time of the time-window for operations is set to 60 minutes. Resequencing with the maximum number of position shifts, k, varying between 1 and 3 is considered, and the arrival and takeoff schedule that minimizes the average delay is determined by the proposed algorithm.

5.3.4 Results: minimizing average delay

The results from the runway schedule optimization for the minimum average delay are summarized in Figure 5-15. (The detailed data are provided in Appendix B.) This figure shows the average delay and the corresponding throughput obtained at various k-CPS and TA conditions.

It is noted that as the average delay is reduced through the optimization, the throughput is also improved. With respect to k-CPS solutions, 1-CPS provides great benefit to average delay savings (about 150 seconds). 2-CPS shows little additional savings, and there is no difference between 2-CPS and 3-CPS. This result suggests that 2-CPS is sufficient in practice, considering air traffic controller complexity and computation time. In the figure, as the amount of time advance increases, the average delay values decrease by the same amount of TA. Similarly, the TA method improves the throughput of the runway.

A closer look at the schedules shown in Appendix B shows that most of time

savings from resequencing are achieved by alternating arrivals and departures. In other words, if a sequence consisting of a group of successive departures and another group of arrivals is rearranged to a sequence in which landings and takeoffs alternate with each other, delay can be reduced. This implies that the benefit from resequencing is potentially more in the case of coupled operations of arrivals and departures than in the case of independent operations.

Chapter 6

Robust Runway Scheduling

In this chapter, a robust scheduling algorithm is developed to determine the runway schedule that optimizes a measure of robustness among all possible schedules for a given group of aircraft under Constrained Position Shifting.

6.1 Dynamic Programming Algorithm for Robust Runway Scheduling

The CPS network that was described in Chapter 4 is extended and used for developing a dynamic programming algorithm for robust runway scheduling.

6.1.1 Minimizing weakness

As mentioned in Chapter 3, the *weakness* of a schedule is defined as the maximum value among the probabilities of violating the minimum separation requirements between two adjacent aircraft in a given sequence. Given that the leading aircraft i is scheduled to arrive at t_i and the trailing aircraft j is scheduled to arrive at t_j, the probability that the spacing constraint between the two aircraft i and j will be violated is denoted by $\Pr\{t_i \nrightarrow t_j\}$. In other words, if the required minimum separation between i and j is $\delta_{i,j}$,

$$\Pr\{t_i \nrightarrow t_j\} = \Pr\{t_j - t_i \leq \delta_{i,j} \mid t_i; t_j\}$$

Using this expression, the weakness of a given sequence of n aircraft for which the scheduled times of arrival are $\{t_1, t_2, \cdots, t_n\}$ can be described as follows.

$$W(t_1, t_2, \cdots, t_n) = \max\{\Pr\{t_1 \nleftrightarrow t_2\}, \Pr\{t_2 \nleftrightarrow t_3\}, \cdots, \Pr\{t_{n-1} \nleftrightarrow t_n\}\}$$

We use the CPS network that was described in Chapter 4. For developing the dynamic programming recursion used for minimizing the weakness of an arrival sequence, the following variables are first defined:

$\ell(x)$: The last aircraft of node x

$\ell'(x)$: The second from last aircraft of node x

$P(x)$: Set of nodes that are predecessors of x

$\mathcal{I}(j)$: Set of times during which aircraft j could land

t_j: Scheduled time of arrival (STA) of aircraft j

Let $J_x(t_{\ell'(x)}, t_{\ell(x)})$ be the minimum value of weakness for a sequence that starts in stage 1 and ends in node x, given that $\ell'(x)$ is scheduled to land at time $t_{\ell'(x)}$ and $\ell(x)$ is scheduled to land at time $t_{\ell(x)}$.

For an arc (x, y) in the CPS network, the weakness of the subsequence that begins with the first aircraft of the sequence and ends with the last aircraft $\ell(x)$ of node x, $J_x(t_{\ell'(x)}, t_{\ell(x)})$, is used to calculate the weakness of the subsequence that begins with the first aircraft of the sequence and ends with the last aircraft $\ell(y)$ of node y, $J_y(t_{\ell'(y)}, t_{\ell(y)})$, through the following dynamic programming recursion:

$$\begin{aligned} J_y(t_{\ell'(y)}, t_{\ell(y)}) = \min_{x \in P(y)} \left\{ \max\left\{ \Pr\left\{ t_{\ell(x)} \nleftrightarrow t_{\ell(y)} \right\}, J_x(t_{\ell'(x)}, t_{\ell(x)}) \right\} \right\}, \\ \forall\ t_{\ell'(x)} \in \mathcal{I}(\ell'(x)),\ t_{\ell(x)} \in \mathcal{I}(\ell(x)),\ t_{\ell(y)} \in \mathcal{I}(\ell(y)), \\ \text{where } t_{\ell(x)} - t_{\ell'(x)} \geq \delta_{\ell'(x),\ell(x)} \text{ and } t_{\ell(y)} - t_{\ell(x)} \geq \delta_{\ell(x),\ell(y)}. \end{aligned} \tag{6.1}$$

The proof of correctness of this recursion is presented below, following standard techniques for proving the validity of dynamic programming recursions.

Proof: We first observe that, by construction, $\ell(x) = \ell'(y)$ for $x \in P(y)$. Therefore, $J_y(t_{\ell'(y)}, t_{\ell(y)}) = J_y(t_{\ell(x)}, t_{\ell(y)})$.

Since $J_y(t_{\ell(x)}, t_{\ell(y)})$ is the minimum value of weakness over all paths leading to node y,

$$J_y(t_{\ell'(y)}, t_{\ell(y)}) = J_y(t_{\ell(x)}, t_{\ell(y)}) \leq \max\left\{\Pr\left\{t_{\ell(x)} \nleftrightarrow t_{\ell(y)}\right\}, J_x(t_{\ell'(x)}, t_{\ell(x)})\right\},$$
$$\forall\ x \in P(y),\ t_{\ell'(x)} \in \mathcal{I}(\ell'(x)),\ t_{\ell(x)} \in \mathcal{I}(\ell(x)),\ t_{\ell(y)} \in \mathcal{I}(\ell(y)),$$
$$\text{where } t_{\ell(x)} - t_{\ell'(x)} \geq \delta_{\ell'(x),\ell(x)} \text{ and } t_{\ell(y)} - t_{\ell(x)} \geq \delta_{\ell(x),\ell(y)}.$$

This means that, in particular,

$$J_y(t_{\ell'(y)}, t_{\ell(y)}) \leq \min_{x \in P(y)} \left\{\max\left\{\Pr\left\{t_{\ell(x)} \nleftrightarrow t_{\ell(y)}\right\}, J_x(t_{\ell'(x)}, t_{\ell(x)})\right\}\right\},$$
$$\forall\ t_{\ell'(x)} \in \mathcal{I}(\ell'(x)),\ t_{\ell(x)} \in \mathcal{I}(\ell(x)),\ t_{\ell(y)} \in \mathcal{I}(\ell(y)), \tag{6.2}$$
$$\text{where } t_{\ell(x)} - t_{\ell'(x)} \geq \delta_{\ell'(x),\ell(x)} \text{ and } t_{\ell(y)} - t_{\ell(x)} \geq \delta_{\ell(x),\ell(y)}.$$

To complete the proof, we only need to show that the above relationship can never hold as a strict inequality. For contradiction, suppose that

$$J_y(t_{\ell(x)}, t_{\ell(y)}) < \max\left\{\Pr\left\{t_{\ell(x)} \nleftrightarrow t_{\ell(y)}\right\}, J_x(t_{\ell'(x)}, t_{\ell(x)})\right\},$$
$$\forall\ x \in P(y),\ t_{\ell'(x)} \in \mathcal{I}(\ell'(x)),\ t_{\ell(x)} \in \mathcal{I}(\ell(x)),\ t_{\ell(y)} \in \mathcal{I}(\ell(y)), \tag{6.3}$$
$$\text{where } t_{\ell(x)} - t_{\ell'(x)} \geq \delta_{\ell'(x),\ell(x)} \text{ and } t_{\ell(y)} - t_{\ell(x)} \geq \delta_{\ell(x),\ell(y)}.$$

When $\Pr\left\{t_{\ell(x)} \nleftrightarrow t_{\ell(y)}\right\} \leq J_x(t_{\ell'(x)}, t_{\ell(x)})$,
$$\max\left\{\Pr\left\{t_{\ell(x)} \nleftrightarrow t_{\ell(y)}\right\}, J_x(t_{\ell'(x)}, t_{\ell(x)})\right\} = J_x(t_{\ell'(x)}, t_{\ell(x)})$$

Then, Equation 6-3 may be simplified as follows.

$$J_y(t_{\ell(x)}, t_{\ell(y)}) < J_x(t_{\ell'(x)}, t_{\ell(x)})$$

However, the weakness of node y should be equal to or greater than the weakness of node x because the value of $J_x(t_{\ell'(x)}, t_{\ell(x)})$ is the weakness of the subsequence of $J_y(t_{\ell(x)}, t_{\ell(y)})$ that ends at node y.

On the other hand, when $\Pr\left\{t_{\ell(x)} \nleftrightarrow t_{\ell(y)}\right\} > J_x(t_{\ell'(x)}, t_{\ell(x)})$,
$$\max\left\{\Pr\left\{t_{\ell(x)} \nleftrightarrow t_{\ell(y)}\right\}, J_x(t_{\ell'(x)}, t_{\ell(x)})\right\} = \Pr\left\{t_{\ell(x)} \nleftrightarrow t_{\ell(y)}\right\}$$

Then, Equation 6-3 may be simplified as follows.

$$J_y(t_{\ell(x)}, t_{\ell(y)}) < \Pr\left\{t_{\ell(x)} \nleftrightarrow t_{\ell(y)}\right\}$$

However, the weakness of node y must be equal to or greater than the value of $\Pr\left\{t_{\ell(x)} \nleftrightarrow t_{\ell(y)}\right\}$ because the weakness of node y should include the probability of violating the separation requirements between the last aircraft of node x and the last aircraft of node y.

procedure Find Minimum Weakness:
begin
Set $J(\cdot)$ for all nodes in the network to ∞;
for each node y in stage 2 **do**
for each $t_{\ell(y)} \in I(\ell(y))$, $t_{\ell'(y)} \in I(\ell'(y)) : t_{\ell(y)} - t_{\ell'(y)} \geq \delta_{\ell'(y),\ell(y)}$ **do**
$J_y(t_{\ell'(y)}, t_{\ell(y)}) \leftarrow \Pr\left\{t_{\ell'(y)} \nleftrightarrow t_{\ell(y)}\right\}$;
for each stage $p = 3, \cdots, n-1$ **do**
for each node x in stage p **do**
for each $t_{\ell(x)} \in I(\ell(x))$, $t_{\ell'(x)} \in I(\ell'(x)) : t_{\ell(x)} - t_{\ell'(x)} \geq \delta_{\ell'(x),\ell(x)}$ **do**
for each arc (x, y) **do**
for each $t_{\ell(y)} \in I(\ell(y)) : t_{\ell(y)} - t_{\ell(x)} \geq \delta_{\ell(x),\ell(y)}$ **do**
$J_y(t_{\ell(x)}, t_{\ell(y)}) =$
$\min\left\{J_y(t_{\ell(x)}, t_{\ell(y)}), \max\left\{J_x(t_{\ell'(x)}, t_{\ell(x)}), \Pr\left\{t_{\ell(x)} \nleftrightarrow t_{\ell(y)}\right\}\right\}\right\}$;
end

Figure 6-1: Algorithm for computing the minimum weakness.

Therefore, Equation (6.2) cannot hold as a strict inequality implying that Equation (6.1) must be valid. ∎

Now, the weakness value $J_y(\cdot)$ for each node in stage n can be computed by unrolling the dynamic programming recursion from the boundary condition $J_x(t_{\ell'(x)}, t_{\ell(x)}) = \Pr\{\ell'(x) \leftrightarrow \ell(x)\}$ for every node x in stage 2, where $t_{\ell'(x)} \in \mathcal{I}(\ell'(x))$ and $t_{\ell(x)} \in \mathcal{I}(\ell(x))$. The pseudocode for the algorithm is presented in Figure 6-1.

Since the state space for $J(\cdot)$ is infinite, the recursion in the current form is computationally impractical. For implementing the algorithm, all times are discretized into the periods of length ϵ. Since the accuracy of measurement in the airspace based on the radar update rates shows the order of seconds [13], it would be reasonable to set ϵ to a value between 1 and 10 seconds.

When the computing procedure described in the pseudocode (Figure 6-1) is complete, the values of $J(\cdot)$ for all nodes in the last stage n in the CPS network are obtained for all feasible time periods. Given a makespan t, the most reliable sequence is the one that has the minimum weakness value among all $J_x(t_{\ell'(x)}, t_{\ell(x)})$ for $t_{\ell(x)} = t$. Within a range of feasible makespan values, the proposed algorithm generates the optimal sequence and schedule to have the minimum weakness value for each makespan. Consequently, a curve that trades off makespan against weakness can be plotted.

6.1.2 Complexity

It was shown in [1] and in Chapter 5 that the number of nodes in the CPS network is $O(n(2k+1)^{(2k+1)})$, and the number of arcs is $O(n(2k+1)^{(2k+2)})$.

While looking for the optimal landing times to minimize the weakness, this algorithm includes two time intervals in which two aircraft involved with each arc (x, y) in the CPS network can be allocated. In other words, for each arc (x, y), we have to consider all possible landing times for the last aircraft in node x and the last aircraft of the current node y. Assumed that the length of the largest interval of feasible arrival times among all aircraft is L and the accuracy is ϵ, the computational work done per arc in the network is therefore $O((L/\epsilon)^2)$.

Lemma 2 : The complexity of the proposed dynamic programming algorithm is $O(n(2k+1)^{(2k+2)}(L/\epsilon)^2)$, where n is the number of aircraft, k is the maximum allowed number of position shifts, L is the largest difference between the latest and earliest arrival times over all aircraft, and ϵ is the desired resolution.

In this algorithm, the probabilities $\Pr\left\{t_{\ell'(x)} \nleftrightarrow t_{\ell(x)}\right\}$ of various types of aircraft, depending on the weight class and the prediction accuracy of the ETA, are computed and stored for repetitive usage during the optimization process. Therefore, the work to calculate these probabilities is done only once, and this computational work is not included in the complexity.

6.2 Tradeoff between Weakness and Throughput

While scheduling aircraft arrivals, it is difficult to accomplish both efficiency (maximizing runway throughput or minimizing makespan) and robustness (minimizing weakness). By adding very large buffer times to the inter-aircraft spacings, it is possible to lay out a robust schedule that scarcely needs any controller interference after the initial scheduling. However, in such a schedule, there may be a very long time before the last aircraft completes its landing. On the other hand, the most efficient landing schedule (which has the maximum throughput) might be achieved by allowing the inter-aircraft separations to be as close to the minimum requirements as possible, but this schedule may be so sensitive to uncertainty that the separation requirements would be frequently violated. In this section, the tradeoff between weakness (as a measure of robustness) and throughput (as a measure of efficiency)

will be discussed in detail.

For this tradeoff study, an illustrative example of a landing schedule on a single runway is considered. This landing sequence consists of 20 aircraft crossing the Center boundary toward the destination airport at crossing times generated using a Poisson distribution at the rate of 45 aircraft per hour. Four jet routes are assigned based on the traffic flow statistics at Denver airport, and precedence conditions that aircraft arriving on the same jet route cannot overtake each other are enforced.

Since the scheduled time of arrivals are estimated when the aircraft enter the Center boundary (about 45-60 min before landing), there can be considerable errors between the scheduled and the actual landing times, depending on the equipage of the aircraft. For instance, aircraft with precise Flight Management Systems (FMS) are likely to be more accurate in meeting their scheduled times than aircraft which are less equipped [15,30,60]. In this example, it is assumed that the probability distribution of the difference between scheduled landing times and actual landing times is triangular, and has a range of ± 300 seconds for aircraft which are not equipped with an accurate FMS, and ± 150 seconds for appropriately equipped aircraft. The aircraft in this sequence are therefore divided into six categories: three classes based on their Maximum Takeoff Weight (MTOW) and two types based on the presence of equipment. The form of a probability distribution (a triangular distribution) is symmetrical with respect to the exact landing time determined by a controller, at which the aircraft has the highest probability of landing, regardless of the equipage of the aircraft.

For the time-window, the earliest arrival time is set to one minute before the estimated time of arrival. The latest possible arrival time is chosen to be 60 minutes after the estimated time of arrival. The separation requirements between successive arriving aircraft during IFR approaches are dependent upon the MTOW classification of aircraft and are already given in Table 3.3.

One way to improve the robustness of the arrival schedule is to add buffer times to the minimum separation requirements. The *buffered FCFS* schedule is obtained by enforcing the minimum spacing requirements with appropriate buffering, while maintaining the sequence in order of the estimated times of arrival. In this example, the size of the buffer time is set to 12 seconds if both the leading and trailing aircraft are equipped with the FMS and 24 seconds if at least one aircraft of them is not equipped [30]. The resultant schedule from this

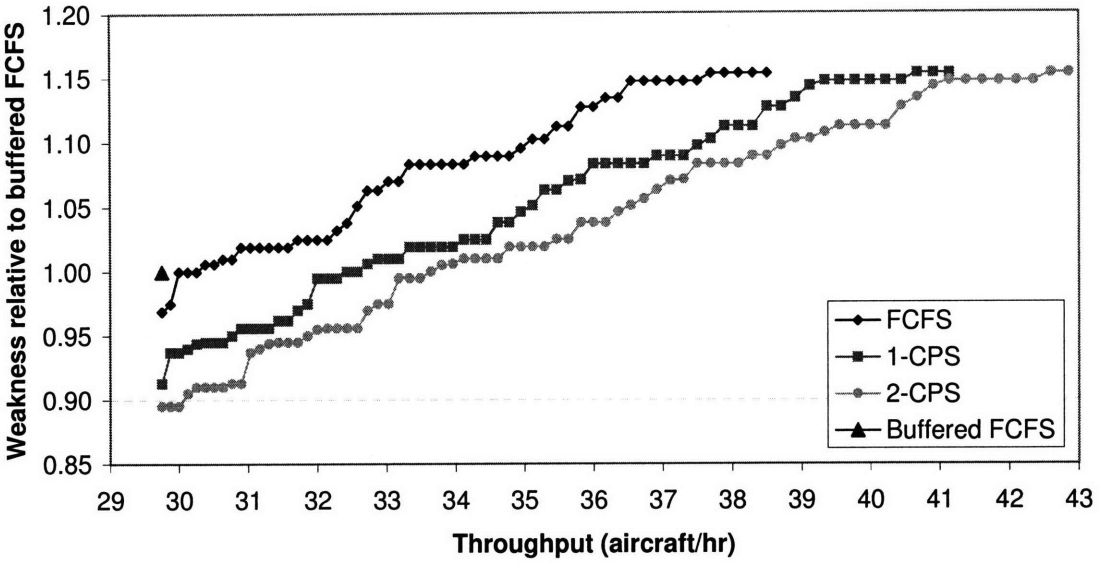

Figure 6-2: An illustration of the tradeoffs between the weakness and the throughput.

approach is used as a baseline schedule for robustness optimization. In other words, this schedule has the baseline value of the robustness expressed by its *weakness*, the maximum value among probabilities that the separation requirements between two successive aircraft will be violated, and its throughput (the number of arriving aircraft in the sequence divided by the time taken to complete the schedule) is the minimum acceptable value (which we hope will be improved through optimization). The initial sequence of 20 aircraft, their weight classes, equipage, jet routes, and scheduled arrival times are presented in Table 6.1 with the buffered FCFS schedule.

The dynamic programming based scheduling algorithm generates the feasible schedules within the range of possible throughput, not a single schedule. The air traffic controller may have to choose an appropriate schedule to satisfy the required conditions for robustness and efficiency among these schedules. The characteristics of these schedules can be represented by a tradeoff curve between weakness and throughput, as shown in Figure 6-2. To show how much the weakness decreases (or increases) over the buffered FCFS case, the ratio of the probability of a feasible schedule to the probability of the buffered FCFS schedule is used in this figure.

Figure 6-2 shows that the proposed algorithm under the CPS method can compute the tradeoff curves between weakness and throughput for k=1 and k=2, as well as a more robust FCFS schedule than the buffered FCFS case. It is noted that the same throughput as the

buffered FCFS schedule's throughput can be achieved through both FCFS and k-CPS, with a lower level of weakness.

Figure 6-3 illustrates how the arrival sequence and schedule changes in order to obtain a lower weakness value as k increases. It shows the triangular probability distributions of the landing times achieved from three resulting schedules: "robust" FCFS (=0-CPS), 1-CPS, and 2-CPS. Each triangle in this figure represents a probability density function for the landing time of each aircraft. A triangle with a narrow base denotes an equipped aircraft with high accuracy, while a triangle with a wide base denotes an aircraft controlled by a pilot. In this figure, the probability of violating the spacing constraint between adjacent aircraft is not equal to the overlapped area between the corresponding two triangular probability distributions (which denotes the probability that the order will be swapped). The derivation of the probabilities of violating separation is described in Appendix C. For the purpose of comparing the robustness, the schedules drawn in this figure have the same throughput (or makespan) as the baseline schedule. Through Figure 6-3, it can be seen that several aircraft in the sequence move their landing times and exchange positions in order to reduce weakness while maintaining throughput (or makespan).

Similarly, the proposed algorithm may also achieve a greater throughput with the same value of weakness. With respect to the robustness of the baseline schedule (buffered FCFS), the throughput improves, as we move from FCFS to 1-CPS, and then to 2-CPS. Figure 6-4 shows the probability distributions of the arrival times obtained from robust FCFS (=0-CPS), 1-CPS, and 2-CPS. Each schedule corresponds to the maximum throughput that can be obtained while maintaining the same value of weakness as the buffered FCFS schedule. In this figure, it is noted that while these optimal schedules have the same value of weakness, the locations at which the minimum weakness value is achieved differ from one schedule to other; in addition, the makespan (the time at which the last aircraft in a given sequence completes its landing) decreases as k increases.

The difference between buffered FCFS and controlled FCFS comes from the fact that while the buffered FCFS allocates the landing times by adding buffer times uniformly, without accounting for the aircraft-specific information such as the estimated times of arrival, the proposed scheduling algorithm determines the optimal schedule using the information available. As before, the CPS schedules are made out from the same strategy and the benefit of position reordering. As a result, as the maximum number of position shifts allowed

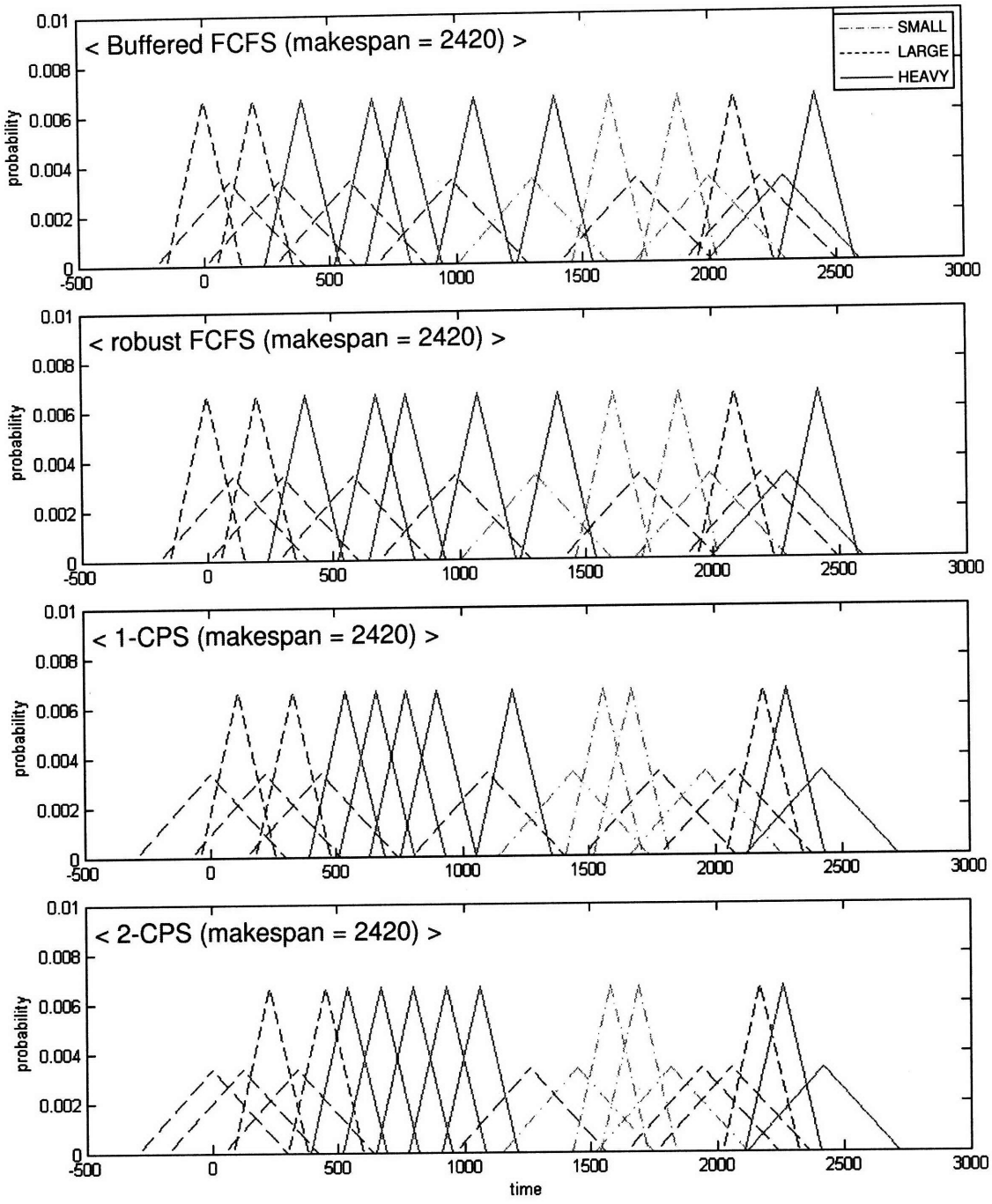

Figure 6-3: An illustration of the probability distribution of landing times for buffered FCFS, robust FCFS, 1-CPS, and 2-CPS from the minimum weakness solution at a fixed throughput.

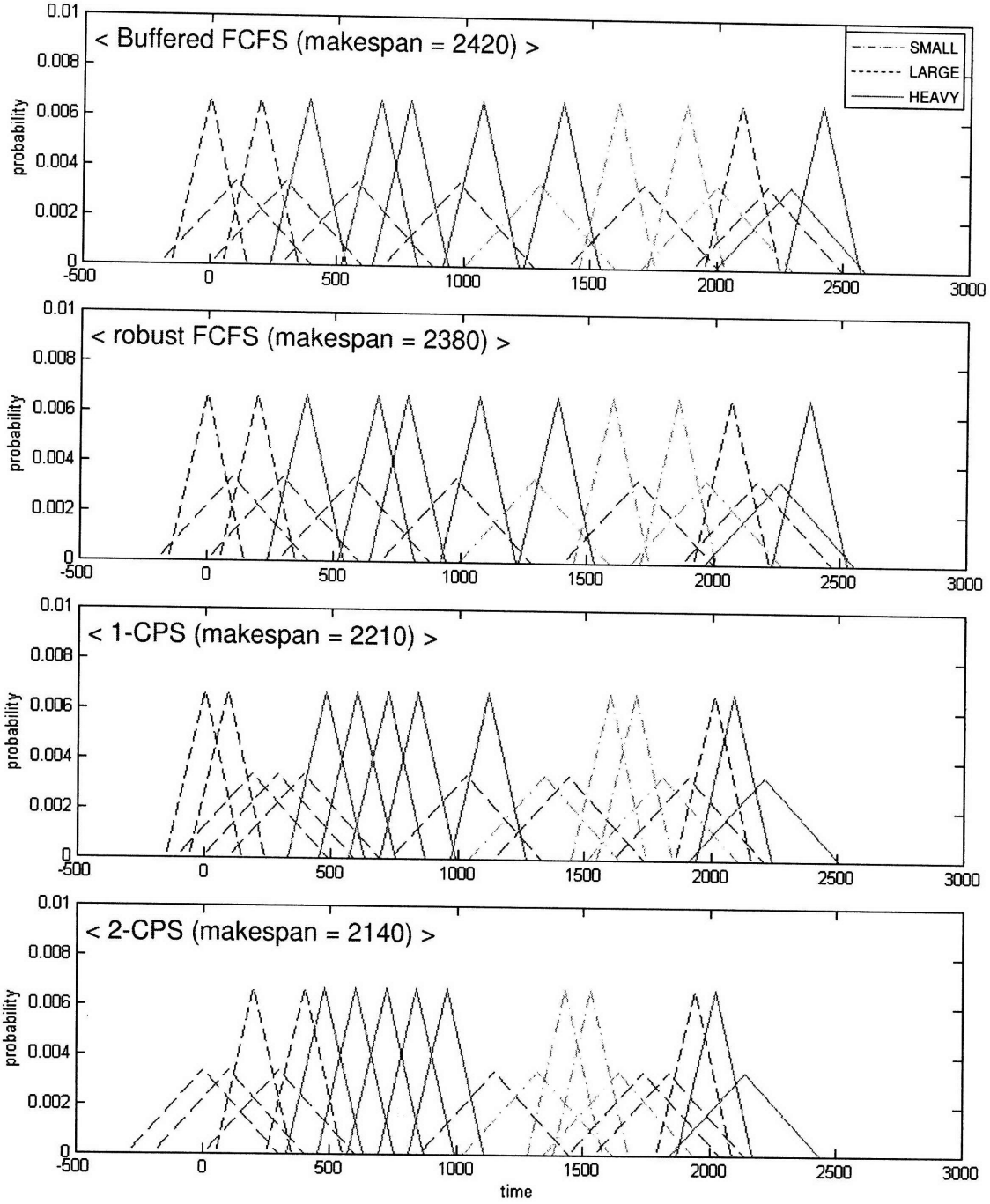

Figure 6-4: An illustration of the probability distribution of landing times for buffered FCFS, robust FCFS, 1-CPS, and 2-CPS from the minimum weakness solution, with a same level of weakness.

(k) increases, the benefit from resequencing, in terms of both robustness and throughput, also increases.

While optimizing runway schedules, it is necessary to tradeoff weakness and throughput: as seen in Figure 6-2, a decrease in weakness (i.e. a more robust schedule) can be obtained with a decrease of throughput (i.e. a less efficient schedule). This is similar to the tradeoffs between reliability and throughput in prior work [32].

Table 6.1 shows the output of the proposed robust scheduling algorithm, that is, the arrival times for the robust FCFS and CPS sequences with the same makespan. The arrival times shown in the table are rounded up to 10 seconds for rapid computation. With this resolution of the time-step, the technique presented in this thesis is amenable to real time implementation.

Aircraft ID	Aircraft type	Equipage	Jet route	Scheduled Time of Arrival (in seconds)			
				buffered FCFS	FCFS	1-CPS	2-CPS
Ac1	Large	Equipped	J4	0	0	110	230
Ac2	Large	Not Equipped	J1	100	100	0	0
Ac3	Large	Equipped	J4	200	200	330	450
Ac4	Large	Not Equipped	J2	300	300	220	120
Ac5	Heavy	Equipped	J1	390	390	540	670
Ac6	Large	Not Equipped	J2	580	580	440	340
Ac7	Heavy	Equipped	J1	670	670	780	930
Ac8	Heavy	Equipped	J2	790	790	660	540
Ac9	Large	Not Equipped	J2	980	980	1100	1260
Ac10	Heavy	Equipped	J3	1070	1070	900	800
Ac11	Small	Not Equipped	J1	1300	1300	1440	1450
Ac12	Heavy	Equipped	J4	1390	1390	1200	1060
Ac13	Small	Equipped	J1	1610	1610	1560	1690
Ac14	Large	Not Equipped	J4	1710	1710	1780	1940
Ac15	Small	Equipped	J2	1880	1870	1670	1580
Ac16	Small	Not Equipped	J2	2000	1990	1960	1820
Ac17	Large	Equipped	J2	2100	2090	2190	2170
Ac18	Large	Not Equipped	J1	2200	2190	2080	2060
Ac19	Heavy	Not Equipped	J2	2290	2290	2420	2420
Ac20	Heavy	Equipped	J1	2420	2420	2280	2260

Table 6.1: Aircraft types, equipage, jet routes, scheduled arrival times for buffered FCFS, "robust" FCFS, and CPS sequences with the same makespan for minimum weakness.

6.3 Comparison of the Minimum Weakness Solution and the Maximum Reliability Solution

In this section, we compare the minimum weakness solution proposed in this thesis with the maximum reliability solution that was suggested in previous research [32].

In [32], the *reliability* of a schedule was defined as the probability that none of the inter-aircraft spacing constraints will be violated. Its mathematical definition is briefly described below.

Let $t_i \leftrightarrow t_j$ represent the event that the minimum spacing between two aircraft i and j will *not* be violated given that i is scheduled to land at t_i and j is scheduled to land at t_j. Given a sequence of aircraft $\{i_1, \cdots, i_n\}$ with corresponding scheduled arrival times $\{t_{i_1}, \cdots, t_{i_n}\}$, the reliability of the schedule, $R(t_{i_1}, \cdots, t_{i_n})$, is defined as follows, under some technical assumptions [32].

$$\begin{aligned} R(t_{i_1}, \cdots, t_{i_n}) &= \Pr\left\{t_{i_1} \leftrightarrow t_{i_2} \wedge t_{i_2} \leftrightarrow t_{i_3} \wedge \cdots \wedge t_{i_{n-1}} \leftrightarrow t_{i_n}\right\} \\ &\approx \Pr\left\{t_{i_1} \leftrightarrow t_{i_2}\right\} \times \Pr\left\{t_{i_2} \leftrightarrow t_{i_3} \mid t_{i_1} \leftrightarrow t_{i_2}\right\} \times \cdots \times \Pr\left\{t_{i_{n-1}} \leftrightarrow t_{i_n} \mid t_{i_{n-2}} \leftrightarrow t_{i_{n-1}}\right\} \end{aligned}$$

For the same scenario as the arrival schedule used in the previous section, the maximum reliability solution produces the tradeoff curve between the throughput and the reliability ratio relative to the buffered FCFS case as shown in Figure 6-5. The shape of the curve in this figure is similar to the result of the other landing sequence example used in the previous work [32], showing that k-CPS as well as FCFS schedule can achieve higher level of the reliability at a given throughput, but the reliability decreases with an increase in throughput.

Figure 6-2 and 6-5 make it possible to compare the minimum weakness solution with the maximum reliability solution. At a given throughput, both algorithms generate better levels of robustness, in terms of weakness or reliability, respectively. In a similar way, while maintaining the level of robustness achieved by the buffered FCFS schedule, both algorithms can increase throughput. In particular, the maximum reliability solution shows a greater amount of throughput increase with respect to the equal level of robustness (as measured by the reliability). Additionally, it seems that the maximum reliability solution leads to significant improvement in terms of reliability (up to 8-fold for 2-CPS).

For a more detailed comparison, the weakness of the maximum reliability solution is

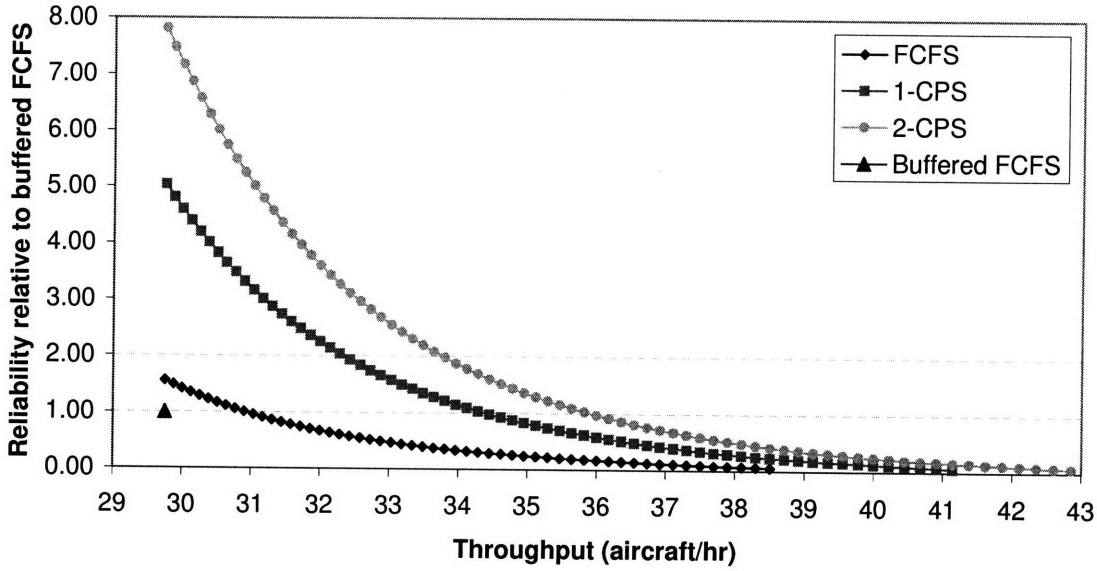

Figure 6-5: An illustration of the tradeoffs between the reliability and the throughput.

computed and compared with the minimum achievable weakness value. Figure 6-6 depicts the probability distribution of actual landing times of the FCFS sequences obtained from three approaches for a given example. The exact landing times determined by a controller are also shown in Table 6.2.

In the buffered FCFS sequence, the weakness value is achieved at the inter-aircraft spacing between Ac18 (Large, Not equipped) and Ac19 (Heavy, Not equipped), with the time difference of 90 seconds. In the minimum weakness solution, the leading aircraft (Ac18) is moved forward by 10 seconds, so the probability of violating the separation constraints between these two aircraft is reduced. The minimum weakness solution enables us to achieve a weakness value for the FCFS sequence that is lower than that of the buffered FCFS schedule. The location having the maximum violation probability is between Ac14 (Large, Not equipped) and Ac15 (Small, equipped), with the time difference of 160 seconds. On the other hand, the maximum reliability solution shifts the spacing between Ac18 and Ac19 close to the minimum separation requirement (60 seconds). This spacing is lower even than the time separation of the same aircraft in the buffered FCFS schedule. This implies that the controller might have to intervene at this point in the schedule more frequently when following the maximum reliability solution. A closer look shows that the actual probabilities of violating the safety constraints between two adjacent aircraft often exceed the weakness (maximum achieved probability of violation) of the schedule that minimizes

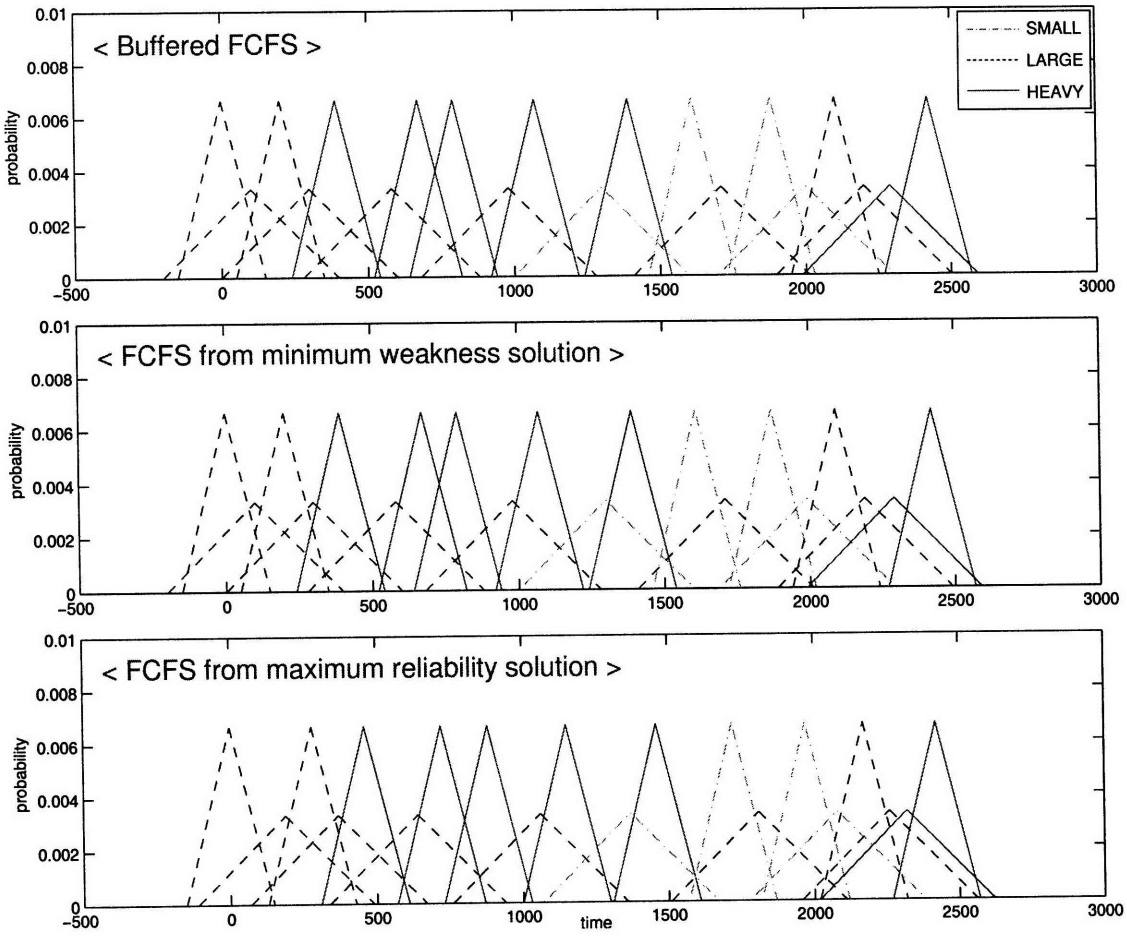

Figure 6-6: An illustration of the probability distribution of landing times for (top) buffered FCFS, (middle) FCFS from the minimum weakness solution, and (bottom) FCFS from the maximum reliability solution.

Aircraft ID	Aircraft type	Equipage	Jet route	Scheduled Time of Arrival (in seconds)			
				buffered FCFS	FCFS	1-CPS	2-CPS
Ac1	Large	Equipped	J4	0	0	0	0
Ac2	Large	Not Equipped	J1	100	190	280	300
Ac3	Large	Equipped	J4	200	280	180	190
Ac4	Large	Not Equipped	J2	300	370	350	380
Ac5	Heavy	Equipped	J1	390	460	520	720
Ac6	Large	Not Equipped	J2	580	640	420	460
Ac7	Heavy	Equipped	J1	670	720	840	1040
Ac8	Heavy	Equipped	J2	790	880	680	560
Ac9	Large	Not Equipped	J2	980	1060	1190	1400
Ac10	Heavy	Equipped	J3	1070	1150	1000	880
Ac11	Small	Not Equipped	J1	1300	1370	1510	1620
Ac12	Heavy	Equipped	J4	1390	1460	1280	1200
Ac13	Small	Equipped	J1	1610	1720	1750	1740
Ac14	Large	Not Equipped	J4	1710	1810	1580	1480
Ac15	Small	Equipped	J2	1880	1970	1900	1890
Ac16	Small	Not Equipped	J2	2000	2080	2020	2010
Ac17	Large	Equipped	J2	2100	2170	2190	2190
Ac18	Large	Not Equipped	J1	2200	2260	2090	2080
Ac19	Heavy	Not Equipped	J2	2290	2320	2420	2420
Ac20	Heavy	Equipped	J1	2420	2420	2320	2320

Table 6.2: Aircraft types, equipage, jet routes, scheduled arrival times for buffered FCFS, "robust" FCFS, and CPS sequences with the same makespan for maximum reliability.

weakness. Similar situations also occur in k-CPS schedules.

The reason why these situations occur is that the maximum reliability approach focuses on increasing the reliability of the sequence as a whole (the probability that the separation requirements will not be violated for any inter-aircraft spacings in the sequence), and as a result, this algorithm may "sacrifice" one pair of aircraft for the sake of further lowering the violation probability values of other pairs, thereby improving the reliability of the whole sequence.

Chapter 7

Conclusion

This thesis presented an algorithm for determining a terminal-area schedule that minimizes the sum of aircraft-dependent delay costs in the presence of constraints such as separation criteria, arrival time windows, limits on deviation from the FCFS sequence and precedence conditions, in a computationally tractable manner. The algorithm was used to optimize schedules and evaluate tradeoffs between different objective functions such as throughput, average delay, fuel costs and operating costs.

The results showed that significant improvements in the average delay (up to 50%) could be achieved through resequencing under constrained position shifting (CPS) and that the suboptimality of the minimum average delay schedule (measured in terms of the optimal throughput) was quite small.

The policy of allowing aircraft to speed up from their nominal profiles and to arrive before their ETAs (known as time advance) was also investigated. The minimum fuel cost schedules were determined by considering, for each aircraft, both the delay cost and the extra fuel cost incurred due to speeding up. The analysis suggested that a time advance of up to 3 minutes is optimal in most practical scenarios.

Using data from Dallas Fort Worth international airport (DFW), the tradeoffs between fuel and operating costs, and runway throughput were also analyzed. The tradeoff analysis showed that minimizing fuel costs or operating costs generally did not result in significant decreases in the throughput of the schedule. It also demonstrated that while on average maximizing the throughput resulted in modest increases in the fuel and operating costs (relative to FCFS), in the worst-case scenarios, throughput maximization could result in

up to a 20% increase in the fuel cost and up to a 9% increase in the direct operating costs relative to FCFS.

We also demonstrated that these methods could be extended to coupled operations of arrivals and departures on a single runway using a case study based on Incheon international airport (ICN).

In addition, We discussed the problem of optimizing robustness, and introduced a new notion of schedule robustness, which we called the "weakness" (the maximum value among the probabilities that the separation requirement between a pair of aircraft will be violated). We developed an algorithm to minimize weakness, and used this algorithm to evaluate the tradeoffs between throughput and weakness.

Finally, by extending the CPS framework to the problem of minimizing the sum of delay costs and new robustness concepts, we have developed a better understanding of the tradeoffs involved in terminal-area scheduling.

Appendix A

DFW Data

This appendix describes the input and output data that are used in tradeoff studies for DFW airport (Chapter 5.2). The input data include the type, estimated arrival time, and hourly fuel cost of each aircraft arriving on DFW airport runway 18R between 8AM and 9AM. The output data show scheduled arrival time of each aircraft which is calculated by the proposed algorithm.

Figure A-1, A-2, and A-3 show the input data and the scheduled times of arrival optimized by Time Advance (TA) and Constrained Position Shifting (CPS) strategies for the minimum fuel costs.

Fig. A-4, A-5, and A-6 show the same input data and the scheduled times of arrival optimized by Time Advance (TA) and Constrained Position Shifting (CPS) strategies for the minimum operating costs.

The extra fuel or operating cost (in dollars) and average delay (in seconds) during a given time period are also shown in the bottom of each figure. These values can be used for comparing different sequencing strategies such as CPS and TA.

A/C ID	A/C Type	ETAs (sec)	Fuel cost ($/hr)	**No TA case**, STAs (sec)				**TA 1min. case**, STAs (sec)			
				FCFS	1-CPS	2-CPS	3-CPS	FCFS	1-CPS	2-CPS	3-CPS
Ac1	LARGE	0	645	0	0	0	0	0	0	0	0
Ac2	LARGE	0	393	70	70	70	70	70	70	70	70
Ac3	LARGE	300	762	300	370	440	440	240	240	380	380
Ac4	LARGE	300	1805	370	300	300	370	310	310	240	310
Ac5	LARGE	300	645	440	510	510	510	380	450	450	450
Ac6	LARGE	300	1805	510	440	370	300	450	380	310	240
Ac7	LARGE	600	839	600	600	670	600	540	540	610	610
Ac8	SMALL	600	295	740	810	810	810	680	750	750	750
Ac9	LARGE	600	839	810	670	600	670	750	610	540	540
Ac10	LARGE	900	645	900	970	970	1130	840	840	840	1130
Ac11	LARGE	900	839	970	900	900	1060	910	910	910	1060
Ac12	HEAVY	900	3111	1030	1030	1030	900	970	970	970	900
Ac13	SMALL	900	295	1230	1230	1320	1480	1170	1170	1260	840
Ac14	SMALL	900	295	1320	1320	1230	1570	1260	1260	1170	1480
Ac15	LARGE	1200	762	1390	1390	1460	1200	1330	1330	1400	1270
Ac16	LARGE	1200	645	1460	1530	1600	1340	1400	1470	1540	1340
Ac17	LARGE	1200	1619	1530	1460	1390	1270	1470	1400	1330	1200
Ac18	LARGE	1500	393	1600	1670	1740	1850	1540	1610	1680	1760
Ac19	LARGE	1500	1805	1670	1600	1530	1640	1610	1540	1470	1550
Ac20	LARGE	1500	762	1740	1740	1670	1710	1680	1680	1610	1620
Ac21	LARGE	1500	645	1810	1810	1810	1780	1750	1750	1750	1690
Ac22	LARGE	2100	645	2100	2100	2170	2170	2040	2040	2110	2110
Ac23	LARGE	2100	393	2170	2240	2240	2240	2110	2180	2180	2180
Ac24	LARGE	2100	645	2240	2170	2100	2100	2180	2110	2040	2040
Ac25	LARGE	2400	839	2400	2400	2400	2400	2340	2410	2410	2410
Ac26	LARGE	2400	393	2470	2470	2470	2470	2410	2340	2480	2480
Ac27	SMALL	2400	295	2610	2610	2610	2610	2550	2550	2340	2340
Ac28	LARGE	2700	839	2700	2700	2770	2770	2640	2640	2640	2640
Ac29	SMALL	2700	295	2840	2910	2910	2910	2780	2850	2850	2850
Ac30	LARGE	2700	1805	2910	2770	2700	2700	2850	2710	2710	2710
Ac31	LARGE	3000	645	3000	3000	3000	3000	2940	3000	3000	3000
Ac32	LARGE	3300	762	3300	3370	3370	3370	3240	3310	3310	3310
Ac33	LARGE	3300	762	3370	3300	3300	3300	3310	3240	3240	3240
Ac34	LARGE	3300	645	3440	3510	3510	3510	3380	3450	3450	3450
Ac35	LARGE	3300	645	3510	3440	3440	3440	3450	3380	3380	3380
		Extra fuel cost due to delay ($)		1113	924	838	748	758	590	538	449
		Average delay (sec)		133	129	129	137	76	74	72	69

Figure A-1: The estimated time of arrivals (ETAs) and scheduled time of arrivals (STAs) controlled by k-CPS and TA methods for the minimum fuel costs at DFW airport between 8AM-9AM

A/C ID	A/C Type	ETAs (sec)	Fuel cost ($/hr)	**TA 2min. case**, STAs (sec)				**TA 3min. case**, STAs (sec)			
				FCFS	1-CPS	2-CPS	3-CPS	FCFS	1-CPS	2-CPS	3-CPS
Ac1	LARGE	0	645	0	0	0	0	0	0	0	0
Ac2	LARGE	0	393	70	70	70	70	70	70	70	70
Ac3	LARGE	300	762	180	180	180	180	140	140	140	140
Ac4	LARGE	300	1805	250	250	320	320	210	210	280	280
Ac5	LARGE	300	645	320	390	390	390	280	350	350	350
Ac6	LARGE	300	1805	390	320	250	250	350	280	210	210
Ac7	LARGE	600	839	480	500	570	550	420	560	560	490
Ac8	SMALL	600	295	620	710	710	690	560	490	490	630
Ac9	LARGE	600	839	690	570	500	480	630	630	630	420
Ac10	LARGE	900	645	780	780	780	1070	720	720	720	790
Ac11	LARGE	900	839	850	850	850	850	790	790	790	860
Ac12	HEAVY	900	3111	910	910	910	910	850	850	850	920
Ac13	SMALL	900	295	1110	1110	1200	780	1050	1050	1140	720
Ac14	SMALL	900	295	1200	1200	1110	1420	1140	1140	1050	1360
Ac15	LARGE	1200	762	1270	1270	1340	1140	1210	1210	1280	1220
Ac16	LARGE	1200	645	1340	1410	1410	1280	1280	1350	1350	1080
Ac17	LARGE	1200	1619	1410	1340	1270	1210	1350	1280	1210	1150
Ac18	LARGE	1500	393	1480	1550	1620	1700	1420	1420	1560	1640
Ac19	LARGE	1500	1805	1550	1480	1480	1490	1490	1490	1490	1500
Ac20	LARGE	1500	762	1620	1620	1550	1560	1560	1560	1420	1430
Ac21	LARGE	1500	645	1690	1690	1690	1630	1630	1630	1630	1570
Ac22	LARGE	2100	645	1980	2050	2050	2050	1920	2030	2030	2030
Ac23	LARGE	2100	393	2050	1980	1980	1980	1990	1960	1960	1960
Ac24	LARGE	2100	645	2120	2120	2120	2120	2060	2100	2100	2100
Ac25	LARGE	2400	839	2280	2350	2350	2350	2220	2290	2400	2400
Ac26	LARGE	2400	393	2350	2280	2420	2420	2290	2220	2330	2330
Ac27	SMALL	2400	295	2490	2490	2280	2280	2430	2430	2260	2260
Ac28	LARGE	2700	839	2580	2650	2720	2720	2520	2630	2630	2630
Ac29	SMALL	2700	295	2720	2580	2580	2580	2660	2560	2560	2560
Ac30	LARGE	2700	1805	2790	2720	2650	2650	2730	2700	2700	2700
Ac31	LARGE	3000	645	2880	3000	3000	3000	2820	3000	3000	3000
Ac32	LARGE	3300	762	3180	3250	3250	3250	3120	3120	3190	3190
Ac33	LARGE	3300	762	3250	3180	3320	3320	3190	3260	3260	3260
Ac34	LARGE	3300	645	3320	3390	3180	3180	3260	3190	3120	3120
Ac35	LARGE	3300	645	3390	3320	3390	3390	3330	3330	3330	3330
		Extra fuel cost due to delay ($)		474	356	324	275	306	236	207	185
		Average delay (sec)		20	19	17	10	-35	-25	-23	-34

Figure A-2: The estimated time of arrivals (ETAs) and scheduled time of arrivals (STAs) controlled by k-CPS and TA methods for the minimum fuel costs at DFW airport between 8AM-9AM

A/C ID	A/C Type	ETAs (sec)	Fuel cost ($/hr)	**TA 4min. case**, STAs (sec)				**TA 5min. case**, STAs (sec)			
				FCFS	1-CPS	2-CPS	3-CPS	FCFS	1-CPS	2-CPS	3-CPS
Ac1	LARGE	0	645	0	0	0	0	0	0	0	0
Ac2	LARGE	0	393	70	70	70	70	70	70	70	70
Ac3	LARGE	300	762	140	140	140	140	140	140	140	140
Ac4	LARGE	300	1805	210	210	280	280	210	210	280	280
Ac5	LARGE	300	645	280	350	350	350	280	350	350	350
Ac6	LARGE	300	1805	350	280	210	210	350	280	210	210
Ac7	LARGE	600	839	420	560	560	490	420	560	560	490
Ac8	SMALL	600	295	560	490	490	630	560	490	490	630
Ac9	LARGE	600	839	630	630	630	420	630	630	630	420
Ac10	LARGE	900	645	700	700	700	790	700	700	700	790
Ac11	LARGE	900	839	770	770	770	860	770	770	770	860
Ac12	HEAVY	900	3111	830	830	830	920	830	830	830	920
Ac13	SMALL	900	295	1030	1030	1120	720	1030	1030	1120	720
Ac14	SMALL	900	295	1120	1120	1030	1360	1120	1120	1030	1360
Ac15	LARGE	1200	762	1190	1190	1260	1220	1190	1190	1260	1220
Ac16	LARGE	1200	645	1260	1330	1330	1080	1260	1330	1330	1080
Ac17	LARGE	1200	1619	1330	1260	1190	1150	1330	1260	1190	1150
Ac18	LARGE	1500	393	1400	1400	1540	1640	1400	1400	1540	1640
Ac19	LARGE	1500	1805	1470	1470	1470	1500	1470	1470	1470	1500
Ac20	LARGE	1500	762	1540	1540	1400	1430	1540	1540	1400	1430
Ac21	LARGE	1500	645	1610	1610	1610	1570	1610	1610	1610	1570
Ac22	LARGE	2100	645	1860	2030	2030	2030	1800	2030	2030	2030
Ac23	LARGE	2100	393	1930	1960	1960	1960	1870	1960	1960	1960
Ac24	LARGE	2100	645	2000	2100	2100	2100	1940	2100	2100	2100
Ac25	LARGE	2400	839	2160	2190	2400	2400	2100	2190	2400	2400
Ac26	LARGE	2400	393	2230	2400	2330	2330	2170	2400	2330	2330
Ac27	SMALL	2400	295	2370	2330	2260	2260	2310	2330	2260	2260
Ac28	LARGE	2700	839	2460	2630	2630	2630	2400	2630	2630	2630
Ac29	SMALL	2700	295	2600	2560	2560	2560	2540	2560	2560	2560
Ac30	LARGE	2700	1805	2670	2700	2700	2700	2610	2700	2700	2700
Ac31	LARGE	3000	645	2760	3000	3000	3000	2700	3000	3000	3000
Ac32	LARGE	3300	762	3060	3090	3160	3300	3000	3090	3160	3300
Ac33	LARGE	3300	762	3130	3230	3230	3160	3070	3230	3230	3160
Ac34	LARGE	3300	645	3200	3160	3090	3090	3140	3160	3090	3090
Ac35	LARGE	3300	645	3270	3300	3300	3230	3210	3300	3300	3230
		Extra fuel cost due to delay ($)		290	215	192	183	320	215	192	183
		Average delay (sec)		-65	-35	-33	-38	-89	-35	-33	-38

Figure A-3: The estimated time of arrivals (ETAs) and scheduled time of arrivals (STAs) controlled by k-CPS and TA methods for the minimum fuel costs at DFW airport between 8AM-9AM

A/C ID	A/C Type	ETAs (sec)	Operating cost ($/hr)	**No TA case**, STAs (sec)				**TA 1min. case**, STAs (sec)			
				FCFS	1-CPS	2-CPS	3-CPS	FCFS	1-CPS	2-CPS	3-CPS
Ac1	LARGE	0	1373	0	0	0	0	0	0	0	0
Ac2	LARGE	0	1284	70	70	70	70	70	70	70	70
Ac3	LARGE	300	1494	300	370	440	440	240	310	380	380
Ac4	LARGE	300	3421	370	300	300	370	310	240	240	310
Ac5	LARGE	300	1373	440	510	510	510	380	450	450	450
Ac6	LARGE	300	3421	510	440	370	300	450	380	310	240
Ac7	LARGE	600	1467	600	600	670	600	540	540	610	610
Ac8	SMALL	600	614	740	810	810	810	680	750	750	750
Ac9	LARGE	600	1467	810	670	600	670	750	610	540	540
Ac10	LARGE	900	1373	900	970	970	1130	840	840	840	1130
Ac11	LARGE	900	1467	970	900	900	1060	910	910	910	1060
Ac12	HEAVY	900	5729	1030	1030	1030	900	970	970	970	900
Ac13	SMALL	900	614	1230	1230	1320	1480	1170	1170	1260	840
Ac14	SMALL	900	614	1320	1320	1230	1570	1260	1260	1170	1480
Ac15	LARGE	1200	1494	1390	1390	1460	1200	1330	1330	1400	1270
Ac16	LARGE	1200	1373	1460	1530	1600	1340	1400	1470	1540	1340
Ac17	LARGE	1200	3835	1530	1460	1390	1270	1470	1400	1330	1200
Ac18	LARGE	1500	1284	1600	1670	1740	1850	1540	1610	1680	1760
Ac19	LARGE	1500	3421	1670	1600	1530	1640	1610	1540	1470	1550
Ac20	LARGE	1500	1494	1740	1740	1670	1710	1680	1680	1610	1620
Ac21	LARGE	1500	1373	1810	1810	1810	1780	1750	1750	1750	1690
Ac22	LARGE	2100	1373	2100	2100	2170	2170	2040	2110	2110	2110
Ac23	LARGE	2100	1284	2170	2240	2240	2240	2110	2040	2040	2040
Ac24	LARGE	2100	1373	2240	2170	2100	2100	2180	2180	2180	2180
Ac25	LARGE	2400	1467	2400	2400	2400	2400	2340	2410	2410	2410
Ac26	LARGE	2400	1284	2470	2470	2470	2470	2410	2340	2340	2340
Ac27	SMALL	2400	614	2610	2610	2610	2610	2550	2550	2550	2550
Ac28	LARGE	2700	1467	2700	2700	2770	2770	2640	2640	2710	2710
Ac29	SMALL	2700	614	2840	2910	2910	2910	2780	2850	2850	2850
Ac30	LARGE	2700	3421	2910	2770	2700	2700	2850	2710	2640	2640
Ac31	LARGE	3000	1373	3000	3000	3000	3000	2940	2940	2940	2940
Ac32	LARGE	3300	1494	3300	3370	3370	3370	3240	3310	3310	3310
Ac33	LARGE	3300	1494	3370	3300	3300	3300	3310	3240	3240	3240
Ac34	LARGE	3300	1373	3440	3510	3510	3510	3380	3450	3450	3450
Ac35	LARGE	3300	1373	3510	3440	3440	3440	3450	3380	3380	3380
		Extra BH operating cost due to delay ($)		2287	1950	1786	1604	1449	1129	1001	835
		Average delay (sec)		133	129	129	137	76	72	72	70

Figure A-4: The estimated time of arrivals (ETAs) and scheduled time of arrivals (STAs) controlled by k-CPS and TA methods for the minimum operating costs at DFW airport between 8AM-9AM

A/C ID	A/C Type	ETAs (sec)	Operating cost ($/hr)	**No 2min. case**, STAs (sec)				**TA 3min. case**, STAs (sec)			
				FCFS	1-CPS	2-CPS	3-CPS	FCFS	1-CPS	2-CPS	3-CPS
Ac1	LARGE	0	1373	0	0	0	0	0	0	0	0
Ac2	LARGE	0	1284	70	70	70	70	70	70	70	70
Ac3	LARGE	300	1494	180	250	320	320	140	210	280	280
Ac4	LARGE	300	3421	250	180	180	250	210	140	140	210
Ac5	LARGE	300	1373	320	390	390	390	280	350	350	350
Ac6	LARGE	300	3421	390	320	250	180	350	280	210	140
Ac7	LARGE	600	1467	480	480	550	550	420	420	490	490
Ac8	SMALL	600	614	620	690	690	690	560	630	630	630
Ac9	LARGE	600	1467	690	550	480	480	630	490	420	420
Ac10	LARGE	900	1373	780	780	780	1070	720	720	720	1010
Ac11	LARGE	900	1467	850	850	850	1000	790	790	790	940
Ac12	HEAVY	900	5729	910	910	910	840	850	850	850	780
Ac13	SMALL	900	614	1110	1110	1200	780	1050	1050	1140	720
Ac14	SMALL	900	614	1200	1200	1110	1420	1140	1140	1050	1360
Ac15	LARGE	1200	1494	1270	1270	1340	1210	1210	1210	1280	1150
Ac16	LARGE	1200	1373	1340	1410	1410	1280	1280	1350	1350	1220
Ac17	LARGE	1200	3835	1410	1340	1270	1140	1350	1280	1210	1080
Ac18	LARGE	1500	1284	1480	1550	1620	1700	1420	1490	1560	1640
Ac19	LARGE	1500	3421	1550	1480	1480	1490	1490	1420	1420	1430
Ac20	LARGE	1500	1494	1620	1620	1550	1560	1560	1560	1490	1500
Ac21	LARGE	1500	1373	1690	1690	1690	1630	1630	1630	1630	1570
Ac22	LARGE	2100	1373	1980	2050	2050	2050	1920	1990	1990	1990
Ac23	LARGE	2100	1284	2050	1980	1980	1980	1990	1920	1920	1920
Ac24	LARGE	2100	1373	2120	2120	2120	2120	2060	2060	2060	2060
Ac25	LARGE	2400	1467	2280	2350	2350	2350	2220	2290	2290	2290
Ac26	LARGE	2400	1284	2350	2280	2280	2280	2290	2220	2220	2220
Ac27	SMALL	2400	614	2490	2490	2490	2490	2430	2430	2430	2430
Ac28	LARGE	2700	1467	2580	2580	2650	2650	2520	2520	2590	2590
Ac29	SMALL	2700	614	2720	2790	2790	2790	2660	2730	2730	2730
Ac30	LARGE	2700	3421	2790	2650	2580	2580	2730	2590	2520	2520
Ac31	LARGE	3000	1373	2880	2880	2880	2880	2820	2820	2820	2820
Ac32	LARGE	3300	1494	3180	3250	3250	3250	3120	3120	3190	3190
Ac33	LARGE	3300	1494	3250	3180	3180	3180	3190	3260	3260	3260
Ac34	LARGE	3300	1373	3320	3390	3390	3390	3260	3190	3120	3120
Ac35	LARGE	3300	1373	3390	3320	3320	3320	3330	3330	3330	3330
		Extra BH operating cost due to delay ($)		683	417	331	210	60	-132	-210	-303
		Average delay (sec)		20	16	16	13	-35	-39	-39	-41

Figure A-5: The estimated time of arrivals (ETAs) and scheduled time of arrivals (STAs) controlled by k-CPS and TA methods for the minimum operating costs at DFW airport between 8AM-9AM

A/C ID	A/C Type	ETAs (sec)	Operating cost ($/hr)	**No 4min. case**, STAs (sec)				**TA 5min. case**, STAs (sec)			
				FCFS	1-CPS	2-CPS	3-CPS	FCFS	1-CPS	2-CPS	3-CPS
Ac1	LARGE	0	1373	0	0	0	0	0	0	0	0
Ac2	LARGE	0	1284	70	70	70	70	70	70	70	70
Ac3	LARGE	300	1494	140	210	280	280	140	210	280	280
Ac4	LARGE	300	3421	210	140	140	210	210	140	140	210
Ac5	LARGE	300	1373	280	350	350	350	280	350	350	350
Ac6	LARGE	300	3421	350	280	210	140	350	280	210	140
Ac7	LARGE	600	1467	420	420	490	490	420	420	490	490
Ac8	SMALL	600	614	560	630	630	630	560	630	630	630
Ac9	LARGE	600	1467	630	490	420	420	630	490	420	420
Ac10	LARGE	900	1373	700	700	700	850	700	700	700	850
Ac11	LARGE	900	1467	770	770	770	920	770	770	770	920
Ac12	HEAVY	900	5729	830	830	830	690	830	830	830	690
Ac13	SMALL	900	614	1030	1030	1120	1270	1030	1030	1120	1270
Ac14	SMALL	900	614	1120	1120	1030	1360	1120	1120	1030	1360
Ac15	LARGE	1200	1494	1190	1190	1260	1130	1190	1190	1260	1130
Ac16	LARGE	1200	1373	1260	1330	1330	990	1260	1330	1330	990
Ac17	LARGE	1200	3835	1330	1260	1190	1060	1330	1260	1190	1060
Ac18	LARGE	1500	1284	1400	1470	1540	1640	1400	1470	1540	1640
Ac19	LARGE	1500	3421	1470	1400	1400	1430	1470	1400	1400	1430
Ac20	LARGE	1500	1494	1540	1540	1470	1500	1540	1540	1470	1500
Ac21	LARGE	1500	1373	1610	1610	1610	1570	1610	1610	1610	1570
Ac22	LARGE	2100	1373	1860	1930	1930	1930	1800	1870	1870	1870
Ac23	LARGE	2100	1284	1930	1860	1860	1860	1870	1800	1800	1800
Ac24	LARGE	2100	1373	2000	2000	2000	2000	1940	1940	1940	1940
Ac25	LARGE	2400	1467	2160	2230	2230	2230	2100	2170	2170	2170
Ac26	LARGE	2400	1284	2230	2160	2160	2160	2170	2100	2100	2100
Ac27	SMALL	2400	614	2370	2370	2370	2370	2310	2310	2310	2310
Ac28	LARGE	2700	1467	2460	2460	2530	2530	2400	2400	2470	2470
Ac29	SMALL	2700	614	2600	2670	2670	2670	2540	2610	2610	2610
Ac30	LARGE	2700	3421	2670	2530	2460	2460	2610	2470	2400	2400
Ac31	LARGE	3000	1373	2760	2760	2760	2760	2700	2700	2700	2700
Ac32	LARGE	3300	1494	3060	3060	3130	3270	3000	3000	3070	3210
Ac33	LARGE	3300	1494	3130	3200	3200	3130	3070	3140	3140	3070
Ac34	LARGE	3300	1373	3200	3130	3060	3060	3140	3070	3000	3000
Ac35	LARGE	3300	1373	3270	3270	3270	3200	3210	3210	3210	3140
		Extra BH operating cost due to delay ($)		-198	-374	-447	-549	-341	-518	-591	-693
		Average delay (sec)		-65	-69	-69	-65	-89	-93	-93	-89

Figure A-6: The estimated time of arrivals (ETAs) and scheduled time of arrivals (STAs) controlled by k-CPS and TA methods for the minimum operating costs at DFW airport between 8AM-9AM

Appendix B

ICN Data

This appendix shows the input and output data used in Section 5.3, which describes the ICN airport case study for minimizing the average delay in coupled operations of arrivals and departures.

Figure B-1, B-2, and B-3 show the aircraft types, jet routes for arrivals including "take-off" for departures, and estimated times of arrival (or departure) of all aircraft using the airport during an observed time period as input data. These figures also provide the scheduled times of arrival (or departure) that are optimized by Time Advance (TA) and Constrained Position Shifting (CPS) strategies for minimizing the average delay. The average delay (in seconds) and throughput (in aircraft per hour), which are used for Figure 5-15, are summarized on the bottom of the figures.

A/C ID	A/C Type	Jet Route	ETAs (sec)	**No TA case**, STAs (sec)				**TA 1min. case**, STAs (sec)			
				FCFS	1-CPS	2-CPS	3-CPS	FCFS	1-CPS	2-CPS	3-CPS
Ac1	HEAVY	B576	0	0	0	0	0	0	0	0	0
Ac2	LARGE	Takeoff	360	360	360	360	360	300	300	300	300
Ac3	HEAVY	Takeoff	480	480	480	480	480	420	420	420	420
Ac4	HEAVY	**Takeoff**	480	570	**610**	**610**	**610**	510	550	550	550
Ac5	HEAVY	B576	540	630	**540**	**540**	**540**	570	480	480	480
Ac6	LARGE	G597	540	760	670	670	670	700	610	610	610
Ac7	HEAVY	G597	600	850	760	760	760	790	700	700	700
Ac8	LARGE	Takeoff	600	920	830	830	830	860	770	770	770
Ac9	LARGE	Y64	660	980	890	890	890	920	830	830	830
Ac10	HEAVY	B576	720	1070	**1070**	980	980	1010	1010	920	920
Ac11	LARGE	Y64	840	1200	**980**	**1110**	**1110**	1140	920	1050	1050
Ac12	HEAVY	G597	960	1290	**1200**	**1200**	**1200**	1230	1140	1140	1140
Ac13	HEAVY	**Takeoff**	1020	1360	**1140**	**1050**	**1050**	1300	1080	990	990
Ac14	HEAVY	G597	1140	1420	1310	**1330**	**1330**	1360	1250	1270	1270
Ac15	LARGE	B576	1200	1550	**1440**	**1460**	**1460**	1490	1380	1400	1400
Ac16	HEAVY	**Takeoff**	1260	1620	**1380**	**1270**	**1270**	1560	1320	1210	1210
Ac17	LARGE	Y64	1320	1680	**1570**	**1590**	**1590**	1620	1510	1530	1530
Ac18	HEAVY	**Takeoff**	1380	1750	**1510**	**1400**	**1400**	1690	1450	1340	1340
Ac19	HEAVY	Takeoff	1380	1840	1640	1530	1530	1780	1580	1470	1470
Ac20	LARGE	**Takeoff**	1440	1960	**1770**	1660	1660	1900	1710	1600	1600
Ac21	HEAVY	Y64	1500	2020	**1700**	1720	1720	1960	1640	1660	1660
Ac22	LARGE	**Takeoff**	1500	2090	**1900**	1790	1790	2030	1840	1730	1730
Ac23	HEAVY	B576	1560	2150	**1830**	1850	1850	2090	1770	1790	1790
Ac24	HEAVY	G597	1680	2260	1960	**1980**	**1980**	2200	1900	1920	1920
Ac25	HEAVY	**Takeoff**	1740	2330	2030	**1920**	**1920**	2270	1970	1860	1860
Ac26	HEAVY	G597	1800	2390	2090	**2110**	**2110**	2330	2030	2050	2050
Ac27	HEAVY	**Takeoff**	1920	2460	2160	**2050**	**2050**	2400	2100	1990	1990
Ac28	HEAVY	Takeoff	2100	2550	2250	2180	2180	2490	2190	2120	2120
Ac29	HEAVY	Takeoff	2340	2640	2340	2340	2340	2580	2280	2280	2280
Ac30	HEAVY	B576	2460	2700	2460	2460	2460	2640	2400	2400	2400
Ac31	LARGE	Takeoff	2700	2770	2700	2700	2700	2710	2640	2640	2640
Ac32	HEAVY	**Takeoff**	2700	2860	**2830**	**2830**	**2830**	2800	2770	2770	2770
Ac33	LARGE	B576	2760	2920	**2760**	**2760**	**2760**	2860	2700	2700	2700
Ac34	HEAVY	G597	2760	3010	2890	2890	2890	2950	2830	2830	2830
Ac35	HEAVY	Takeoff	2760	3080	2960	2960	2960	3020	2900	2900	2900
Ac36	HEAVY	B576	2820	3140	3020	3020	3020	3080	2960	2960	2960
Ac37	LARGE	Takeoff	2820	3210	3090	3090	3090	3150	3030	3030	3030
Ac38	HEAVY	Takeoff	3060	3300	3180	3180	3180	3240	3120	3120	3120
Ac39	HEAVY	Takeoff	3240	3390	3270	3270	3270	3330	3210	3210	3210
Ac40	HEAVY	Takeoff	3480	3480	3480	3480	3480	3420	3420	3420	3420
Ac41	HEAVY	Takeoff	3480	3570	3570	3570	3570	3510	3510	3510	3510
		Average delay (sec)		305.1	159.0	140.7	140.7	246.6	100.5	82.2	82.2
		Throughput (sec)		41.3	41.3	41.3	41.3	42.1	42.1	42.1	42.1

Figure B-1: The estimated time of arrivals (ETAs) and scheduled time of arrivals (STAs) controlled by k-CPS and TA methods at ICN airport

A/C ID	A/C Type	Jet Route	ETAs (sec)	**TA 2min. case**, STAs (sec)				**TA 3min. case**, STAs (sec)			
				FCFS	1-CPS	2-CPS	3-CPS	FCFS	1-CPS	2-CPS	3-CPS
Ac1	HEAVY	B576	0	0	0	0	0	0	0	0	0
Ac2	LARGE	Takeoff	360	240	240	240	240	180	180	180	180
Ac3	HEAVY	Takeoff	480	360	360	360	360	300	300	300	300
Ac4	HEAVY	Takeoff	480	450	490	490	490	390	430	430	430
Ac5	HEAVY	B576	540	510	420	420	420	450	360	360	360
Ac6	LARGE	G597	540	640	550	550	550	580	490	490	490
Ac7	HEAVY	G597	600	730	640	640	640	670	580	580	580
Ac8	LARGE	Takeoff	600	800	710	710	710	740	650	650	650
Ac9	LARGE	Y64	660	860	770	770	770	800	710	710	710
Ac10	HEAVY	B576	720	950	950	860	860	890	890	800	800
Ac11	LARGE	Y64	840	1080	860	990	990	1020	800	930	930
Ac12	HEAVY	G597	960	1170	1080	1080	1080	1110	1020	1020	1020
Ac13	HEAVY	Takeoff	1020	1240	1020	930	930	1180	960	870	870
Ac14	HEAVY	G597	1140	1300	1190	1210	1210	1240	1130	1150	1150
Ac15	LARGE	B576	1200	1430	1320	1340	1340	1370	1260	1280	1280
Ac16	HEAVY	Takeoff	1260	1500	1260	1150	1150	1440	1200	1090	1090
Ac17	LARGE	Y64	1320	1560	1450	1470	1470	1500	1390	1410	1410
Ac18	HEAVY	Takeoff	1380	1630	1390	1280	1280	1570	1330	1220	1220
Ac19	HEAVY	Takeoff	1380	1720	1520	1410	1410	1660	1460	1350	1350
Ac20	LARGE	Takeoff	1440	1840	1650	1540	1540	1780	1590	1480	1480
Ac21	HEAVY	Y64	1500	1900	1580	1600	1600	1840	1520	1540	1540
Ac22	LARGE	Takeoff	1500	1970	1780	1670	1670	1910	1720	1610	1610
Ac23	HEAVY	B576	1560	2030	1710	1730	1730	1970	1650	1670	1670
Ac24	HEAVY	G597	1680	2140	1840	1860	1860	2080	1780	1800	1800
Ac25	HEAVY	Takeoff	1740	2210	1910	1800	1800	2150	1850	1740	1740
Ac26	HEAVY	G597	1800	2270	1970	1990	1990	2210	1910	1930	1930
Ac27	HEAVY	Takeoff	1920	2340	2040	1930	1930	2280	1980	1870	1870
Ac28	HEAVY	Takeoff	2100	2430	2130	2060	2060	2370	2070	2000	2000
Ac29	HEAVY	Takeoff	2340	2520	2220	2220	2220	2460	2160	2160	2160
Ac30	HEAVY	B576	2460	2580	2340	2340	2340	2520	2280	2280	2280
Ac31	LARGE	Takeoff	2700	2650	2580	2580	2580	2590	2520	2520	2520
Ac32	HEAVY	Takeoff	2700	2740	2710	2710	2710	2680	2650	2650	2650
Ac33	LARGE	B576	2760	2800	2640	2640	2640	2740	2580	2580	2580
Ac34	HEAVY	G597	2760	2890	2770	2770	2770	2830	2710	2710	2710
Ac35	HEAVY	Takeoff	2760	2960	2840	2840	2840	2900	2780	2780	2780
Ac36	HEAVY	B576	2820	3020	2900	2900	2900	2960	2840	2840	2840
Ac37	LARGE	Takeoff	2820	3090	2970	2970	2970	3030	2910	2910	2910
Ac38	HEAVY	Takeoff	3060	3180	3060	3060	3060	3120	3000	3000	3000
Ac39	HEAVY	Takeoff	3240	3270	3150	3150	3150	3210	3090	3090	3090
Ac40	HEAVY	Takeoff	3480	3360	3360	3360	3360	3300	3300	3300	3300
Ac41	HEAVY	Takeoff	3480	3450	3450	3450	3450	3390	3390	3390	3390
		Average delay (sec)		188.0	42.0	23.7	23.7	129.5	-16.6	-34.9	-34.9
		Throughput (sec)		42.8	42.8	42.8	42.8	43.5	43.5	43.5	43.5

Figure B-2: The estimated time of arrivals (ETAs) and scheduled time of arrivals (STAs) controlled by k-CPS and TA methods at ICN airport

A/C ID	A/C Type	Jet Route	ETAs (sec)	**TA 4min. case**, STAs (sec)				**TA 5min. case**, STAs (sec)			
				FCFS	1-CPS	2-CPS	3-CPS	FCFS	1-CPS	2-CPS	3-CPS
Ac1	HEAVY	B576	0	0	0	0	0	0	0	0	0
Ac2	LARGE	Takeoff	360	120	120	120	120	70	70	70	70
Ac3	HEAVY	Takeoff	480	240	240	240	240	180	180	180	180
Ac4	HEAVY	Takeoff	480	330	370	370	370	270	310	310	310
Ac5	HEAVY	B576	540	390	300	300	300	330	240	240	240
Ac6	LARGE	G597	540	520	430	430	430	460	370	370	370
Ac7	HEAVY	G597	600	610	520	520	520	550	460	460	460
Ac8	LARGE	Takeoff	600	680	590	590	590	620	530	530	530
Ac9	LARGE	Y64	660	740	650	650	650	680	590	590	590
Ac10	HEAVY	B576	720	830	830	740	740	770	770	680	680
Ac11	LARGE	Y64	840	960	740	870	870	900	680	810	810
Ac12	HEAVY	G597	960	1050	960	960	960	990	900	900	900
Ac13	HEAVY	Takeoff	1020	1120	900	810	810	1060	840	750	750
Ac14	HEAVY	G597	1140	1180	1070	1090	1090	1120	1010	1030	1030
Ac15	LARGE	B576	1200	1310	1200	1220	1220	1250	1140	1160	1160
Ac16	HEAVY	Takeoff	1260	1380	1140	1030	1030	1320	1080	970	970
Ac17	LARGE	Y64	1320	1440	1330	1350	1350	1380	1270	1290	1290
Ac18	HEAVY	Takeoff	1380	1510	1270	1160	1160	1450	1210	1100	1100
Ac19	HEAVY	Takeoff	1380	1600	1400	1290	1290	1540	1340	1230	1230
Ac20	LARGE	Takeoff	1440	1720	1530	1420	1420	1660	1470	1360	1360
Ac21	HEAVY	Y64	1500	1780	1460	1480	1480	1720	1400	1420	1420
Ac22	LARGE	Takeoff	1500	1850	1660	1550	1550	1790	1600	1490	1490
Ac23	HEAVY	B576	1560	1910	1590	1610	1610	1850	1530	1550	1550
Ac24	HEAVY	G597	1680	2020	1720	1740	1740	1960	1660	1680	1680
Ac25	HEAVY	Takeoff	1740	2090	1790	1680	1680	2030	1730	1620	1620
Ac26	HEAVY	G597	1800	2150	1850	1870	1870	2090	1790	1810	1810
Ac27	HEAVY	Takeoff	1920	2220	1920	1810	1810	2160	1860	1750	1750
Ac28	HEAVY	Takeoff	2100	2310	2010	1940	1940	2250	1950	1880	1880
Ac29	HEAVY	Takeoff	2340	2400	2100	2100	2100	2340	2040	2040	2040
Ac30	HEAVY	B576	2460	2460	2220	2220	2220	2400	2160	2160	2160
Ac31	LARGE	Takeoff	2700	2530	2460	2460	2460	2470	2400	2400	2400
Ac32	HEAVY	Takeoff	2700	2620	2590	2590	2590	2560	2530	2530	2530
Ac33	LARGE	B576	2760	2680	2520	2520	2520	2620	2460	2460	2460
Ac34	HEAVY	G597	2760	2770	2650	2650	2650	2710	2590	2590	2590
Ac35	HEAVY	Takeoff	2760	2840	2720	2720	2720	2780	2660	2660	2660
Ac36	HEAVY	B576	2820	2900	2780	2780	2780	2840	2720	2720	2720
Ac37	LARGE	Takeoff	2820	2970	2850	2850	2850	2910	2790	2790	2790
Ac38	HEAVY	Takeoff	3060	3060	2940	2940	2940	3000	2880	2880	2880
Ac39	HEAVY	Takeoff	3240	3150	3030	3030	3030	3090	2970	2970	2970
Ac40	HEAVY	Takeoff	3480	3240	3240	3240	3240	3180	3180	3180	3180
Ac41	HEAVY	Takeoff	3480	3330	3330	3330	3330	3270	3270	3270	3270
		Average delay (sec)		71.0	-75.1	-93.4	-93.4	12.7	-133.4	-151.7	-151.7
		Throughput (sec)		44.3	44.3	44.3	44.3	45.1	45.1	45.1	45.1

Figure B-3: The estimated time of arrivals (ETAs) and scheduled time of arrivals (STAs) controlled by k-CPS and TA methods at ICN airport

Appendix C

Violation Probability Calculation for Triangular Distribution

The probability of violating the separation requirement between two successive aircraft, *violation probability*, is discussed in this appendix. The weakness, which is used in Chapter 6, is determined by the maximum value among the violation probabilities between two consecutive aircraft in a given sequence.

The two consecutive aircraft may have different arrival time accuracies according to the performance of the equipped flight management systems. It is assumed that the probability of arrival times forms triangular distribution which is symmetric with respect to the estimated time of arrival (ETA). Given the standard deviation, σ, of estimated time of arrival for an aircraft that represents the performance of the aircraft, the aircraft can arrive at a destination airport 3σ earlier than ETA or 3σ later than ETA. Then, the probability that this aircraft lands on time is $\frac{1}{3\sigma}$ because the sum of all probabilities should be equal to one.

The violation probability for the triangular distribution is calculated as follows.

$$(\textit{Violation probability}) = \int_{-\infty}^{\infty} p_1(t) \left\{ \int_{-\infty}^{t} p_2(s)\, ds \right\} dt$$

$$\text{where } p_1(t) = \begin{cases} 0, & \text{if } -\infty < t < -3\sigma_1; \\ \frac{t+3\sigma_1}{(3\sigma_1)^2}, & \text{if } -3\sigma_1 \le t < 0; \\ -\frac{t-3\sigma_1}{(3\sigma_1)^2}, & \text{if } 0 \le t < 3\sigma_1; \\ 0, & \text{if } 3\sigma_1 \le t < \infty; \end{cases} \quad p_2(t) = \begin{cases} 0, & \text{if } -\infty < t < r - 3\sigma_2; \\ \frac{t-r+3\sigma_2}{(3\sigma_2)^2}, & \text{if } r - 3\sigma_2 \le t < r; \\ -\frac{t-r-3\sigma_2}{(3\sigma_2)^2}, & \text{if } r \le t < r + 3\sigma_2; \\ 0, & \text{if } r + 3\sigma_2 \le t < \infty; \end{cases}$$

$p_1(t)$: probability when a leading aircraft lands at time t

$p_2(t)$: probability when a following aircraft lands at time t

σ_1: standard deviation for actual arrival time of the leading aircraft

σ_2: standard deviation for actual arrival time of the trailing aircraft

d: estimated arrival time difference between two successive arriving aircraft

$\delta_{1,2}$: separation requirement between two successive arriving aircraft

$r = d - \delta_{1,2}$: virtual difference between two aircraft defined for violation probability calculation

In the equation described above, the inner integral can be calculated as follows.

$$q(t) = \int_{-\infty}^{t} p_2(s)\,ds = \begin{cases} 0, & \text{if } -\infty < t < r - 3\sigma_2; \\ \frac{(t-r+3\sigma_2)^2}{2(3\sigma_2)^2}, & \text{if } r - 3\sigma_2 \le t < r; \\ \frac{1}{2} - \frac{(t-r)^2 - 2(3\sigma_2)(t-r)}{2(3\sigma_2)^2}, & \text{if } r \le t < r + 3\sigma_2; \\ 1, & \text{if } r + 3\sigma_2 \le t < \infty; \end{cases}$$

Therefore, the equation for calculating the violation probability is simplified as follows:

$$(Violation\ probability) = \int_{-3\sigma_1}^{3\sigma_1} p_1(t)q(t)\,dt$$

$$\text{where } p_1(t) = \begin{cases} \frac{t+3\sigma_1}{(3\sigma_1)^2}, & (-3\sigma_1 \le t < 0) \\ -\frac{t-3\sigma_1}{(3\sigma_1)^2}, & (0 \le t < 3\sigma_1) \end{cases} \quad q(t) = \begin{cases} 0, & (-\infty < t < r - 3\sigma_2) \\ \frac{(t-r+3\sigma_2)^2}{2(3\sigma_2)^2}, & (r - 3\sigma_2 \le t < r) \\ \frac{1}{2} - \frac{(t-r)^2 - 2(3\sigma_2)(t-r)}{2(3\sigma_2)^2}, & (r \le t < r + 3\sigma_2) \\ 1, & (r + 3\sigma_2 \le t < \infty) \end{cases}$$

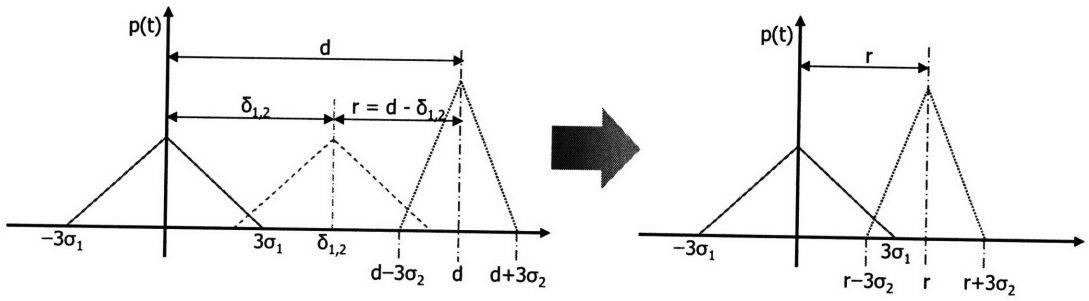

Figure C-1: Triangular distribution of estimated arrival times for two successive aircraft

The violation probability value calculated by the above equation is dependent on the time difference between two successive aircraft (r) and their standard deviations (σ_1, σ_2). In other words, the violation probability depends on the time difference between two arriving aircraft, aircraft types of two aircraft which determine the separation requirement, and the accuracies of flight management systems equipped in these aircraft.

$$(Violation\ probability) = f(r, \sigma_1, \sigma_2)$$

According to the combination of the r, σ_1, and σ_2 values, we can categorize the violation probability as 14 cases. These cases are shown in Fig C-2 and C-3, and the detailed equation for each case is described below. In this appendix, a negative r is not considered because the time difference, d, between successive aircraft should be set to be greater than separation requirement, $\delta_{1,2}$, by an air traffic controller. If this case ($r < 0$) exists, its violation probability might be equal to one.

Case 1-1) $\sigma_1 \leq \sigma_2,\ r = 0$

$$\begin{aligned}(Violation\ probability) &= \int_{-3\sigma_1}^{0} \frac{1}{(3\sigma_1)^2}(t+3\sigma_1)\,\{\frac{1}{2(3\sigma_2)^2}(t-r+3\sigma_2)^2\}\,dt \\ &+ \int_{0}^{3\sigma_1} -\frac{1}{(3\sigma_1)^2}(t-3\sigma_1)\,[\,\frac{1}{2} - \frac{1}{2(3\sigma_2)^2}\{(t-r)^2 - 2(3\sigma_2)(t-r)\}\,]\,dt \\ &= \frac{1}{2}\end{aligned}$$

Case 1-2) $\sigma_1 \leq \sigma_2,\ 0 < r < \min\{3\sigma_1,\ 3\sigma_2 - 3\sigma_1\}$

$$\begin{aligned}(Violation\ probability) &= \int_{-3\sigma_1}^{0} \frac{1}{(3\sigma_1)^2}(t+3\sigma_1)\,\{\frac{1}{2(3\sigma_2)^2}(t-r+3\sigma_2)^2\}\,dt \\ &+ \int_{0}^{r} -\frac{1}{(3\sigma_1)^2}(t-3\sigma_1)\,\{\frac{1}{2(3\sigma_2)^2}(t-r+3\sigma_2)^2\}\,dt \\ &+ \int_{r}^{3\sigma_1} -\frac{1}{(3\sigma_1)^2}(t-3\sigma_1)\,[\,\frac{1}{2} - \frac{1}{2(3\sigma_2)^2}\{(t-r)^2 - 2(3\sigma_2)(t-r)\}\,]\,dt \\ &= \frac{1}{2(3\sigma_1)^2(3\sigma_2)^2}[-\frac{1}{6}r^4 + \frac{2}{3}(3\sigma_1)r^3 + \{\frac{2}{3}(3\sigma_1)^3 - 2(3\sigma_1)^2(3\sigma_2)\}r + (3\sigma_1)^2(3\sigma_2)^2]\end{aligned}$$

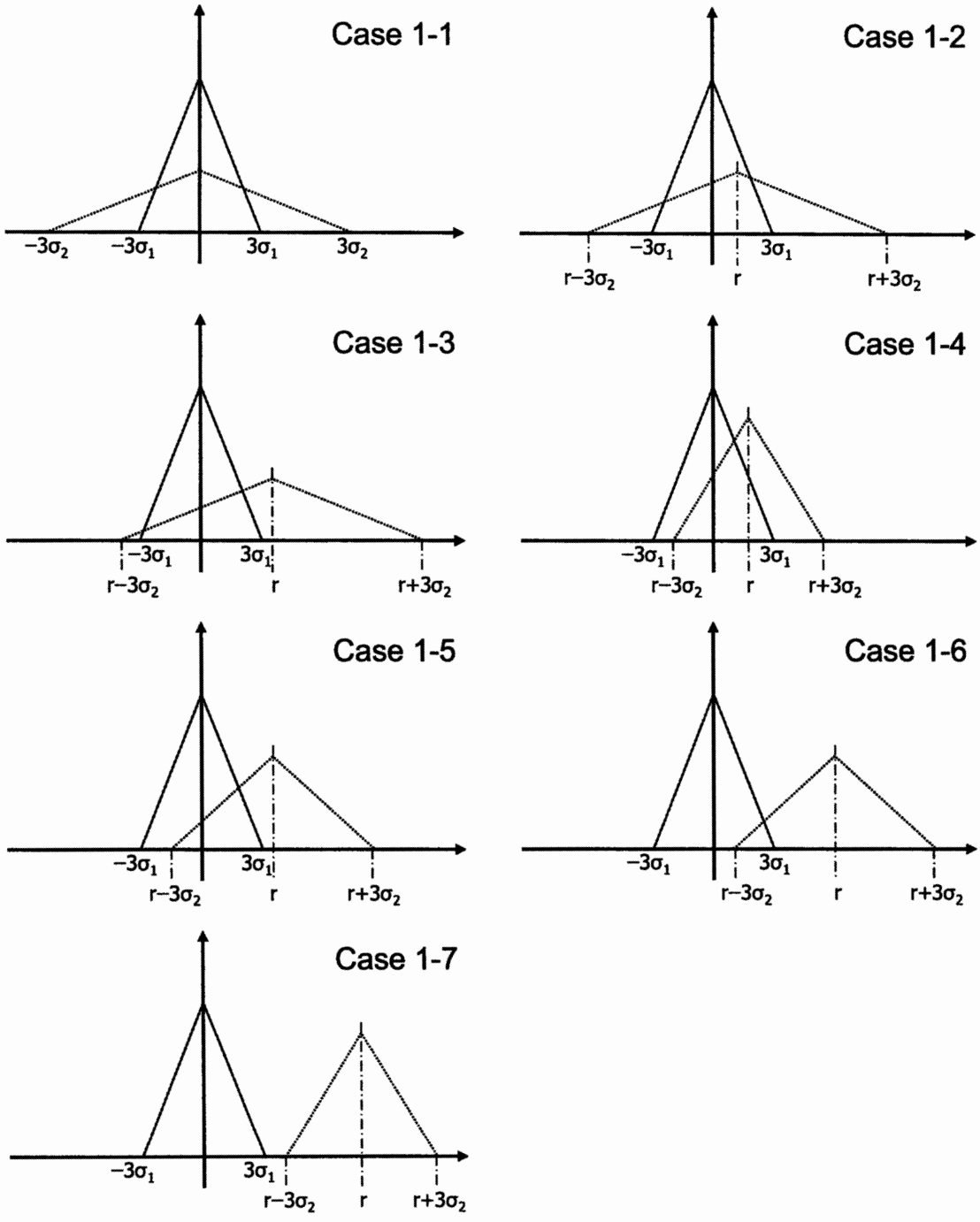

Figure C-2: 7 cases for the violation probability ($\sigma_1 \leq \sigma_2$)

Case 1-3) $\sigma_1 \leq \sigma_2,\ 2(3\sigma_1) \leq 3\sigma_2,\ 3\sigma_1 \leq r < 3\sigma_2 - 3\sigma_1$

$$
\begin{aligned}
(\textit{Violation probability}) &= \int_{-3\sigma_1}^{0} \frac{1}{(3\sigma_1)^2}(t+3\sigma_1)\,\{\frac{1}{2(3\sigma_2)^2}(t-r+3\sigma_2)^2\}\,dt \\
&\quad + \int_{0}^{3\sigma_1} -\frac{1}{(3\sigma_1)^2}(t-3\sigma_1)\,\{\frac{1}{2(3\sigma_2)^2}(t-r+3\sigma_2)^2\}\,dt \\
&= \frac{1}{2(3\sigma_1)^2(3\sigma_2)^2}[(3\sigma_1)^2r^2 - 2(3\sigma_1)^2(3\sigma_2)r + \frac{1}{6}(3\sigma_1)^4 + (3\sigma_1)^2(3\sigma_2)^2]
\end{aligned}
$$

Case 1-4) $\sigma_1 \leq \sigma_2,\ 2(3\sigma_1) > 3\sigma_2,\ 3\sigma_2 - 3\sigma_1 \leq r < 3\sigma_1$

$$
\begin{aligned}
(\textit{Violation probability}) &= \int_{r-3\sigma_2}^{0} \frac{1}{(3\sigma_1)^2}(t+3\sigma_1)\,\{\frac{1}{2(3\sigma_2)^2}(t-r+3\sigma_2)^2\}\,dt \\
&\quad + \int_{0}^{r} -\frac{1}{(3\sigma_1)^2}(t-3\sigma_1)\,\{\frac{1}{2(3\sigma_2)^2}(t-r+3\sigma_2)^2\}\,dt \\
&\quad + \int_{r}^{3\sigma_1} -\frac{1}{(3\sigma_1)^2}(t-3\sigma_1)\,[\,\frac{1}{2} - \frac{1}{2(3\sigma_2)^2}\{(t-r)^2 - 2(3\sigma_2)(t-r)\}\,]\,dt \\
&= \frac{1}{2(3\sigma_1)^2(3\sigma_2)^2}[-\frac{1}{4}r^4 + \frac{1}{3}(3\sigma_1+3\sigma_2)r^3 - \frac{1}{2}(3\sigma_1-3\sigma_2)^2r^2 \\
&\quad + \frac{1}{3}\{(3\sigma_1)^3 - 3(3\sigma_1)^2(3\sigma_2) - 3(3\sigma_1)(3\sigma_2)^2 + (3\sigma_2)^3\}r \\
&\quad - \frac{1}{12}\{(3\sigma_1)^4 - 4(3\sigma_1)^3(3\sigma_2) - 6(3\sigma_1)^2(3\sigma_2)^2 - 4(3\sigma_1)(3\sigma_2)^3 + (3\sigma_2)^4\}]
\end{aligned}
$$

Case 1-5) $\sigma_1 \leq \sigma_2,\ \max\{3\sigma_1,\ 3\sigma_2 - 3\sigma_1\} \leq r < 3\sigma_2$

$$
\begin{aligned}
(\textit{Violation probability}) &= \int_{r-3\sigma_2}^{0} \frac{1}{(3\sigma_1)^2}(t+3\sigma_1)\,\{\frac{1}{2(3\sigma_2)^2}(t-r+3\sigma_2)^2\}\,dt \\
&\quad + \int_{0}^{3\sigma_1} -\frac{1}{(3\sigma_1)^2}(t-3\sigma_1)\,\{\frac{1}{2(3\sigma_2)^2}(t-r+3\sigma_2)^2\}\,dt \\
&= \frac{1}{2(3\sigma_1)^2(3\sigma_2)^2}[-\frac{1}{12}r^4 + \frac{1}{3}(-3\sigma_1+3\sigma_2)r^3 + \{\frac{1}{2}(3\sigma_1)^2 + (3\sigma_1)(3\sigma_2) - \frac{1}{2}(3\sigma_2)^2\}r^2 \\
&\quad + \{-\frac{1}{3}(3\sigma_1)^3 - (3\sigma_1)^2(3\sigma_2) - (3\sigma_1)(3\sigma_2)^2 + \frac{1}{3}(3\sigma_2)^3\}r \\
&\quad + \{\frac{1}{12}(3\sigma_1)^4 + \frac{1}{3}(3\sigma_1)^3(3\sigma_2) + \frac{1}{2}(3\sigma_1)^2(3\sigma_2)^2 + \frac{1}{3}(3\sigma_1)(3\sigma_2)^3 - \frac{1}{12}(3\sigma_2)^4\}]
\end{aligned}
$$

Case 1-6) $\sigma_1 \leq \sigma_2,\ 3\sigma_2 \leq r < 3\sigma_1 + 3\sigma_2$

$$
\begin{aligned}
(Violation\ probability) &= \int_{r-3\sigma_2}^{3\sigma_1} -\frac{1}{(3\sigma_1)^2}(t-3\sigma_1)\,\{\frac{1}{2(3\sigma_2)^2}(t-r+3\sigma_2)^2\}\,dt \\
&= \frac{1}{2(3\sigma_1)^2(3\sigma_2)^2}[\frac{1}{12}r^4 - \frac{1}{3}(3\sigma_1+3\sigma_2)r^3 + \frac{1}{2}(3\sigma_1+3\sigma_2)^2r^2 \\
&\quad - \frac{1}{3}(3\sigma_1+3\sigma_2)^3r + \frac{1}{12}(3\sigma_1+3\sigma_2)^4]
\end{aligned}
$$

Case 1-7) $\sigma_1 \leq \sigma_2,\ r \geq 3\sigma_1 + 3\sigma_2$

$$(Violation\ probability) = 0$$

Case 2-1) $\sigma_1 > \sigma_2,\ r = 0$

$$
\begin{aligned}
(Violation\ probability) &= \int_{-3\sigma_2}^{0} \frac{1}{(3\sigma_1)^2}(t+3\sigma_1)\,\{\frac{1}{2(3\sigma_2)^2}(t-r+3\sigma_2)^2\}\,dt \\
&\quad + \int_{0}^{3\sigma_2} -\frac{1}{(3\sigma_1)^2}(t-3\sigma_1)\,[\,\frac{1}{2} - \frac{1}{2(3\sigma_2)^2}\{(t-r)^2 - 2(3\sigma_2)(t-r)\}\,]\,dt \\
&\quad + \int_{3\sigma_2}^{3\sigma_1} -\frac{1}{(3\sigma_1)^2}(t-3\sigma_1)\,dt \\
&= \frac{1}{2}
\end{aligned}
$$

Case 2-2) $\sigma_1 > \sigma_2,\ 0 < r < \min\{3\sigma_2,\ 3\sigma_1 - 3\sigma_2\}$

$$
\begin{aligned}
(Violation\ probability) &= \int_{r-3\sigma_2}^{0} \frac{1}{(3\sigma_1)^2}(t+3\sigma_1)\,\{\frac{1}{2(3\sigma_2)^2}(t-r+3\sigma_2)^2\}\,dt \\
&\quad + \int_{0}^{r} -\frac{1}{(3\sigma_1)^2}(t-3\sigma_1)\,\{\frac{1}{2(3\sigma_2)^2}(t-r+3\sigma_2)^2\}\,dt \\
&\quad + \int_{r}^{r+3\sigma_2} -\frac{1}{(3\sigma_1)^2}(t-3\sigma_1)\,[\,\frac{1}{2} - \frac{1}{2(3\sigma_2)^2}\{(t-r)^2 - 2(3\sigma_2)(t-r)\}\,]\,dt \\
&\quad + \int_{r+3\sigma_2}^{3\sigma_1} -\frac{1}{(3\sigma_1)^2}(t-3\sigma_1)\,dt \\
&= \frac{1}{2(3\sigma_1)^2(3\sigma_2)^2}[-\frac{1}{6}r^4 + \frac{2}{3}(3\sigma_2)r^3 + \{\frac{2}{3}(3\sigma_2)^3 - 2(3\sigma_1)(3\sigma_2)^2\}r + (3\sigma_1)^2(3\sigma_2)^2]
\end{aligned}
$$

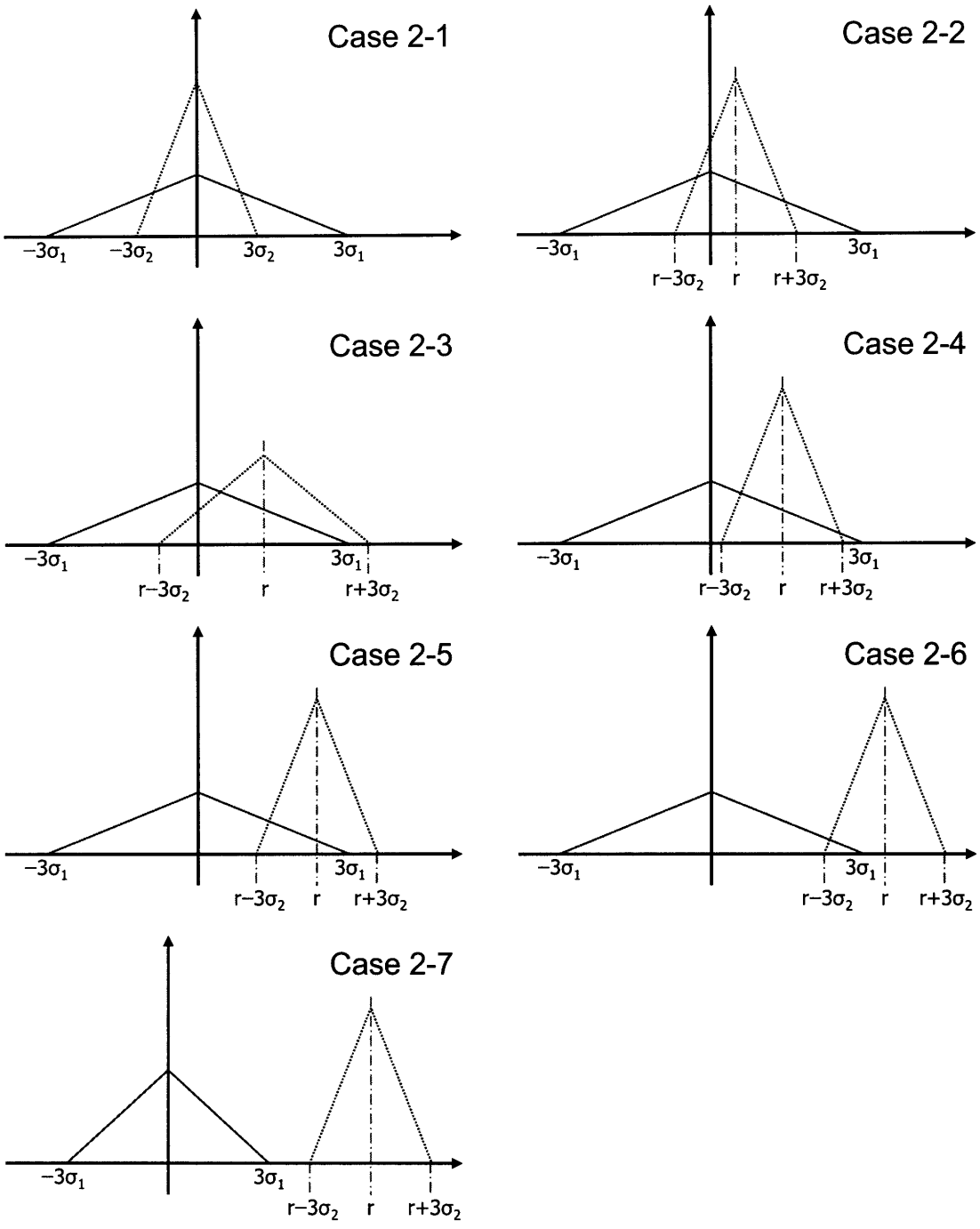

Figure C-3: 7 cases for the violation probability ($\sigma_1 > \sigma_2$)

Case 2-3) $\sigma_1 > \sigma_2,\ 3\sigma_1 \le 2(3\sigma_2),\ 3\sigma_1 - 3\sigma_2 \le r < 3\sigma_2$

$$
\begin{aligned}
(Violation\ probability) &= \int_{r-3\sigma_2}^{0} \frac{1}{(3\sigma_1)^2}(t+3\sigma_1)\,\{\frac{1}{2(3\sigma_2)^2}(t-r+3\sigma_2)^2\}\,dt \\
&+ \int_{0}^{r} -\frac{1}{(3\sigma_1)^2}(t-3\sigma_1)\,\{\frac{1}{2(3\sigma_2)^2}(t-r+3\sigma_2)^2\}\,dt \\
&+ \int_{r}^{3\sigma_1} -\frac{1}{(3\sigma_1)^2}(t-3\sigma_1)\,[\,\frac{1}{2} - \frac{1}{2(3\sigma_2)^2}\{(t-r)^2 - 2(3\sigma_2)(t-r)\}\,]\,dt \\
&= \frac{1}{2(3\sigma_1)^2(3\sigma_2)^2}[-\frac{1}{4}r^4 + \frac{1}{3}(3\sigma_1+3\sigma_2)r^3 - \frac{1}{2}(3\sigma_1-3\sigma_2)^2r^2 \\
&+ \frac{1}{3}\{(3\sigma_1)^3 - 3(3\sigma_1)^2(3\sigma_2) - 3(3\sigma_1)(3\sigma_2)^2 + (3\sigma_2)^3\}r \\
&- \frac{1}{12}\{(3\sigma_1)^4 - 4(3\sigma_1)^3(3\sigma_2) - 6(3\sigma_1)^2(3\sigma_2)^2 - 4(3\sigma_1)(3\sigma_2)^3 + (3\sigma_2)^4\}]
\end{aligned}
$$

Case 2-4) $\sigma_1 > \sigma_2,\ 3\sigma_1 > 2(3\sigma_2),\ 3\sigma_2 \le r < 3\sigma_1 - 3\sigma_2$

$$
\begin{aligned}
(Violation\ probability) &= \int_{r-3\sigma_2}^{r} -\frac{1}{(3\sigma_1)^2}(t-3\sigma_1)\,\{\frac{1}{2(3\sigma_2)^2}(t-r+3\sigma_2)^2\}\,dt \\
&+ \int_{r}^{r+3\sigma_2} -\frac{1}{(3\sigma_1)^2}(t-3\sigma_1)\,[\,\frac{1}{2} - \frac{1}{2(3\sigma_2)^2}\{(t-r)^2 - 2(3\sigma_2)(t-r)\}\,]\,dt \\
&+ \int_{r+3\sigma_2}^{3\sigma_1} -\frac{1}{(3\sigma_1)^2}(t-3\sigma_1)\,dt \\
&= \frac{1}{2(3\sigma_1)^2(3\sigma_2)^2}[(3\sigma_2)^2r^2 - 2(3\sigma_1)(3\sigma_2)^2r + \{\frac{1}{6}(3\sigma_2)^4 + (3\sigma_1)^2(3\sigma_2)^2\}]
\end{aligned}
$$

Case 2-5) $\sigma_1 > \sigma_2,\ \max\{3\sigma_2,\ 3\sigma_1 - 3\sigma_2\} \le r < 3\sigma_1$

$$
\begin{aligned}
(Violation\ probability) &= \int_{r-3\sigma_2}^{r} -\frac{1}{(3\sigma_1)^2}(t-3\sigma_1)\,\{\frac{1}{2(3\sigma_2)^2}(t-r+3\sigma_2)^2\}\,dt \\
&+ \int_{r}^{3\sigma_1} -\frac{1}{(3\sigma_1)^2}(t-3\sigma_1)\,[\,\frac{1}{2} - \frac{1}{2(3\sigma_2)^2}\{(t-r)^2 - 2(3\sigma_2)(t-r)\}\,]\,dt \\
&= \frac{1}{2(3\sigma_1)^2(3\sigma_2)^2}[-\frac{1}{12}r^4 + \frac{1}{3}(3\sigma_1-3\sigma_2)r^3 + \{-\frac{1}{2}(3\sigma_1)^2 + (3\sigma_1)(3\sigma_2) + \frac{1}{2}(3\sigma_2)^2\}r^2 \\
&+ \{\frac{1}{3}(3\sigma_1)^3 - (3\sigma_1)^2(3\sigma_2) - (3\sigma_1)(3\sigma_2)^2 - \frac{1}{3}(3\sigma_2)^3\}r \\
&+ \{-\frac{1}{12}(3\sigma_1)^4 + \frac{1}{3}(3\sigma_1)^3(3\sigma_2) + \frac{1}{2}(3\sigma_1)^2(3\sigma_2)^2 + \frac{1}{3}(3\sigma_1)(3\sigma_2)^3 + \frac{1}{12}(3\sigma_2)^4\}]
\end{aligned}
$$

Case 2-6) $\sigma_1 > \sigma_2,\ 3\sigma_1 \leq r < 3\sigma_1 + 3\sigma_2$

$$
\begin{aligned}
(Violation\ probability) &= \int_{r-3\sigma_2}^{3\sigma_1} -\frac{1}{(3\sigma_1)^2}(t-3\sigma_1)\,\{\frac{1}{2(3\sigma_2)^2}(t-r+3\sigma_2)^2\}\,dt \\
&= \frac{1}{2(3\sigma_1)^2(3\sigma_2)^2}[\frac{1}{12}r^4 - \frac{1}{3}(3\sigma_1+3\sigma_2)r^3 + \frac{1}{2}(3\sigma_1+3\sigma_2)^2r^2 \\
&\quad - \frac{1}{3}(3\sigma_1+3\sigma_2)^3r + \frac{1}{12}(3\sigma_1+3\sigma_2)^4]
\end{aligned}
$$

Case 2-7) $\sigma_1 > \sigma_2,\ r \geq 3\sigma_1 + 3\sigma_2$

$$(Violation\ probability) = 0$$

The violation probability distribution for several combinations of two successive aircraft which can be made by types of weight classes and equipment is plotted in Figure C-4 along with the difference between their estimated times of arrival.

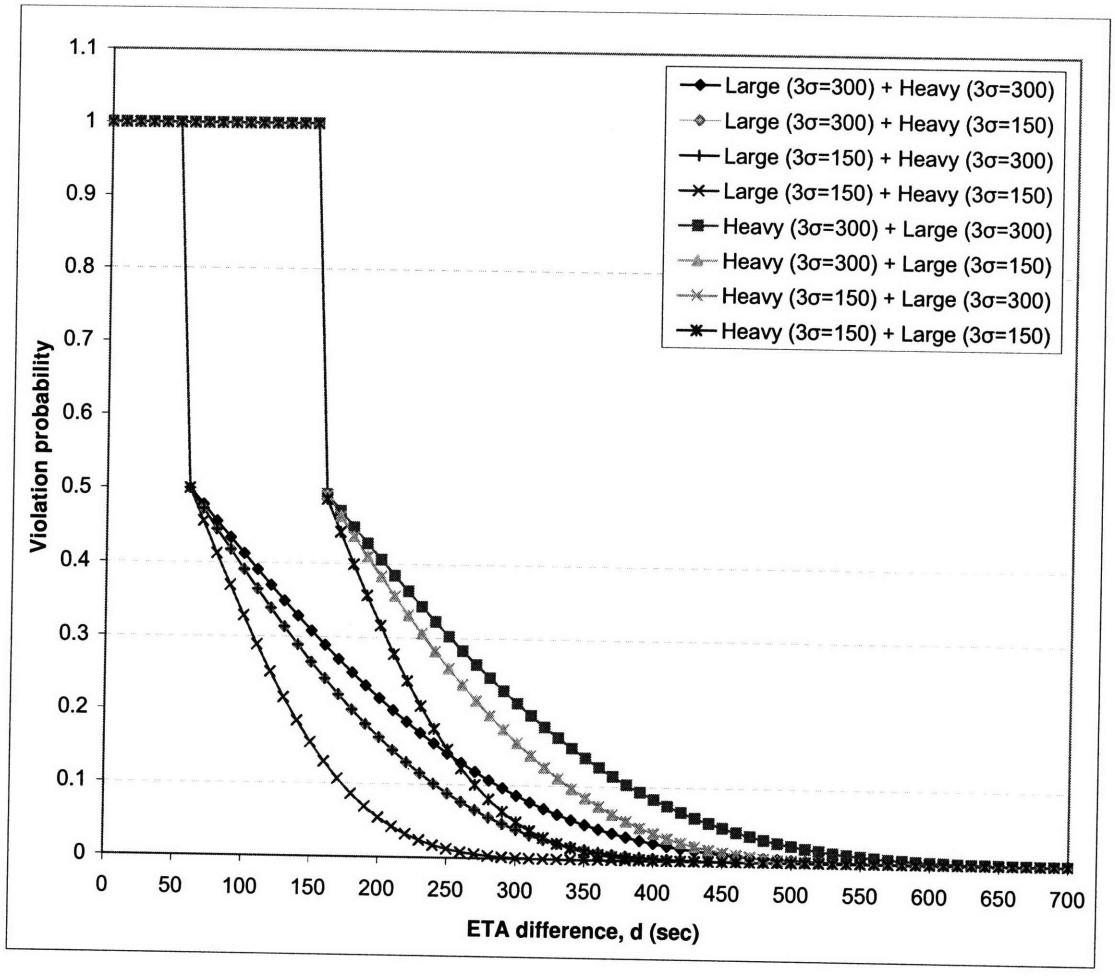

Figure C-4: An illustration of the violation probability distribution between large and heavy aircraft with different accuracy (3σ=150 or 300 seconds)

Bibliography

[1] H. Balakrishnan and B. Chandran. Scheduling Aircraft Landings under Constrained Position Shifting. In *AIAA Guidance, Navigation, and Control Conference and Exhibit*, Keystone, CO, 2006.

[2] Federal Aviation Administration (FAA). OPSNET website. http://aspm.faa.gov/.

[3] James Ott. Tactical Decision Aids Used by ZFW CWSU, April 2007. http://www.wrh.noaa.gov/psr/aviation/SAWS_Workshop/25_TDAs_ZFW.ppt.

[4] Federal Aviation Administration (FAA). Airport Capacity Benchmark Report 2004: Dallas/Fort Worth International (DFW).

[5] Richard de Neufville and Amadeo Odoni. *Airport Systems: Planning, Design and Management.* McGraw-Hill, 2003.

[6] U.S. Department of Transportation. FY 2004 Performance Plan, February 2003.

[7] International Air Transport Association (IATA). IATA website. http://www.iata.org.

[8] T.S. Perry. In Search of the Future of Air Traffic Control. In *IEEE Spectrum*, volume 34 of *8*, pages 18–35, August 1997.

[9] C. S. Venkatakrishnan. *Analysis and Optimization of Terminal Area Air Traffic Control Operations.* PhD thesis, Massachusetts Institute of Technology, 1991.

[10] U. Volckers. Arrival Planning and Sequencing with COMPAS-OP at the Frankfurt ATC-Center. In *American Control Conference*, 1990.

[11] J. Garcia. MAESTRO - A Metering and Spacing Tool. In *American Control Conference*, 1990.

[12] National Aeronautics and Space Administration (NASA), accessed May 2008. http://www.aviationsystemsdivision.arc.nasa.gov/research/foundations/index.html.

[13] H. Erzberger, T. J. Davis, and S. M. Green. Design of Center-TRACON Automation System. In *AGARD Meeting on Machine Intelligence in Air Traffic Management*, 1993. http://www.ctas.arc.nasa.gov/.

[14] W. Nedell and H. Erzberger. The Traffic Management Advisor. In *Proceedings of the American Control Conference*, San Diego, CA, May 1990.

[15] H. N. Swenson, T. Hoang, S. Engelland, D. Vincent, T. Sanders, B. Sanford, and K. Heere. Design and Operational Evaluation of the Traffic Management Advisor at the Fort Worth Air Route Traffic Control Center. In *1st USA/Europe Air Traffic Management R&D Seminar*, Saclay, France, June 1997.

[16] S. M. Green. Time-Based Operations in an Advanced ATC Environment. *Operations Research*, 28:1347–1359, 1980.

[17] S. M. Green and R. A. Vivona. En Route Descent Advisor Concept for Arrival Metering. In *AIAA Guidance, Navigation, and Control Conference*, Montreal, Canada, August 2001. AIAA 2001-4114.

[18] T. J. Davis, K. J. Krzeczowski, and C. C. Bergh. The Final Approach Spacing Tool (FAST): A Cooperative Controller-Engineer Design Approach. In *Proceedings of the 14th IFAC Symposium on Automatic Control in Aerospace*, Berlin, Germany, September 1995.

[19] K. K. Lee and T. J. Davis. The Development of the Final Approach Spacing Tool (FAST): A Cooperative Controller-Engineer Design Approach. NASA Technical Memorandum 110359, August, 1995.

[20] Joint Planning and Development Office (JPDO). Concept of Operations for the Next Generation Air Transportation System, Version 1.2, February 2007.

[21] Joint Planning and Development Office (JPDO). Next Generation Air Transportation System Integrated Plan, December 2004. http://www.jpdo.aero/integrated_plan.html.

[22] H. Erzberger and R. Paielli. Concept for Next Generation Air Traffic Control System. In *Air Traffic Control Quarterly*, volume 10 of *4*, pages 355–378, 2002.

[23] EUROCONTROL. SESAR website. http://www.eurocontrol.int/sesar/.

[24] NASA. Next Generation Air Transportation System (NGATS) Air TrafficManagement (ATM)-Airspace Project: Reference Material, June 2006. External Release Version.

[25] NASA. Next Generation Air Transportation System (NGATS) Air TrafficManagement (ATM)-Airportal Project: Reference Material, May 2007. External Release Version.

[26] EUROCONTROL. Single European Sky ATM Research Brochure, 2007.

[27] SESAR Consortium. Air Transport Framework: The Performance Target, December, 2006.

[28] G. L. Wong. The Dynamic Planner: The Sequencer, Scheduler, and Runway Allocator for Air Traffic Control Automation. NASA/TM-2000-209586, April, 2000.

[29] M. G. Ballin and H. Erzberger. Benefits Analysis of Terminal-area Air Traffic Automation at the Dallas/Fort Worth International Airport. In *AIAA Guidance, Navigation, and Control Conference*, San Diego, CA, 1996.

[30] L. A. Meyn and H. Erzberger. Airport Arrival Capacity Benefits Due to Improved Scheduling Accuracy. In *AIAA Aviation, Technology, Integration and Operations (ATIO) Conference*, Arlington, VA, 2005.

[31] F. R. Carr. *Robust Decision-Support Tools for Airport Surface Traffic.* PhD thesis, Massachusetts Institute of Technology, 2004.

[32] B. Chandran and H. Balakrishnan. A Dynamic Programming Algorithm for Robust Runway Scheduling. In *American Control Conference*, New York, NY, July 2007.

[33] H. Balakrishnan and B. Chandran. Efficient and Equitable Departure Scheduling in Real-time: New Approaches to Old Problems. In *7th USA/Europe Air Traffic Management R&D Seminar*, Barcelona, Spain, July 2007.

[34] S. Atkins and C. Brinton. Concept Description and Development Plan for the Surface Management System. *Journal of Air Traffic Control*, 44(1), January-March 2002.

[35] F. Neuman and H. Erzberger. Analysis of Delay Reducing and Fuel Saving Sequencing and Spacing Algorithms for Arrival Spacing. NASA Technical Memorandum 103880, October, 1991.

[36] F. Neuman and H. Erzberger. Analysis of Sequencing and Scheduling Methods for Arrival Traffic. NASA Technical Memorandum 102795, April, 1990.

[37] R. G. Dear. *The Dynamic Scheduling of Aircraft in the Near Terminal Area.* PhD thesis, Massachusetts Institute of Technology, 1976. Flight Transportation Laboratory Report R76-9.

[38] D. Böhme. Tactical Departure Management With The Eurocontrol/DLR DMAN. In *6th USA/Europe Air Traffic Management R&D Seminar*, Baltimore, MD, 2005.

[39] I. Anagnostakis, H. R. Idris, J. P. Clarke, E. Feron, R. J. Hansman, A. R. Odoni, and W. D. Hall. A Conceptual Design of A Departure Planner Decision Aid. In *3rd USA/Europe Air Traffic Management R&D Seminar*, Napoli, Italy, June 2000.

[40] J. E. Beasley, M. Krishnamoorthy, Y. M. Sharaiha, and D. Abramson. Scheduling Aircraft Landings - The Static Case. *Transportation Science*, 34(2):180–197, 2000.

[41] W. W. Cooper, R. H. Cormier, J. G. Foster, M. J. Mills, and S. C. Mohleji. Use of the Departure Enhanced Planning and Runway/Taxiway Assignment System (DEPARTS) for optimal departure scheduling at busy airports. In *Digital Avionics Systems Conference*, 2002.

[42] I. Anagnostakis, J.-P. Clarke, D. Böhme, and U. Völckers. Runway Operations Planning and Control: Sequencing and Scheduling. *Journal of Aircraft*, 38(6), 2001.

[43] R. G. Dear and Y. S. Sherif. An Algorithm for Computer Assisted Sequencing and Scheduling of Terminal Area Operations. *Transportation Research, Part A, Policy and Practice*, 25:129–139, 1991.

[44] H. N. Psaraftis. A Dynamic Programming Approach for Sequencing Groups of Identical Jobs. *Operations Research*, 28:1347–1359, 1980.

[45] C. S. Venkatakrishnan, A. Barnett, and A. R. Odoni. Landings at Logan Airport: Describing and Increasing Airport Capacity. *Transportation Science*, 27(3):211–227, 1993.

[46] D. A. Trivizas. Optimal Scheduling with Maximum Position Shift (MPS) Constraints: A Runway Scheduling Application. *Journal of Navigation*, 51(2):250–266, May 1998.

[47] L. Bianco, G. Rinaldi, and A. Sassano. A Combinatorial Optimization Approach to Aircraft Sequencing Problem. In A. R. Odoni, L. Bianco, and G. Szego, editors, *Flow Control of Congested Networks*, volume 38 of *NATO ASI Series, Series F: Computer Systes and Systems Science*, pages 323–339, Springer-Verlag, Berlin, 1987.

[48] L. Bianco, S. Ricciardelli, G. Rinaldi, and A. Sassano. Scheduling Tasks with Sequence-dependent Processing Times. *Naval Research Logistics*, 35(2):177–184, 1988.

[49] J. Abela, D. Abramson, M. Krishnamoorthy, A. De Silva, and G. Mills. Computing Optimal Schedules for Landing Aircraft. In *The 12th National ASOR Conference*, pages 71–90, Adelaide, Australia, 1993.

[50] A.T. Ernst, M. Krishnamoorthy, and R.H. Storer. Heuristic and Exact Algorithms for Scheduling Aircraft Landings. *Networks*, 34:229–241, 1999.

[51] A. M. Bayen, C. J. Tomlin, Y. Ye, and J. Zhang. An Approximation Algorithm for Scheduling Aircraft with Holding Time. In *IEEE Conference on Decision and Control (CDC)*, 2004.

[52] K. Roy, A. M. Bayen, and C. J. Tomlin. Polynomial Time Algorithms for Scheduling of Arrival Aircraft. In *AIAA Guidance, Navigation, and Control Conference and Exhibit*, San Francisco, CA, August 2005.

[53] J. Milan. The Flow Management Problem in Air Traffic Control: A Model of Assigning Priorities for Landings at a Congested Airport. *Transp. Plan. Technol*, 20:131–162, 1997.

[54] G. C. Carr, H. Erzberger, and F. Neuman. Airline Arrival Prioritization in Sequencing and Scheduling. In *2nd USA/Europe Air Traffic Management R&D Seminar*, Orlando, FL, December 1998.

[55] Federal Aviation Administration (FAA). Air Traffic Control: Order 7110.65R. Includes Change 3, February 16, 2006. (Appendix A). http://www.faa.gov/atpubs.

[56] R. Slattery. Terminal Area Trajectory Synthesis for Air Traffic Control Automation. In *Proceedings of the 1995 American Control Conference*, Seattle, WA, June 21-23 1995.

[57] Eclat Consulting. Aircraft Operating Costs and Statistics. *Aviation Daily*, 368, June, 2007.

[58] DFW Airport Arrivals, July 2 2007. http://www.flightstats.com.

[59] F. Carr, A. Evans, J.-P. Clarke, and E. Feron. Modeling and Control of Airport Queueing Dynamics under Severe Flow Restrictions. In *Proceedings of the American Control Conference*, Anchorage, AK, May 8-10 2002.

[60] J. Scharl, A. Haraldsdottir, and E. Schoemig. A Trajectory Modeling Environment for the Study of Arrival Traffic Delivery Accuracy. In *AIAA Modeling and Simulation Technologies Conference and Exhibit*, Keystone, CO, 2006.